Molecular determinants for the outcome in gemcitabine-treated pancreatic cancer

Doctoral Thesis

In partial fulfillment of the requirements for the degree
"Doctor rerum naturalium (Dr. rer. nat.)"
in the Molecular Medicine Study Program
at the Georg-August University Göttingen

submitted by

Claudia Lüske

born in Oldenburg

Göttingen 2015

Members of the Thesis Committee:

Supervisor:

Name, Institute: **Prof. Dr. med. Jürgen Brockmöller**, Institute of Clinical Pharmacology, University Medical Center Göttingen, Georg-August University Göttingen

Second member of the thesis committee:

Name, Institute: **Prof. Dr. rer. nat. Peter Burfeind**, Institute of Human Genetics, University Medical Center Göttingen, Georg-August University Göttingen

Third member of the thesis committee:

Name, Institute: **Prof. Dr. med. Michael Zeisberg**, Department of Nephrology and Rheumatology, University Medical Center Göttingen, Georg-August University Göttingen

Date of disputation: 26th of November 2015

Affidavit

Here I declare that my doctoral thesis entitled "**Molecular determinants for the outcome in gemcitabine-treated pancreatic cancer**" has been written independently with no other sources and aids than quoted.

_____

Claudia Lüske

Göttingen, September 2015

Table of Contents

List of Publications

GROH, I. A., CHEN, C., **LÜSKE, C.**, CARTUS, A. T., ESSELEN, M. (2013). "Plant polyphenols and oxidative metabolites of the herbal alkenylbenzene methyeugenol suppress histone deacetylase activity in human colon carcinoma cells." J Nutr Metab **2013**: 821082.

Acknowledgments

Abstract

Pancreatic ductal adenocarcinoma (PDAC) is a mostly lethal disease which represents the fourth common cause of all deaths related to cancer. The nucleoside analogue gemcitabine constitutes a currently widely used treatment standard both in a palliative and adjuvant setting. However, variability in response to gemcitabine is high with a substantial impact of genetic variations assumed. Two previously identified single nucleotide polymorphisms (SNPs) associated with the overall survival of gemcitabine treated patients suffering from PDAC were characterized in this thesis concerning the underlying molecular mechanisms: Rs11644322 pertinent to the tumor suppressor gene *WWOX*, and rs1130609 pertinent to the ribonucleotide reductase *RRM2.*

A panel of 89 lymphoblastoid cell lines (LCLs) with publicly available genotype information was used as model system to study genomic causes of variable gemcitabine sensitivity. Cytotoxicity of gemcitabine was assessed by flow cytometry-based measurement of proliferation inhibition, and gene expression was determined by quantitative real-time PCR. For extended experiments the pancreatic cancer cell lines AsPC1, MiaPaca-II, PaTu8988t, PancI, and L3.6 were used. Modification of gemcitabine response upon *WWOX* knock-down by siRNA and shRNA (verified by Western Blotting) or upon *WWOX* overexpression was ascertained. As the transcription factor SP1 bound to the *WWOX* rs11644322, overexpression of this factor was conducted and the consequences on *WWOX* transcription with and without gemcitabine, 5-fluorouracil and irinotecan were studied. Whole transcriptome analysis was determined for gemcitabine effects in AsPC1 and MiaPaca-II cells, in PaTu8988t upon shRNA-mediated *WWOX* knock down, and in pooled LCLs defined by homozygous wild type and variant allele at the *WWOX* index SNP site, respectively.

Regarding the molecular mechanisms behind the *RRM2* polymorphism, electrophoretic mobility shift assays (EMSA) were performed to discern allele-specific transcription factor binding at rs1130609. An *in vitro* coupled Transcription/Translation system was utilized to study allele-specific differences regarding protein translation.

In LCLs, cytotoxicity of gemcitabine was reduced in dependence of the number of *A* alleles at *WWOX* rs11644322, consistent with the worse prognosis of patients with this allele. No transcripts were detected in close vicinity to rs11644322. However, homozygosity for the *AA* allele at rs11644322 was accompanied by lower *WWOX*

expression of both, the core coding region and of the last exon, separated by 730 kb. A specific gemcitabine-related correlation was identified in LCLs between transcription of *WWOX* and the growth arrest and DNA damage-inducible gene *GADD45A*, which was correlated with increased gemcitabine cytotoxicity.

Whole transcriptome analysis in AsPC1 and MiaPaca-II cells revealed that *RRM2* expression increased more strongly than any other protein-coding transcript upon gemcitabine exposure. Quantitative relations of the two *RRM2* transcripts differing in the noncoding 5' sequence length revealed the major one amounting to 96 to 99 % of the entire transcript numbers, depending on the cell type. This major *RRM2* transcript isoform was also increased upon gemcitabine exposure in LCLs and in peripheral blood of patients subjected to gemcitabine-containing chemotherapy. In EMSA experiments stronger protein binding at the *RRM2* rs1130609 *G* allele (the same allele which was associated with worse prognosis) was identified. However, no impact of this SNP on the transcription of the major *RRM2* isoform was seen. In contrast, increased expression of the minor isoform with an extended 5'-region was observed in presence of the *T* variant allele at rs1130609, intensified upon gemcitabine treatment. Preliminary results for cloned RRM2 suggested less translation efficacy for the *T* compared to the *G* allele.

Based on previous data and those of my thesis, mechanistic hypotheses for *WWOX* and *RRM2* are suggested: The variant *A* allele at the *WWOX* index SNP might bind SP1 to a lesser extent, resulting in decreased expression probably mediated via interaction with the promoter region by looping. By that, epithelial-mesenchymal transition may be increased resulting in reduced cell proliferation and enhanced resistance to gemcitabine, finally providing a mechanistic basis for worse clinical outcome. Regarding RRM2, phosphorylated gemcitabine can block physiological DNA synthesis resulting in *RRM2* transcription induction, primarily of the major variant isoform. In case of the *T* variant allele at the *RRM2* index SNP site, RRM2 protein synthesis is presumed to be impaired, what might stimulate transcription of the minor isoform.

The obtained data provide new insights in functional mechanisms. By corroborating the clinical associations, these data further supported the two predictive SNPs in *WWOX* and *RRM2* as valid biomarkers for gemcitabine-based chemotherapy in PDAC.

List of Figures

List of Tables and Equations

Tables

Equations

List of Abbreviations

36B4	Acidic ribosomal phosphoprotein P0
5-FU	5-Fluorouracil
ADP	Adenosine diphosphate
APS	Ammonium persulfate
AJCC	American Joint Committee on Cancer
AMT	Ataxia telangiectasia-mutated
B2MG	Beta-2 microglobulin
BCL2	B-cell lymphoma 2
bp	Base pair
BSA	Bovine Serum Albumin
cAMP	Cyclic adenosine monophosphate
CDA	Cytidine deaminase
cDNA	Copy DNA (complementary DNA)
CDP	Cytidine diphosphate
hCNT	Human concentrative nucleoside transporter
CFSE	Carboxy fluoresceinsuccinimidyl ester
CI	Confidence interval
CMPK	Cytidine monophosphate kinase
CRE	cAMP response element
d-	Deoxy
Da	Dalton
DCTD	Deoxycytidylate deaminase
dCTP	Deoxycytidine triphosphate
dd-	Dideoxy
ddH$_2$O	Bi-distilled water
DDR	DNA damage response
dFdC	2', 2'-difluorodeoxycytidine (Gemcitabine)
dFdCMP	2', 2'-difluorodeoxycytidine-monophosphate
dFdCDP	2', 2'-difluorodeoxycytidine-diphosphate
dFdCTP	2', 2'-difluorodeoxycytidine-triphosphate
dFdUMP	2', 2'-difluorodeoxyuridine-monophosphate
DMEM	Dulbecco's modified Eagle Medium
DMSO	Dimethylsulfoxide
DNA	Deoxyribonucleic acid
dNTP	Desoxynucleosidetriphosphate
DPD	Dihydropyrimidine dehydrogenase
dsDNA	Double standed DNA
DTT	Dithiothreitol
E. coli	*Escherichia coli*
EC$_{50}$	Half maximal effect concentration
EDTA	Ethylene di-amine tetra-acetic acid
e.g.	*Exempli gratia*
EGFR	Epidermal growth factor receptor
eGFP	Enhanced Green Fluorescent Protein
EMT	Epithelial-mesenchymal Transition

hENT	Human equilibrative nucleoside transporter
et al.	*et alii/et aliae/et alia*
FACS	Fluorescence-activated cell sorting
FCS	Fetal calf serum
FRT	Flp (recombinase) recognition target
g	Gravity acceleration (9.81 m/s^2)
GADD45A	Growth arrest and DNA-damage-inducible gene alpha
GAPDH	Glyceraldehyde 3-phosphate dehydrogenase
GDP	Guanosine diphosphate
GWAS	Genome-wide association study
h	Hour
HEK-293	Human embryonic kidney 293 cell line
HEPES	2-[4-(2-hydroxyethyl)piperazin-1-ly]ethanesulfonic acid
HPRT1	Hypoxanthine-guanine phosphoribosyltransferase 1
HR	Hazard ratio
HRP	Horseradish peroxidase
ID	Identification
IgG	Immunoglobulin G
kV	Kilo volt
kb	Kilo base
kDa	Kilodalton
LB medium	Luria-Bertani medium
LCL	Lymphoblastoid cell line
LD	Linkage disequilibrium
M	Molarity
MAF	Minor allele frequency
MET	Mesenchymal-epithelial Transition
min	Minute
mRNA	Messenger RNA
NDPK	Nucleoside diphosphate kinase
NER	Nucleotide excision repair
NP-40	Nonyl-phenoxypolyethoxylethanol
NT	Nucleotidase
ORF	Open reading frame
p	Probability
PAGE	Polyacrylamide gel electrophoresis
PBS	Phosphate buffered saline
PCR	Polymerase chain reaction
PDAC	Pancreatic ductal adenocarcinoma
pH	pH-value
PMSF	Phenylmethanesulfonyl fluoride
PS	Penicillin-Streptomycin
qRT-PCR	Quantitative real-time PCR
RNA	Ribonucleic acid
RNase	Ribonuclease
RNAseq	RNA sequencing
RPKM	Reads per kilobase of transcript per million mapped reads

RPMI	Roswell Park Memorial Institute Medium 1640
RRM1	Ribonucleotide reductase subunit 1
RRM2	Ribonucleotide reductase subunit 2
rpm	Rotations per minute
rs	Reference SNP
RT	Room temperature
SDS	Sodiumdodecylsulfate
sec	Second
shRNA	Short hairpin RNA
siRNA	Small interfering RNA
SNP	Single Nucleotide Polymorphism
SP1	Specificity protein 1
ssDNA	Single stranded DNA
Taq	Thermus aquaticus
TBE-Buffer	Tris-Borat-EDTA-buffer
TE-Buffer	Tris-hydroxymethyl-aminomethane-EDTA-buffer
TEMED	N,N,N',N'-Tetramethylethane-1,2-diamine
TNM	Tumor classification system (tumor, lymph node, metastasis)
TP53	Tumor protein 53
Tris	Tris(hydroxymethyl)-aminomethane
TS	Thymidylate synthase
U	Unit
UBC	Ubiquitin C
UDP	Uridine diphosphate
UICC	Union internationale contre le cancer
UV	Ultraviolet
Var	Variant
v/v	Volume per volume
Vol	Volume
vs.	*Versus*
v/w	Weight per volume
W	Tryptophan
w/o	Without
WT	Wild type
WWOX	WW domain containing oxidoreductase

In this thesis all gene names are denotes *in italics* and the protein names in roman letters, respectively.

1 Introduction

1.1 Pancreatic cancer: Incidence and prognosis

Pancreatic cancer is one of the most aggressive and lethal diseases with a dismal prognosis. The current lifetime risk in the Western countries amounts to 1.49 % (1 in 67) with no marked gender preference (HOWLADER *et al.* 2013, BECKER *et al.* 2014). In Germany there are up to 16,000 new cases per year and the average age to be affected is 75 years for women, and 71 for men (ROBERT-KOCH INSTITUT 2012). With regard to all malignancies, the incidence of pancreatic ductal adenocarcinoma (PDAC) amounts to 3.5 % and it represents the fourth most common cause of cancer-related deaths, for men ranked behind lung, prostate and colorectal cancer and for women behind lung, breast, and colorectal cancer, respectively (SIEGEL *et al.* 2013).

No early detection methods are available so far and at the time of diagnosis the disease state is often advanced, because at the early stages most patients have no or no specific symptoms indicating the disease (WOLFGANG *et al.* 2013). The overall five-year survival is less than 5 % and even patients after surgery, performed in curative intention, show an overall five-year survival which does not exceed 20 - 25 % with a median survival of 17 to 23 months (VINCENT *et al.* 2011). Patients presenting metastatic disease (50 - 60 %) have the shortest survival time of three to six months (SHRIKHANDE *et al.* 2007, CHUE 2009). Among all malignant tumors of the pancreas, PDAC, arising from the exocrine pancreas, account for more than 90 % (DELPERO *et al.* 2015). Approximately 65 % of the pancreatic tumors are located in the head, 15 % in the body and the tail and the remaining ones diffusely occur inside the gland (Figure 1, GREENLEE *et al.* 2000, ARTINYAN *et al.* 2008).
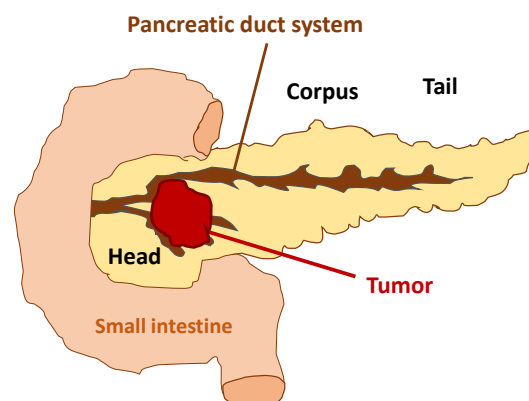
Figure 1: Anatomy of pancreatic ductal adenocarcinoma (PDAC)

1.2 Molecular features of pancreatic cancer

Treatment response to cytostatics is highly variable and a substantial contribution of tumor and host genome variability is presumed. DNA sequencing technologies have shown that pancreatic carcinomas carry on average about 63 acquired somatic mutations, which are predominantly point mutations (JONES *et al.* 2008).

Ninety five percent of pancreatic cancers harbor activating mutations in the proto-oncogene *KRAS,* which is known to drive pancreatic neoplasia (SMIT *et al.* 1988, DI MAGLIANO AND LOGSDON 2013, ESER *et al.* 2014). *KRAS* mutations correlate with a shortened median survival of 17 *vs.* 30 months for *KRAS* wild type (RACHAKONDA *et al.* 2013). Somatic mutations in *SMAD4*, which mediated the *TGFβ* signaling pathway suppressing epithelial cell growth, have been reported in approximately 50 % of human pancreatic tumors (HAHN *et al.* 1996, MIYAKI AND KUROKI 2003). Also, the known tumor suppressor gene *TP53* belongs to the frequently mutated genes in pancreatic cancer. *TP53* is involved in diverse biological effects concerning cell-cycle arrest, DNA replication and repair, apoptosis, angiogenesis inhibition, proliferation and response to cellular stresses. This is due to transcriptional activation of several target genes, e.g. *IGF-BP3* (negative regulator of cell proliferation), *PCNA* (involved in DNA replication and nucleotide excision repair *in vitro*), *BAX* (linked to regulation of apoptosis) and *GADD45* (encodes a protein that binds to PCNA) (CHAN *et al.* 1999, HAINAUT AND HOLLSTEIN 2000, TOKINO AND NAKAMURA 2000). Further genes often mutated in PDAC are *CDKN2A* (CALDAS *et al.* 1994), *APC* (HORII *et al.* 1992), *BRAF* and *FBXW7* (CALHOUN *et al.* 2003). Targeted therapies according to the somatic mutation pattern extend treatment options for distinct pancreatic adenocarcinoma subsets.

Some genes like *TP53*, *SMAD4*, *CDKN2A*, and *ATM* are not only affected by somatic mutations but also carry germline genetic polymorphisms some of them possibly predisposing to PDAC. For another group of genes, germline polymorphisms rather than somatic mutations are reported as relevant in PDAC carcinogenesis (e.g. in *BRCA1*, *BRCA2* or the DNA mismatch-associated genes *MLH1* and *MSH2*) (STOFFEL 2015). Notably, pancreatic cancer cells have inherited the genetic make-up of the host germ-line variability. Regarding the complex biological reactions upon drug exposure it is thus likely that germline variability contributes substantially to treatment response.

1.3   Therapy options

PDAC is described to have a high tendency for local invasion, distant metastases and limited response to chemotherapeutic agents (MARECHAL *et al.* 2012).

The only potentially curative approach for PDAC is the complete resection of the tumor. Regrettably, less than 20 % of the patients exhibit a resectable disease at time of diagnosis (BRENNAN *et al.* 1996). To enhance the chance of curative resection, patients not suitable for surgery or patients with borderline resectable tumors may undergo neoadjuvant treatment (NANDA *et al.* 2015). Either a combination of chemo- and radiotherapy or a monotherapy of either is commonly used as neoadjuvant treatment (GILLEN *et al.* 2010). After surgery, adjuvant chemotherapy is commonly used due to the high risk of local tumor recurrence (STALEY *et al.* 1996, SPERTI *et al.* 1997). Because most patients suffer from advanced, non resectable disease the optimization of palliative systemic therapy is still ongoing. Monotherapy or combination chemotherapy may enhance the survival time for patients having no chance for cure (VAN LAETHEM *et al.* 2012).

As standard first-line therapy for PDAC, the nucleoside analogue gemcitabine has been approved for over a decade (VACCARO *et al.* 2015). With regard to the overall survival (OS) after palliative and adjuvant therapy, the benefit of gemcitabine is very moderate, compared to the former traditionally used chemotherapeutic agent 5-FU (5-Fluorouracil) with an OS of 5.7 *vs.* 4.4 months after palliative, and 23.6 *vs.* 23 months (5-FU plus folinic acid) after adjuvant therapy, respectively. However, gemcitabine improved disease-related symptoms and caused less side effects (BURRIS *et al.* 1997, NEOPTOLEMOS *et al.* 2010). The combination of capecitabine (a prodrug of 5-FU) and gemcitabine, used against locally advanced and metastatic pancreatic cancer, had a positive effect on the response rate (19.1 % *vs.* 12.4 %) as well as on progression-free (Hazard ratio [HR], 0.78; 95 % CI (confidence interval), 0.66 to 0.93; p = 0.004) and the overall survival (HR, 0.86, 95 % CI, 0.72 to 1.02; p = 0.08), compared to single gemcitabine treatment with tolerable side-effects (CUNNINGHAM *et al.* 2009). Also nab-paclitaxel (albumin-bound paclitaxel) plus gemcitabine, compared to gemcitabine monotherapy, significantly enhanced the overall (8.5 *vs.* 6.7 months respectively) and progression-free survival (5.5 *vs.* 3.7 months, respectively) in patients with metastatic disease (VON HOFF *et al.* 2013). Combinations of gemcitabine with platin compounds in

most studies did not show an improvement regarding survival time and may just be useful for patients with a good performance status (S‌AIF AND K‌IM 2007). A combined treatment of gemcitabine plus the epidermal growth factor receptor (EGFR) tryosine kinase showed an enhanced progression-free (3.8 *vs.* 2.4 months) and overall survival (7.2 *vs.* 4.4 months), compared to single gemcitabine administration. Survival time was longer for patients with an EGFR mutation (W‌ANG *et al.* 2015).

As an alternative treatment to gemcitabine FOLFIRINOX, a combined chemotherapy regimen, including folinic acid (leucovorin, FOL), 5-FU (F), irinotecan (IRIN) and oxaliplatin (OX), approved in 2010, showed a prolonged overall (11 *vs.* 6.8 months) and progression-free survival (6.4 *vs.* 3.3 months), but was accompanied by higher toxicity. Therefore, this treatment is an option for patients with metastatic pancreatic cancer showing a good physical condition (C‌ONROY *et al.* 2011, C‌ONROY *et al.* 2013). In summary, more aggressive regimens in advanced pancreatic cancer are restricted to patients with a good performance state, otherwise the single-agent gemcitabine is still regarded as gold standard (H‌EINEMANN *et al.* 2007).

1.4   The nucleoside analogue gemcitabine

Gemcitabine (2',2'-difluorodeoxycytidine, dFdC, marketed as Gemzar® from Eli Lilly and Company) is a nucleoside analogue of deoxycytidine with two additional fluorine atoms in the deoxyribofuranosyl ring (Figure 2).
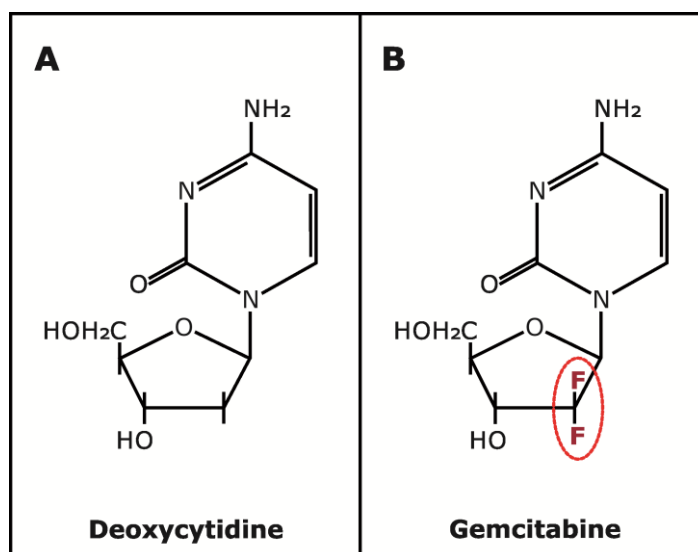
Figure 2: Skeletal formula of desoxycytidine (A) and gemcitabine (B)

1.4.1 Clinical indications, administration and toxicity

Gemcitabine represents a cytostatic drug which is approved for the systemic therapy of advanced (nonresectable Stage II or Stage III) or metastatic (Stage IV) pancreatic cancer since 1995 (PLUNKETT *et al.* 1995, CONROY AND MITRY 2011, ELLI LILY AND COMPANY DRUG INFORMATION SHEET GEMZAR 2014, updated version), as single agent or in combination as outlined above (see chapter 1.3). In combination regimens, gemcitabine is also used for non-small-lung and bladder cancer (with cisplatin), ovarian cancer (with carboplatin), and breast cancer (with paclitaxel), respectively (MINI *et al.* 2006).

The recommended dose of gemcitabine is 1000 - 1250 mg/m² administered as a 30-minutes infusion once a week for the first seven weeks, followed by one week of rest. After week 8 a weekly dosing on day 1, 8 and 15 of a 28-day cycle is advised (ELLI LILY AND COMPANY DRUG INFORMATION SHEET GEMZAR 2014). Following a standard 30 minute infusion of the recommended gemcitabine dose, plasma concentration of 20 - 60 µM could be achieved at the end of infusion. Though, after intravenous administration, plasma level of gemcitabine decrease rapidly due to rapid deamination to dFdU (difluorodeoxyuridine) which is mostly occuring before the active drug can enter the tumor cell (ABBRUZZESE *et al.* 1991, GRUNEWALD *et al.* 1991). The half-life of gemcitabine varies from 42 to 94 minutes and appears to be affected by gender and age. Gemcitabine (< 10 %) and the inactivated dFdU (difluorodeoxyuridine) metabolite represent 99 % of the excreted dose measured in the urine of patients, who received a radiolabeled drug infusion (ELLI LILY AND COMPANY DRUG INFORMATION SHEET GEMZAR 2014).

Though, it shows several side-effects, of which myelosuppression, with thrombocytopenia and anemia, represents the dose-limiting toxicity (ABBRUZZESE *et al.* 1991, CONROY *et al.* 2011).

1.4.2 Route of gemcitabine

The transport of gemcitabine into the cell is essential for its efficacy. Gemcitabine is highly hydrophilic resulting in a limited intracellular diffusion potential and therefore needs nucleoside transporter (NTs) to enter the cell (PAPROSKI *et al.* 2013). The equilibrative nucleoside transporter ENT1 (also called SLC29A1) is known as the primary transport protein for gemcitabine and other nucleoside analogues. Also concentrative nucleoside transporter (CNTs), like CNT1 and CNT3 are involved, but to a

less extent.

As a prodrug, gemcitabine has to be activated inside the cell through phosphorylation by kinases to its derivates dFdCDP (2', 2'-difluorodeoxycytidine-diphosphate) and dFdCTP (2', 2'-difluorodeoxycytidine-triphosphate), which are responsible for the cytotoxic effects. The biotransformation of nucleoside analogues to their mononucleotides by phosphorylation is catalyzed by deoxycytidine kinase (DCK) representing the rate-limiting enzyme (FARRELL *et al.* 2009). Further essential phosphorylation steps of dFdCMP (2', 2'-difluorodeoxycytidine-monophosphate) to di- and triphosphate are mediated by the kinases CMPK1 (cytidine monophosphate kinase) and NDPK (nucleoside diphosphate kinase), respectively (Figure 3) (MINI *et al.* 2006, KOCABAS *et al.* 2008).
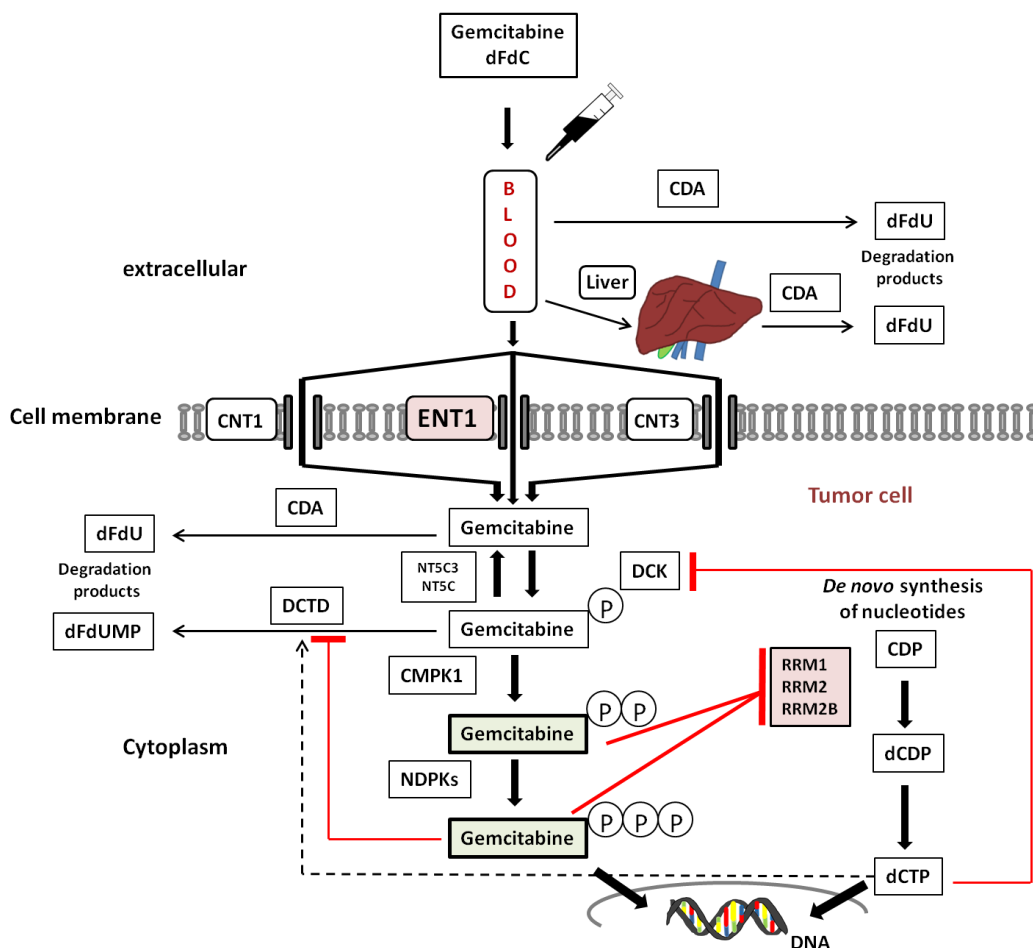
Figure 3: Pathways of gemcitabine (dFdC) transport, metabolism of action and self-potentiation. Black arrows denote uptake and metabolic processes with the involved proteins indicated: Transport proteins ENT1 (equilibrative nucleoside transporter 1), CNT1 (concentrative nucleoside transporter 1) and CNT3 (concentrative nucleoside transporter 3) and the enzymes DCK (deoxycytidine kinase), NT5C3 (cytosolic 5'-nucleotidase 3), NT5C (cytosolic 5'-nucleotidase), CMPK1 (cytidine monophosphate kinase 1) and NDPKs (nucleoside diphosphate kinases). The "P" symbols represent phosphates attached to gemcitabine. Competing physiological cytidine metabolites are denoted as CDP (cytidine diphosphate), dCDP (deoxycytidine diphosphate) and dCTP (deoxycytidine triphosphate). The degradation products are dFdU (difluorodeoxyuridine) and dFdUMP (difluorodeoxyuridine-monophosphate). Details are described in the text. Modified according to MINI *et al.* 2006, WONG *et al.* 2009.

Gemcitabine underlies a self-potentiation mechanism. The metabolite dFdCDP is known to inhibit ribonucleotide reductases (RR) and its regulatory and catalytic subunits (RRM1, RRM2), which are essential for the *de novo* synthesis of deoxynucleotides. A decreased deoxyribonucleotide pool potentiates the cytotoxic effect of dFdCTP, which competes with physiological dCTPs (deoxycytidine triphosphate) for incorporation into the DNA (MINI *et al.* 2006). Furthermore, dCTP is a potent feedback inhibitor of DCK, so that low dCTP level cause an increased phosphorylation of gemcitabine (WONG *et al.* 2009).

When incorporated into DNA as false nucleotide by DNA polymerase alpha, dFdCTP inhibits further DNA synthesis through masked chain termination, initiated by incorporation of only one additional deoxynucleotide preventing DNA repair mechanisms and fostering cytotoxic effects (HUANG *et al.* 1991, RUIZ VAN HAPEREN *et al.* 1993). The described enrichment of dFdCTP as well as the reduction of the dCTP pool lead to an inhibition of the dFdCMP inactivation step mediated by DCTD (deoxycytidylate deaminase), which needs sufficient concentrations of dCTP to be active (HEINEMANN *et al.* 1992).

Gemcitabine has a short plasma half-life (see chapter 1.4.1) due to its rapid degradation (90 %) to dFdU (2', 2'-difluorodeoxyuridine) catalyzed by cytidine deaminase (CDA), an enzyme which is expressed in the liver and blood and to a less extent inside tumor cells (HEINEMANN *et al.* 1992). Cytosolic 5'-Nucleotidases (5'-NT) are responsible for further gemcitabine inactivation and convert nucleoside monophosphates back to nucleosides, acting as antagonists of DCK (BERGMAN *et al.* 2002). Another degradation pathway of gemcitabine is the deamination of gemcitabine monophosphate (dFdCMP, 2', 2'-difluorodeoxycytidine-monophosphate) to dFdUMP (2', 2'-difluorodeoxyuridine-monophosphate) by DCTD (HEINEMANN *et al.* 1992).

1.5 Outcome predictors in gemcitabine-treated pancreatic cancer

1.5.1 Candidate genes affecting gemcitabine efficacy

Candidate genes involved in gemcitabine activity are depicted in Figure 3 (section 1.4.2). The determination of a score comprising tumor expression of *ENT1, DCK, RRM1* and *RRM2* was suggested as a putative biomarker for gemcitabine therapy (NAKANO *et al.* 2007, FUJITA *et al.* 2010).

The relevance of the ENT1 transporter in PDAC has been repeatedly confirmed in several studies as a predictive biomarker for gemcitabine efficacy. Strong ENT1 protein expression detected by immunostaining in the tumor cells was related to longer survival of patients (SPRATLIN *et al.* 2004, MARECHAL *et al.* 2009, GREENHALF *et al.* 2014). Similar relations were noticed for tumoral *ENT1* mRNA expression (GIOVANNETTI *et al.* 2006).

A significantly prolonged median survival upon gemcitabine treatment was observed in case of low *RRM2* mRNA expression (ITOI *et al.* 2007). On protein level, higher tumoral expression of RRM2 was correlated with a shorter time to disease recurrence and a reduced OS after resection in patients who underwent gemcitabine adjuvant regimen (FISHER *et al.* 2013). Consistent with the clinical findings, *RRM2* overexpression conveys chemoresistance in pancreatic adenocarcinoma and siRNA-mediated knock-down of *RRM2* leads to an increased chemosensitivity towards gemcitabine, both *in vivo* and *in vitro*. Specifically, the IC_{50} value of gemcitabine was four times higher upon recombinant *RRM2* transfection compared to the empty vector (DUXBURY *et al.* 2004). In a multi-modal approach with simultaneous overexpression of *DCK* and uridine monophosphatase (*UMP*) and gene silencing of *RRM2* and *TS* (thymidylate synthetase) gemcitabine sensitivity of resistant pancreatic cancer cells could be restored (REJIBA *et al.* 2009). In the gemcitabine resistant pancreatic cancer cell line PancI *RRM2* expression gets sharply induced when exposed to gemcitabine via an *E2F1*-dependent transcriptional activation. CG-5, a glucose transporter inhibitor, was hypothesized to re-establish the sensitivity of gemcitabine-resistant PancI cells by induction of microRNA-520f (LAI *et al.* 2014).

Regarding *RRM1,* low *RRM1* mRNA expression levels were related to increased gemcitabine sensitivity in pancreatic cancer cell lines and in PDAC (NAKAHIRA *et al.* 2007). However, in other studies a correlation between RRM1 expression and treatment outcome could not be confirmed (KIM *et al.* 2011, FISHER *et al.* 2013). Subsequent studies also could not identify *RRM1* as a clear predictive or prognostic parameter in resected PDAC patients exposed to gemcitabine (VALSECCHI *et al.* 2012).

To ease future clinical use it might be beneficial if variability in gene expression could be referred to genetic markers which can be determined in a more easy and robust fashion compared to tumor-specific expression of mRNA and proteins. For candidate genes of gemcitabine effects, inherited single nucleotide polymorphisms (SNPs) may substantially contribute to treatment outcome. Several SNPs have been associated with the efficacy and toxicity of gemcitabine, e.g. polymorphisms in *CDA* and *DCTD*

(gemcitabine inactivation enzymes), *ENT1* or *RRM1* (Okazaki *et al.* 2010, Fukunaga *et al.* 2004, Ueno *et al.* 2007, Tanaka *et al.* 2010).

An in-house conducted retrospective analysis highlighted a SNP in *RRM2* associated with OS (Figure 4, Zimmer 2013). However, this *RRM2* SNP was not analyzed functionally so far.
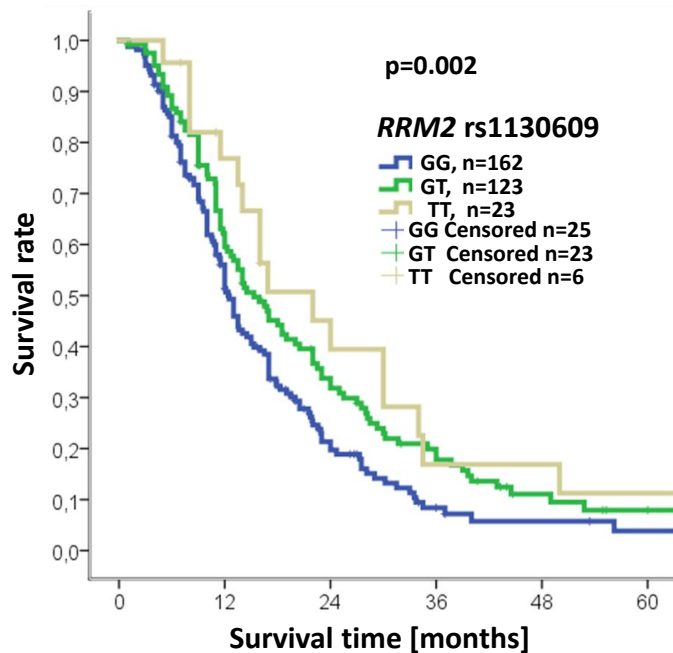
Figure 4: Impact of the inherited *RRM2* polymorphism rs1130609 on overall survival. Data is from a set of 308 patients for whom R0 or R1 resections could be achieved. Patients were recruited at three different study sites (Göttingen, Heidelberg, Hamburg) and patient numbers were specified in 12 month intervals. The p-value refers to unadjusted log-rank test (data from Zimmer 2013).

1.5.2 Genome-wide association studies (GWAS)

Genome-wide association studies (GWAS) represent an approach to identify clinically or functionally relevant SNPs in a broad scale (in a so-called hypothesis free approach not restricting the analysis to genes for which specific hypotheses exist). Typically, arrays covering a panel of several hundred thousand SNPs more or less uniformly distributed over the entire genome were applied. More recently, GWAS with complete coverage of genomic varibility have become feasible with emerging of deep sequencing technologies.

In 2012, a comprehensive array-based GWAS was undertaken to screen for markers associating with clinical outcome in gemcitabine-treated PDAC. In that study, 351 patients were recruited and ~ 550,000 markers were assayed in germline DNA samples isolated of peripheral blood cells. Thereby, the SNP *IL17F* rs763780 showed the strongest association with OS (Innocenti *et al.* 2012). The variant allele of this SNP was

hypothesized to mitigate the function of the anti-angiogenic *IL17F*, thus possibly promoting tumor growth and hampering therapy responsiveness (ARISAWA *et al.* 2007, ARISAWA *et al.* 2008). Other SNPs in or near the genes *PRB2*, *DCP1B*, *WWOX* and *BTRC* were also associated with overall survival. However, considering multiple testing their role was statistically not significant (INNOCENTI *et al.* 2012). To assess the clinical relevance of those findings from INNOCENTI *et al.* an independent validation appeared to be mandatory. In a cooperation between the University Medical Centers in Göttingen, Hamburg, and Heidelberg a statistically significant association of the *WWOX* SNP, found among the top hits of the mentioned GWAS, could be demonstrated for the first time (Figure 5). However, the role of the SNP *IL17F* rs763780 could not be confirmed in these german samples. Pilot functional assessment identified members of the specificity protein (SP) family as transcription factors with allele-specific affinity to this *WWOX* index SNP site. According to those analyses it is unlikely that any other polymorphism as rs11644322 in high linkage disequilibrium (LD) with the latter is causatively functional (ROPPEL 2013). Detailed functional elucidations linking this SNP to *WWOX* gene expresssion, gemcitabine sensitivity and the clinical finding are not yet performed and might be worthy for potential use as biomarker. Moreover, the pathways in which *WWOX* acts are still poorly understood.
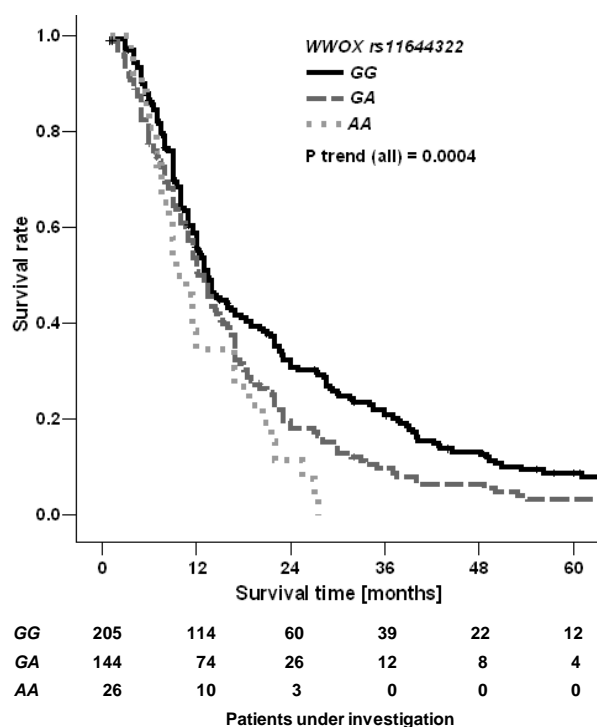
Figure 5: Impact of *WWOX* rs11644322 on overall survival. Data is from a set of 381 patients for whom R0 or R1 resections could be achieved. Patients were recruited at three different study sites (Göttingen, Heidelberg, Hamburg) and patient numbers were specified in 12 month intervals. The p-value refers to unadjusted log-rank test (data from ROPPEL 2013).

GG	205	114	60	39	22	12
GA	144	74	26	12	8	4
AA	26	10	3	0	0	0

Patients under investigation

1.6   Aims of this thesis

The aim of my doctoral thesis was the detailed molecular characterization of genetic polymorphisms in *WWOX* and *RRM2,* previously identified, to determine gemcitabine response in pancreatic cancer. Knowledge of funtional relationship might contribute to overcome treatment resistance. In the next subchapters, a detailed description of single steps to achieve the aims is provided.

1.6.1 WWOX

Based on the clinical association found with the *WWOX* SNP rs11644322, SNP-specific (items 1-3) and general functions of *WWOX* (items 4-6) in relation to gemcitabine sensitivity should be addressed:

1. The variant *A* allele at rs11644322 conferred worse outcome in the clinical setting. It should be delineated whether this variant alters cellular sensitivity to cytostatic drugs in general or specifically to gemcitabine.

2. Is rs11644322 related to gene expression? This genetic polymorphism is located in an extraordinarily huge intron far away from any known coding region. First, the expression levels of the *WWOX* coding regions upstream and downstream of this index SNP should be quantified in detail. It should be elucidated whether rs11644322 affects global transcriptome in general and specifically the *WWOX* expression. Furthermore, possible gemcitabine-induced alterations of WWOX expresson should be evaluated in dependence on rs11644322.

3. Since *WWOX* rs11644322 was identified as a site at which SP proteins bind in an allele-specific fashion, effects of this SNP are presumed to be linked to SP binding. As the expression of SP may be rate-limiting in this issue, the functional consequences of *SP1* overexpression in pancreatic cancer cell lines should be explored in conjunction with cytostatic drug exposure.

4. A pro-apoptotic role of *WWOX* has been suggested. The relationship between *WWOX* expression level and cytotoxicity of gemcitabine should be analyzed. In addition, potential relationships with known apoptotic genes should be evaluated.

5. The relevance of *WWOX* in cancer has recently emerged. The role of enhanced or suppressed *WWOX* expression in pancreatic cancer cell lines should be investigated

in terms of cell proliferation with a specific focus on interactions with gemcitabine.

6. Knock-down of *WWOX* might be accompanied by expression alterations affecting cellular proliferation. By means of whole transcriptome analysis consequences of transient and stable RNAi targeting *WWOX* on gene expression patterns should be delineated.

1.6.2 RRM2

A previous study conducted in the institute of Clinical Pharmacology in Göttingen found a SNP pertinent to the *RRM2* gene associated with the outcome of patients suffering from PDAC and treated with gemcitabine. An ambiguous relation to *RRM2* protein expression in pancreatic cancer tissue has also been reported (ZIMMER 2013). To the best of my knowledge, no functional assessments for this SNP have been conducted so far. The following questions and hypotheses should be elucidated:

1. There are two transcript isoforms of *RRM2*. The index SNP differs in the relative position to these isoforms. The proportions of the two known transcript isoforms should be illustrated in detail in different cell types.

2. *RRM2* counteracts gemcitabine effects and and its up-regulation might be a feature of drug resistance. Upon exposure to gemcitabine the extent of *RRM2* induction should be evaluated in comparison with the global transcriptome. Thus differential expression of *RRM2* transcript variants upon gemcitabine exposure should be delineated and stratified according to the *RRM2* index SNP genotypes.

3. The hypothesis of *RRM2* induction upon gemcitabine should be verified in patients during chemotherapy in a prospective fashion.

4. The *RRM2* index SNP is located in the so-called Kozak sequence at position -6 relative to the start codon of the major transcript variant. The Kozak sequence has been reported as a major region for transcription factor binding (FITZGERALD *et al.* 2004). Thus, it should be analyzed whether nuclear protein extracts bind in an allele-specific manner as a possible mechanism for the observed clinical association.

5. The Kozak sequence is known to be essential for translation initiation. Thus, it should be addressed if the mutation causes by the index SNP affects translation efficiency.

Detailed functional characterizations of the two considered genetic polymorphism in *RRM2* and *WWOX* should provide further evidence for the medical relevance with the perspective to tailor future treatment.

2 Materials

2.1 Reagents and kits

Reagents, kits	Manufacturer
[α-^{32}P]-dCTP (for EMSA)	Hartmann Analytic GmbH, Braunschweig
1 kb standard ladder (for agarose gel)	ABgene, Fermentas, St. Leon-Rot
100 bp standard ladder (for agarose gel)	ABgene, Fermentas, St. Leon-Rot
40 % (w/v) Acrylamide:Bisacrylamide (Mix 37.5:1)	Biomol, Hamburg
5-FU (Fluorouracil)	Central Pharmacy, Clinic Hospital Göttingen
ABI PRISM® SNaPshot™ Multiplex Kit	Applies Biosystems, Darmstadt
Agar (for bacteriology)	AppliChem, Darmstadt
Agarose Ultra Pure (gel electrophoresis)	Invitrogen, Karlsruhe
All oligonucleotides (for PCR or EMSA)	Eurofins MWG synthesis GmbH, Ebersberg
Ammoniumpersulfate (APS)	AppliChem, Darmstadt
Ampicillin 99 %	AppliChem, Darmstadt
AMPure® XP beads	Agencourt Bioscience Corporation, Beverly, Massachusetts
Anti-Protease	Roche, Mannheim
Anti-Phosphatase	Roche, Mannheim
Aquasafe 500 Plus, Safty Scintillator	Zinsser Analytic, Berkshire, UK
Attractene Transfection Reagent	Qiagen, Hilden
BigDye® v1.1 Sequencing Kit (Fluorescence based Sanger sequencing)	Applied Biosystems, Darmstadt
Bovine serum albumin (BSA)	Sigma-Aldrich, Deisenhofen
Bromphenolblue Na-Salt (Electrophoresis)	Roth, Karlsruhe
CFSE Proliferation Dye	eBioscience, Frankfurt

Chloroform ≥ 99.8 %	J.T. Baker, Phillipsburg, USA
CompactPrep kit (for midi-prep)	Qiagen, Hilden
CountBright^{TM} Absolute Counting Beads	Invitrogen, Karlsruhe
Dimethyl sulfoxide (DMSO)	AppliChem, Darmstadt
Disodium hydrogen phosphate ≥ 99.9 %	Merck, Darmstadt
DNaseI solution	USB, Staufen
DNeasy Blood & Tissue Kit (DNA extraction)	Qiagen, Hilden
dNTP Set	ABgene, Hamburg
Dual-Luciferase® Reporter Assay System	Promega, Mannheim
EDTA 0.5 M in water solution	Sigma-Aldrich, Deisenhofen
EDTA pure	Merck, Darmstadt
Ethanol 96 %	Merck, Darmstadt
Ethanol denatured 99 %	Chemie-Vertrieb Hannover
Ethidiumbromide 1 % in H_2O	Merck, Darmstadt
EZ1 DNA Blood Card (No. 9015585)	Qiagen, Hilden
EZ1 DNA Blood Kit	Qiagen, Hilden
Expand Long Template PCR System	Roche Diagnostics, Mannheim
FACS Safe Clean	Beckton Dickinson, Franklin Lakes, USA
FACS Flow	Beckton Dickinson, Franklin Lakes, USA
FACS Rinse	Beckton Dickinson, Franklin Lakes, USA
FAST-AP (1U/µl)	Life Technologies Corporation, Darmstadt
FuGene 6 (Transfection reagent)	Roche, Mannheim
Gemcitabine (dFdC)	Central Pharmacy, University Medical Center, Göttingen
GeneScanLIZ120 (For SNaPshot^{TM})	Applied Biosystems, Darmstadt

15

Glycerol 85 %	Central pharmacy, University Medical Center, Göttingen
GoScript™ Reverse Transcriptase	Promega, Mannheim
Helipur® H plus N (Desinfection reagent)	Braun, Melsungen
Hi-Di™ Formamid (for SNapshot™)	Applied Biosystems, Darmstadt
HotStarTaq Master Mix Kit (250 units)	Qiagen, Hilden
Hydrogen chloride	Merck, Darmstadt
Hygromycin B (50 mg/ml)	Invitrogen, Karlsruhe
Irinotecan	Sigma-Aldrich, Deisenhofen
Isoamylalcohol 98 %	Schuchardt, Hohenbrunn
Isopropanol ≥ 99.9 %	Merck, Darmstadt
Kanamycin ≥ 750U/mg	AppliChem, Darmstadt
Klenow-Fragment (for EMSA)	Fermentas, St. Leon-Roth
KOD HotStart DNA Polymerase	Novagen Merck, Darmstadt
Ligate-IT™ Rapid Ligation Kit	USB, Staufen
Lipofectamine™ 2000	Invitrogen, Karlsruhe
Lipofectamine® RNAiMAX (Transfection Reagent)	Invitrogen, Karlsruhe
Luminata™ Forte Western HRP Substrate	MerckMillipore, Darmstadt
Magic Mark™ standard	Life Technologies Corporation, Darmstadt
Magnesium chloride ≥ 99 %	Riedel-De Haën AG, Seelze
Magnesium sulfate ≥ 99.5 %	Merck, Darmstadt
Methanol for analysis	Merck, Darmstadt
Milk powder, blotting grade	Roth, Karlsruhe
Mini Quick Spin Oligo Columns	Roche, Mannheim

Multiplex PCR Kit	Qiagen, Hilden
Neodisher® A 8 (Cleaning powder)	Chem. Fabrik Dr. Weigert, Mühlenhagen
Nonidet P-40 (NP-40)	AppliChem, Darmstadt
NuPage LDS sample buffer (4x)	Invitrogen, Karlsruhe
PAXgene Blood miRNA Kit	Qiagen, Hilden
PBS	Invitrogen, Karlsruhe
PBS Powder (Dulbeccos 10-fold)	AppliChem, Darmstadt
Penicillin/Streptomycin-Solution	Invitrogen, Karlsruhe
Pierce™ BCA Protein Assay Kit	Life Technologies Corporation, Darmstadt
Plasmid Midi Kit	Qiagen, Hilden
Poly(deoxyinosinic-deoxycytidylic)	Sigma-Aldrich, Deisenhofen
Poly-d-lysine hydrobromide	Sigma-Aldrich, Deisenhofen
Polymer POP6 und POP7 for sequencing	Applied Biosystems, Darmstadt
Prestained Marker (for Western Blotting)	BioFroxx, Einhausen
PrestoBlue® Cell Viability Reagent	Invitrogen, Karlsruhe
QIAquick Gel Extraction Kit	Qiagen, Hilden
5x HOT FIREPol® EvaGreen® qPCR Mix Plus	Solis BioDyne, Estonia
QuantiFluor™ Dye System	Promega, Mannheim
Quickszint Flow 302, Liquid Scintillator	Zinsser Analytic, Berkshire, United Kingdom
Random hexanucleotide primers *dN6*	Roche, Mannheim
RLT Plus Buffer	Qiagen, Hilden
RNAse A ~ 70 %	AppliChem, Darmstadt
RNAse Inhib P/N 71571 (40 un/µl)	USB, Staufen
RNase ZAP	Sigma-Aldrich, Deisenhofen

RNeasy Plus Mini Kit	Qiagen, Hilden
Rotiphorese® Gel 30 solution	Roth, Karlsruhe
Sephadex™ G-50 Superfine	Amersham Bioscience, Freiburg
SnapShot™ Multiplex Kit	Applied Biosystems, Darmstadt
Sodium acetate	Merck, Darmstadt
Sodium chloride	Merck, Darmstadt
Sodium dodecyl sulfate	BioRad, Hercules, USA
Sodium Dodecyl Sulfate (SDS) Solution 10 %	AppliChem, Darmstadt
Sodium hydroxide pellets pure	Merck, Darmstadt
Sure Silencing shRNA Plasmid Kit	Qiagen, Hilden
SYTOX® Blue Dead Cell Stain, for flow cytometry	Life Technologies Corporation, Darmstadt
T4 DNA Ligase	Fermentas, St. Leon-Roth
Taq DNA polymerase	Qiagen, Hilden
TEMED ≥ 99 % (N,N,N',N'- Tetramethylethylenediamine)	Sigma-Aldrich, Deisenhofen
TNT® T7 Quick Coupled Transcription/Translation System	Promega, Mannheim
TopTaq Polymerase	Qiagen, Hilden
Tris 100 % (Tris hydroxymethyl aminomethane)	Roth, Karlsruhe
Tris ultrapure	AppliChem, Darmstadt
Triton X-100	Roth, Karlsruhe
Trypan blue solution (0.4 %)	Sigma-Aldrich, Deisenhofen
TrypLE™ Express	Gibco/Invitrogen, Karlsruhe
Tryptone	AppliChem, Darmstadt

Tween20	Sigma, Steinheim
Vybrant® DyeCycle™ Ruby stain	Life Technologies Corporation, Darmstadt
X-ray film developer G150	AGFA, Leverkusen
X-ray film fixer G354	AGFA, Leverkusen
X-tremeGENE HP DNA Transfection Reagent	Roche, Mannheim
Xylene cyanol FF (for molecular biology)	AppliChem, Darmstadt
Yeast extract	AppliChem, Darmstadt

2.2 Used materials

Used materials	Manufacturer
5 ml Polysterene Round-Botton Tube (FACS Tube)	BD Falcon, Durham, USA
6-Well plate, Nunclon™ Delta Surface	Thermo Scientific, Schwerte
12-Well plate (for Cell culturing)	Greiner, Frickenhausen
24-Well plate (for Cell culturing)	Greiner, Frickenhausen
96 Millipore MAHV N45 plate	Millipore, Bedford, USA
96-Well PCR-Plate	ABgene, Epsom
96-Well Cell Culture Microplate (PS, F-Bottom, chimey well, black)	Greiner, Frickenhausen
Absolute QPCR Seal (Optical Foil for Taqman)	Thermo Scientific, Schwerte
Blotting filter paper	Whatman, Kent, United Kingdom
Culture flask 25 cm² and 75 cm²	Sarstedt, Nümbrecht
Cuvette (UVette®) 50 - 1000 µl	Eppendorf, Hamburg
Cuvette 10 x 4 x 45 mm	Sarstedt, Hamburg
Dialysis filter VSWP01300	Millipore, Schwalbach

Electroporation cuvette 2 mm	PEQLAB Biotechnologie GmbH, Erlangen
Flat 12-cap strips	ABgene, Epsom, United Kingdom
Flat 8-cap strips	ABgene, Epsom, United Kingdom
FrameStar® 384	4titude, Wotton, United Kingdom
Freezing container, Nalgene®, Mr. Frosty	Sigma-Aldrich, Deisenhofen
Gel System PerfectBlue™ (for electrophoresis)	PEQLAB Biotechnologie GmbH, Erlangen
Gel electrophoresis chamber (SDS-minigel)	Biometra, Göttingen
Glass Pasteur pipette 230 mm	WU, Mainz
Nanodrop cuvette	Implen, München
Neubauer-Cell chamber	Schütt, Göttingen
Nunclon™ Multidishes 6 and 12 wells	Nunc, Wiesbaden
Parafilm®	Brand, Wertheim
PAXgene™ Blood RNA tube (2.5 ml)	PreanalytiX GmbH, Hombrechtikon, CH
Petri Dish	Sarstedt, Hamburg
Petri Dish for Cell culture, Falcon 353003	Schütt, Göttingen
Pipette Tip (10 µl, 100 µl, 1000 µl)	Sarstedt, Hamburg
PVDF membrane Hybond-P	Amersham Biosciences, Freiburg
Quali-Filterpipette tip sterile	Kisker, Steinfurt
Reactions vessel 0.2 ml (RNase-free)	Biozym, Hessisch Oldendorf
Reactions vessel (1.5 ml and 2 ml)	Sarstedt, Hamburg
Sterile pipettes (5 ml, 10 ml, 25 ml)	Sarstedt, Hamburg
Sterile Polypropylen-tube (15 ml)	Greiner, Frickenhausen
Sterile Polypropylen-tube (50 ml)	Sarstedt, Hamburg
Thermo-Fast 384-well plate	ABgene Epsom, United Kingdom

Thermo-Fast 96-well plate   ABgene Epsom, United Kingdom

Quanti Fluor™ Dye System   Promega, Mannheim

2.3   Equipment

Equipment	Manufacturer
Accu-jet®	Brand, Wertheim
2100 Bioanalyzer	Agilent Technologies, Santa Clara, USA
3130xl Genetic Analyser	Applied Biosystems, Darmstadt
Bacteria Incubator-Incudrive	Schütt, Göttingen
Biofuge 15 R	Heraeus, Hanau
Biofuge fresco	Heraeus, Hanau
Biofuge pico	Heraeus, Hanau
BioPhotometer	Eppendorf, Hamburg
BioRobot® EZ1	Qiagen, Hilden
Bunsen Burner Phoenix ‖	Schütt, Göttingen
cBot for Cluster generation (RNAseq)	Illumina, San Diego, CA, USA
Centrifuge 5810 R	Eppendorf, Hamburg
Centrifuge JA-20 Rotor	Beckman, München
CO_2-Incubator BB 16 Function Line	Heraeus, Hanau
CO_2-Incubator New Brunswick™ Galaxy 170S	Eppendorf, Hamburg
ComPhor L Mini Gel-chamber	Biozym, Hessisch Oldendorf
Concentrator 5301	Eppendorf; Hamburg
Cryo Storage Tank ARPEGE 140	German-cryo, Jüchen
Electroporator Gene Pulser II	BioRad, Hercules, USA

Eppendorf Research and Reference® Pipettes, 0,1 - 10 µl, 10 - 100 µl, 100 - 1000 µl	Eppendorf, Hamburg
Eppendorf Research® 8 channel Pipettes, 10 µl, 100 µl	Eppendorf, Hamburg
Fine weight machine	Sartorius, Göttingen
Flow cytometer BD LSRII, special order system	Becton Dickinson, Franklin Lakes, USA
Fluor-S™ MultiImager	BioRad, Hercules, USA
Gel-drying-system (DrygelSr)	Hoffer scientific instruments, San Francisco, USA
Gel electrophoresis power supply, (Standard Power Pack P 25)	Biometra, Göttingen
Gel tray, 40-0708-UVT (UV-transmissible)	PEQLAB Biotechnologie GmbH, Erlangen
Gene Pulser capacitance extender II	BioRad, Hercules, USA
Gene Pulser controller II	BioRad, Hercules, USA
GloMax® Fluorometer	Promega, Mannheim
HiSeq2000	Illumina, San Diego, CA, USA
Image Quant™ LAS 4000 Mini	GE Healthcare Bio-Sciences AB, Uppsala, Sweden
Laboklav for sterile materials	SHP Steriltechnik AG, Detzel Schloss/Satuelle
Labor centrifuge 400R	Heraeus, Hanau
Laminar Flow Clean Air type DFL/REC4 KL2A	Mahl, Trendelburg
Magnetic stirrer	Ika, Staufen
Mastercycler gradient (for 384-well plate), PCR-Gradient Cycler	Eppendorf, Hamburg
Membrane-Vacuum pump	Vacuubrand, Wertheim
Microscope TELAVAL 31	Zeiss, Jena

Microwave MWS 2820	Bauknecht, Schorndorf
MS 2 Mini shaker-Vortexer	IKA, Staufen
Multipette® plus	Eppendorf, Hamburg
pH meter, PB-11	Sartorius, Göttingen
Phosphor Imager	Raytest, Sprockhövel
PTC-200 Peltier Thermal Gradient Cycler (for 96-well plate)	MJ Research/BioRad, Hercules, USA
QiaCube	Qiagen, Hilden
Qualitron® Microcentrifuges	Fairport, USA
Scintillation instrument LS1801	Beckman, München
Semidry Electroblotter (PerfectBlue™)	PEQLAB Biotechnologie GmbH, Erlangen
Shaker for Bacteria K2 260 basic	IKA, Staufen
SpeedVac® Plus SC 110A Concentrator	Schütt, Göttingen
Standard Power Pack P25	Biometra, Göttingen
TaqMan 7900HT	Applied Biosystems, Darmstadt
Tecan Ultra Plate Reader (Fluorescence reader)	Tecan Deutschland GmbH, Crailsheim
Thermomixer 5436	Eppendorf, Hamburg
Transilluminator TI 2	Biometra, Göttingen
Vertical-Autoclave KSG 40/60	KSG, Olching
Vertical-Autoclave: FV for sterile materials	Tecnorama, Fernwald
Victor X4 Light Multilabel Reader	PerkinElmer, Wiesbaden, Germany
Warming cupboard FP	Binder, Tuttlingen

2.4   Software

Software	Manufacturer
3100 Data Collection Software	Applied Biosystems , Darmstadt
Advanced Image Data Analyzer (AIDA) V.4.15 025	Raytest Isotopenmeßgeräte GmbH, Sprockhövel
BASReader (FujiFilm BAS1800-II)	Raytest, Sprockhövel
BD-FACSDIVA™ SOFTWARE	Becton Dickinson, Franklin Lakes, USA
Clone Manager Suite v6.0	Sci-Ed Software, Cary NC, USA
CorelDRAW X3	Corel corporation, Ontario, Canada
CurveExpert Professional 2.0	www.curveexpert.net
Cyflogic 1.2.1	www.cyflogic.com
DNA Sequencing Analysis v5.2	Applied Biosystems, Darmstadt
DNASTAR® v11.2	DNASTAR, Madison WI, USA
EndNote X7	Thomson Reuters, Philadelphia PA, USA
Gene mapper v3.7 software®	Applied Biosystems , Darmstadt
HaploView® v4.2	Broad institute, Cambridge MA, USA
Image Quant™ LAS 4000 mini Control Software, v1.2	GE Healthcare Bio-Sciences AB, Uppsala, Sweden
MS Office	Microsoft, USA
Oligo® v6.58	Molecular Biology Insights, Cascade CO, USA
Quantity One® S v4.3.1	BioRad, München
SDS v2.1	Applied Biosystems, Darmstadt
SigmaPlot v12.0	Systat Software, Technology Drive, San Jose, CA
SPSS v12	SPSS Inc., Chicago, USA

Staden Package   Medical research council laboratory of
                                        molecular Biology, Cambridge, United
                                        Kingdom

XFluor4 Software   Tecan, Crailsheim

2.5   Databases

Databases	URL
1000 Genomes, Catalog of Human genetic Variation	http://www.1000genomes.org/
International HapMap Project	http://hapmap.ncbi.nlm.nih.gov/
National Center for Biotechnology Information	NCBI, Bethesda, USA http://www.ncbi.nlm.nih.gov/
TRANSFAC-Database	BIOBASE, Göttingen (http://www.biobase-international.com/product/explain)
UCSC Genome Browser	http://genome.ucsc.edu/

2.6   Enzymes

Restriction Enzymes	Manufacturer
*Bsa*I-HF®	New England Biolabs, Beverly, USA
*Dpn*I	New England Biolabs, Beverly, USA
*Exo*I	Fermentas, St. Leon-Roth
*Eco*RI	Fermentas, St. Leon-Roth
*Fas*t-AP	Life Technologies Corporation, Darmstadt
*Hin*dIII	Fermentas, St. Leon-Roth
*Not*I	New England Biolabs, Beverly, USA
*Pst*I	Fermentas, St. Leon-Roth
*Pvu*II	Fermentas, St. Leon-Roth
*Sac*I	Fermentas, St. Leon-Roth
*Sal*I	Fermentas, St. Leon-Roth
*Xho*I	Fermentas, St. Leon-Roth

2.7   Strains of bacteria

Strain of bacteria	Origin	Application for transfection	Manufacturer
TOP10 (One shot TOP10 Electro-comp. *E.coli*)	*Escherichia coli*	Electro-competent	Invitrogen, Karlsruhe

2.8   Plasmid vectors

Clone-No.	Resistance	Manufacturer
pcDNA3.1	Ampicillin	Invitrogen, Karlsruhe
pcDNA5:FRT	Ampicillin	Invitrogen, Karlsruhe
pcDNA5/FRT/TO GFP (Plasmid 19444)	Ampicillin	Addgene, Cambridge, United Kingdom
pOTB7:*RRM2* (IRAUp969F0415D)	Chloramphenicol	ImaGenes GmbH, Berlin (now Source Bioscience, Nottingham, United Kingdom)
pOTB7:*SP1* (IRAU97D03 Image ID: 5928633)	Chloramphenicol	SourceBioscience, Nottingham, United Kingdom

2.9   Commercial culture media

Medium	Manufacturer
Dulbecco´s Modified Eagle Medium (DMEM, 1x), 4,5 g/L D-Glucose, L-Glutamine	Gibco/Invitrogen, Karlsruhe
Roswell Park Memorial Institute (RPMI) 1640 Medium ™ + GlutaMax – I	Gibco/Invitrogen, Karlsruhe
OPTI-MEM® I Reduced Serum Medium	Gibco/Invitrogen, Karlsruhe

2.10 Cell lines

Cell line	Origin	Characteristics	Manufacturer
HEK-293	Human	Embryonic kidney cell line immortalized by *human adenovirus type 5* DNA	DMSZ, Braunschweig
AsPC1	Human	Pancreatic cancer cell line	ATCC, Wesel
CFPac	Human	Pancreatic cancer cell line	ATCC, Wesel
L3.6	Human	Pancreatic cancer cell line	ATCC, Wesel
MiaPacaII	Human	Pancreatic cancer cell line	ATCC, Wesel
PancI	Human	Pancreatic cancer cell line	ATCC, Wesel
PaTu8988t	Human	Pancreatic cancer cell line	ATCC, Wesel
Lymphoblastoid cell lines (LCLs HapMap and 1000 Genome Project)	Human	Peripheral B lymphocytes that are immortalized by Epstein-Barr (EB) virus	Coriell Cell Repositorie, Camden, New Jersey USA

3 Methods

3.1 Patient cohorts

3.1.1 Retrospective patient cohort

According to the inclusion criteria, i.e. histopathologically confirmed PDAC (without ampullary carcinoma) with adjuvant or palliative gemcitabine-containing chemotherapy, 381 Caucasian patients were recruited for a retrospective study performed in our department in collaboration with the relevant clinical centers, for detecting putative clinical marker in gemcitabine-treated pancreatic cancer. The entire cohort includes patients from three german medical center in Göttingen (n = 142), Hamburg (n = 159), and Heidelberg (n = 80) hospitalized between 2003 and 2010. For genotyping (see section 3.4) isolated DNA of peripheral blood leukocytes (see section 3.2.2) was used and the primary outcome was overall survival. Staging and grading was performed according to current standard classification procedure (published by AJCC (American Joint Commitee on Cancer) and UICC (Union internationale contre le cancer)).

3.1.2 Prospective patient cohort

To evaluate gene expression patterns during gemcitabine-based chemotherapy, a pilot cohort comprising 32 patients suffering from PDAC was followed prospectively. At three time points RNA expression was assessed: Prior to the first gemcitabine application, four weeks and ten weeks thereafter. Therefore, 2.5 ml of peripheral blood was immediately filled in PAX tubes containing a RNA-stabilizing reagent, which then was stored at -20 °C. RNA was isolated using the PAXgene Blood miRNA Kit (Qiagen, Hilden). For reverse transcripton 1 μg of total RNA per sample was used (see chapter 3.6.3 for reverse transcription).

3.2 Standard DNA workflow

3.2.1 DNA isolation from eukaryotic cells

Genomic DNA from eukaryotic cells was isolated with the *DNeasy Blood & Tissue Kit* (Qiagen, Hilden), using the *QiaCube* robot (Qiagen, Hilden) according to the maufacturer's recommendation. Therefor, approximately 5×10^6 cells were harvested

and dissolved in 100 µl of PBS buffer before. The quantification of isolated DNA was performed photometrically (see chapter 3.2.3).

3.2.2 DNA isolation from peripheral leukocytes

Genomic DNA from peripheral leukocytes was isolated with the *EZ1 DNA Blood Kit* (Qiagen, Hilden). For this the *BioRobot EZ1* (Qiagen, Hilden) was used and all steps were performed according to the maufacturer's recommendation with an elution volume of 200 µl.

3.2.3 Quantification of DNA

The amount of DNA was determined with a *BioPhotometer* (Eppendorf, Hamburg), measuring the absorbance at 260 nm. An extinction of 1 at 260 nm (E_{260}) equates to 50 µg DNA per µl. The absorbance ratio 260/280 nm characterizes the sample purity. A value near 2 is defined as "high purity" and allows sample usage for further experiments. For DNA quantification 3 µl of the DNA sample was pipetted on a nanodrop cuvette (Implen, München). This quantification method is based on the following Beer-Lambert law (Equation 1):

Equation 1: Beer-Lambert law

$$A = \varepsilon * c * l$$

A = Absorbance
*ε = Molar attenuation coefficient [L * mol^{-1} * cm^{-1}]*
*c = Solute concentration [mol * L^{-1}]*
l = Path length of the light through the material [cm]

3.2.4 Polymerase chain reaction (PCR)

The polymerase chain reaction is an *in vitro* method to amplify DNA. For cloning experiments the KOD Hot Start polymerase was used, which has a proofreading function to make the reaction more efficient. First, double-stranded DNA is denatured to single strands at 95 °C. Next, oligonucleotide primer anneal to the single DNA strand in a selective way. The annealing step takes place at temperatures between 50 and 70 °C. Thereafter, the temperature rises for the elongation step (65 - 75 °C), where the DNA polymerase synthesizes a copied DNA strand which is complementary to the template DNA, by adding dNTPs in 5' to 3' direction. Using the right conditions, the amount of

DNA is duplicated per cycle what leads to an exponential increase of the DNA region of interest. These steps were repeated 35 times to achieve an adequate amount of DNA. A final elongation step is advised, depending on the length of the DNA fragment. The PCR reactions (see Table 1) were performed in gradient thermal cyclers under conditions listed in Table 2.

Table 1: Standard KOD HotStart PCR reaction

Reagent	Volume for one sample [µl]
10x buffer	2.2
dNTPs (2 mM)	2.2
MgSO$_4$ (25 mM)	0.9
Q-Solution (optional)	4.4
Primer forward (10 µM)	0.5
Primer reverse (10 µM)	0.5
DNA (300 µg/ml)	2
KOD HotStart polymerase (1.0 U/µl)	0.5
ddH2O	8.8
In total	**20**

Table 2: Standard KOD PCR conditions

Phase	Duration	Temperature	
Initial Denaturation	3 min	95 °C	
Denaturation	30 sec	95 °C	
Annealing	30 sec	50 - 70 °C	**35 x**
Elongation	1 min	72 °C	
Terminal Elongation	10 min	72 °C	
Cooling down	for ever	8 °C	

3.2.5 Gradient PCR

To determine the optimal annealing temperature for new primers, a gradient PCR was performed. Therefor five identical PCR reactions were undertaken simultaneously to test different annealing conditions (60 - 72 °C). For each temperature two reaction mixtures were prepared, one with and one without Q-Solution (included in the *Taq*

polymerase or *Multiplex PCR Kit* from Qiagen, Hilden). Q-Solution is used to enhance the DNA amplification for templates comprising a high GC content. To identify the optimal annealing temperature subsequent to the gradient PCR, samples were run on a 0.8 to 3 % agarose gel, where the amount of the PCR product and the fragment size could be assessed.

3.2.6 Site-directed mutagenesis

Site-directed mutagenesis is a method which is used to introduce mutations (one to four bases) into a DNA sequence by mutagenesis primers. In this work the 5' single nucleotide polymorphism *RRM2* rs1130609 in the full length cDNA clone (for construct generation see section 3.5.3) of *RRM2* (pcDNA5:*RRM2*) was mutated at the rs1130609 SNP site from G > T with primers listed in Table 3 to obtain the variant allele in addition to the wild type allele.

Table 3: Oligonucleotide primers for the Site-directed mutagenesis (*RRM2* rs1130609)

Name of primer	Sequence (5' → 3')
Mut_rs1130609for	GTTTAAACTTAAGCTTCGCC**T**CCACTATGCTCTCC
Mut_rs1130609rev	GGAGAGCATAGTGG**A**GGCGAAGCTTAAGTTTAAAC

The mutated base is **bolded** and underlined

For the performance of the mutagenesis PCR it is important that used plasmids were isolated from bacteria and show bacteria specific methylation patterns. The new products synthesized by this PCR did not have these methylations and thus could not be degraded by *Dpn*1 endonuclease (methylation dependend restriction enzyme), in contrast to the not mutated original constructs. For site-directed mutagenesis the *KOD HotStart polymerase* (Novagen Merck, Darmstadt) was used. To identify the optimal annealing temperature for the mutagenesis primers a gradient PCR (see chapter 3.2.5) was conducted, previous to the described mutagenesis PCR (see Table 4 for reaction mixture and Table 5 for PCR conditions).

Following to the DNA amplification, 2 µl of the *Dpn*1 enzyme was added to the PCR product for 1 hour at 37 °C to get the newly mutated constructs. Then, the PCR product was dialyzed for 30 minutes, transformed into *E. coli* TOP10 strain by electroporation and plated on agar plates containing ampicillin as selction marker. Based on the grown

clones on agar plates, plasmid DNA was isolated by mini-preparation (see 3.7.5.1). To verify successful mutagenesis, the open reading frame of *RRM2* was sequenced with sequencing primers listed in Table 6.

Table 4: PCR-reaction mixture for the site-directed mutagenesis

Reagent	Volume [µl]
10x buffer	5
dNTP (2 mM each)	5
MgSO$_4$ (25 mM)	2
Q-Solution (optional)	10
Primer forward (10 nM)	1.3
Primer reverse (10 nM)	1.3
KOD HotStart polymerase	1
Plasmid DNA (50 ng)	1
ddH$_2$O	**Add to 50**

Table 5: PCR consitions used for site-directed mutagenesis

Phase	Duration	Temperature	
Initial Denaturation	3 min	95 °C	
Denaturation	30 sec	95 °C	
Annealing	30 sec	60 °C	**19 x**
Elongation	3 min 30 sec	72 °C	
Cooling down	for ever	8 °C	

Table 6: Sequencing primers for the construct pcDNA5-*RRM2*-eGFP

Name of primer	Sequence (5' → 3')
RRM2-Seq-F1	CACGGAGCCGAAAACTAAAGC
RRM2-Seq-F2	TCTGCCTTCTTATACATCTGCCA
RRM2-Seq-F3	ACATTGAGTTTGTGGCAGACAGAC
RRM2-Seq-F4	GCCTACTCTCTTCTCAAAGAAGTTAGTC
RRM2-Seq-F5_eGFP	AAGGACGACGGCAACTACAAG
RRM2-Seq-F6_eGFP	GCGGATCTTGAAGTTCACCTTG
RRM2-Seq-F7_eGFP	AACAGATGGCTGGCAACTAGAAG

3.2.7 Agarose gel electrophoresis

Agarose gel electrophoresis is used to determine the size and presence of DNA fragments. Nucleic acids are negatively charged and migrate through an agarose matrix by an electric field towards the anode. Because of lower molecular weight, shorter fragments move faster in comparison to longer ones. Dependent on the expected DNA fragment size agarose concentrations between 0.8 and 3 % were used. For the gel preparation the aquired amount of agarose (Agarose Ultrapure, Invitrogen, Karlsruhe) was dissolved in boiling TBE buffer. The solution was cooled down to ~ 60 °C, then 0.5 μg/ml of ethidium bromide (EtBr) was added and stirred with a magnetic mixer. Then, the liquid gel was transferred into a gel tray and gel combs were put into the gel tray to form gel pockets. After 30 minutes the solid gel was placed in a Gel System for electrophoresis, covered with TBE buffer (supplemented with 0.5 μg/ml of EtBr, see Table 8). Before loading the gel, the DNA samples were mixed with 5x loading dye (see Table 7) in a sample-dye ratio of 5:1. To identify the DNA fragment sizes, DNA ladders with 100 bp or 1 kb (ABgene, Fermentas, St. Leon-Rot) were used. The electrophoresis was conducted with 140 V for approximately 30 - 40 minutes in a *PerfectBlue Gel System* (PEQLAB, Erlangen). To visualize the DNA bands the *Fluor-S*^{TM} *MultiImager* (BioRad, Hercules, USA) and its corresponding *QuantityOne® S version 4.3.1* (BioRad) software were employed.

Table 7: 5x Loading Dye

Reagent	Concentration
Glycerol	30 % (v/v)
EDTA	50 mM
Bromphenol blue	0.25 % (v/v)
Xylene cyanol	0.25 % (v/v)

Table 8: TBE buffer

Reagent (pH = 8.3, RT)	Concentration [mM]
Tris	100
Boric acid	100
EDTA	3

3.2.8 DNA purification from agarose gel

To extract DNA from an agarose gel after electrophoresis, the desired band was cut under UV light, using the *transilluminator TI2* (Biometra, Göttingen). The cut slices should not exceed an amount of 400 mg of a 2 % agarose gel. The DNA purification was performed with the *QiaCube robot* (Qiagen, Hilden), using the *QiaQuick Gel Extraction Kit* (Qiagen, Hilden) and following the manufacturer's instructions.

3.2.9 Restriction digestion

Restriction digestion is used to split double stranded DNA at a specific nucleotide sequence of 4 to 8 bases, which are often palindromic. For this, restriction enzymes, which are endonucleases, are used. The separation of the resultant fragments was performed by agarose gel electrophoresis (see section 3.2.7). This method is used during cloning procedures, either for an analytical or preparative purpose.

3.2.9.1 Analytical digestion

Analytical digestion was used to verify plasmid DNA isolated by mini-preparation (see chapter 3.7.5.1). Independent digestion mixtures with at least two digestion enzymes were prepared. For each enzyme a specific fragmentation pattern should be detected. The number of fragments depends on the number of restriction sites for the enzyme. The analytical digestion mixtures (Table 9) were incubated for 1 hour at 37 °C before loading them on an agarose gel. For fast digestion enzymes the icubation time was reduced to 15 minutes.

Table 9: Reaction mixture for analytical digestion

Reagent	Volume [µl]
10x Restriction buffer	1
BSA (optional)	0.1
DNA ($\sim$ 1 µg)	1
Enzyme	1
ddH$_2$O	**Add to 10**

3.2.9.2 Preparative digestion

Preparative digestion was used to generate restriction fragments for cloning, allowing ligation of the digested vector and the digested insert fragment in the next step because of matching DNA ends. The reaction mixture (Table 10) was incubated for two hours or overnight. After this, 1 µl of the enzyme was added for one more hour before loading the digestion mixture on an agarose gel. A double digestion is also possible by proceeding in the same way, using the tango universal buffer or a buffer which is compatible with both enzymes. If different buffers are needed, DNA was digested with one enzyme first, followed by agarose gel electrophoresis (see chapter 3.2.7) and agarose gel purification (see chapter 3.2.8). Afterwards, digestion was performed with the second restriction enzyme.

Table 10: Reaction mixture for preparative digestion

Reagent	Volume [µl]
10x Restriction buffer	5
BSA (optional)	0.5
DNA	max. 10 µg
Enzyme *(dependent on star activity)*	5
ddH$_2$O	**Add to 50**

3.2.10 Ligation

The ligation process is used to integrate DNA fragments into a plasmid vector. For that purpose, DNA ends (cut by restriction enzymes) which are complementary to each other and which can be ligated using a DNA ligating enzyme (*Ligate-IT^{TM} rapid Ligation Kit*, USB Staufen, Germany) are needed. Prior to the ligation performance the DNA was concentrated with a vacuum centrifuge (SpeedVac Plus SC110A) for 5 - 10 minutes. The concentrated DNA, which was attached to the wall of the reaction tube, was dissolved from there by wishing the wall with a drop of the remaining sample. The ligation mixture was prepared as follows (Table 11) with an insert *versus* vector ratio of 13:2 (v/v).

Table 11: Ligation reaction mixture

Reagent	Volume [µl]
5x Ligase buffer	4
Plasmid vector	2
Insert (DNA fragment)	13
Ligase	1
In total	**20**

This mixture was incubated for 10 minutes at room temperature, followed by 10 minutes of incubation on ice. To verify that the used vector does not ligate with itself an extra ligation mixture was prepared where the insert was replaced by ddH$_2$O as negative control.

3.2.11 Dialysis

Prior to the transformation of ligated DNA into bacteria cells (see section 3.7.2) a dialysis step is required to remove salts. Therefor, the whole ligation mixture was pipetted on top of a semipermeable membrane (Dialysis filter, *VSWP01300*, Millipore, Schwalbach), which was placed with the shiny site up on a petri dish filled with ddH$_2$O. After 30 minutes the desalted DNA was transferred into a new reaction tube.

3.3 DNA Sequencing analysis

The DNA sequencing process was used to ascertain the nucleotides within DNA strands. Primarily, this concept was developed by Sanger and Coulson in 1975 (SANGER AND COULSON 1975). The chain-termination principle uses dideoxy nucleotide triphosphates (ddNTPs) additional to the desoxy-nucleotide triphosphates (dNTPs). The ddNTPs are fluorescently labeled with different dyes. During the chain extension in the sequencing PCR the DNA polymerase either adds a corresponding dNTP or ddNTP. In case of incorporated ddNTPs this leads to the termination of the DNA chain due to the absence of the hydroxyl group (OH) at the 3' carbon. Thus, the Sanger dideoxy sequencing results in the extension of products with a various length, terminated with a ddNTP at the end. Afterwards, using the capillary-gel electrophoresis, the newly synthesized extension products were separated by size at a resolution of one base. The number of DNA fragments which can be sequenced in one run is about 500 base pairs.

In detail, the sequencing PCR was performed in a 384 well plate (FrameStar®, 4titude, Wotton, UK), using the *BigDye® terminator v1.1 Sequencing Kit* (Applied Biosystems, Darmstadt). The sequencing PCR was conducted as follows (Table 12 and Table 13):

Table 12: Reaction mix for sequencing PCR

Reagent	Volume [µl] per sample
DMSO	0.25
Primer (10 µM)	0.5
BigDye®	1
ddH$_2$O	2.25
DNA from mini preparation ($\sim$ 300 µg/ml)	1
In total	**5**

Table 13: Sequencing PCR conditions

Phase	Duration	Temperature	
Initial Denaturation	2 min	94 °C	
Denaturation	15 sec	96 °C	
Annealing	15 sec	56.5 °C	**25 x**
Elongation	4 min	60 °C	
Terminal Elongation	7 min	72 °C	
Cooling down	for ever	8 °C	

Before sequencing, the PCR product was purified to eliminate unincorporated ddNTPs. For this, 35 mg of *Sephadex G50 superfine* (Amersham Bioscience, Freiburg) was distributed per well of a 96-well filter plate (MAHV-N45, Millipore). Each well of the sephadex plate was filled up with 300 µl of ddH$_2$O and was incubated for 3 hours at room temperature for swelling. Then, the excess water was removed by centrifugation at 700 rpm for 5 minutes at RT (Centrifuge 5810 R, Eppendorf), followed by addition of 150 µl of ddH$_2$O for another incubation time of half an hour. Again, the excess water was removed by centrifugation, using the same conditions. The prepared sephadex plate was placed on top of a sequencing plate. The sequencing-PCR-mixtures were filled up with ddH$_2$O to a total volume of 40 µl and were pipetted into the wells of the sephadex plate, which was then centrifuged at 700 rpm for 5 minutes at RT. Finally, the purified samples (collected in the sequencing plate) were sequenced with the *3130xl Genetic Analyser*

(Applied Biosystems, Darmstadt). The data was analyzed with the *SequencingAnalysis version 5.2 software®* (Applied Biosystems, Darmstadt) first. For the detailed sequence analysis the software *Staden Package version 4.0* (Cambridge, UK) or *DNASTAR® version 11.2* (Madison WI, USA) and *CloneManager* (SECentral) were used.

3.4   Genotyping by Single Base Primer Extension Method (SNaPshot™)

For the determination of single nucleotide polymorphisms (SNPs) in genomic DNA the Single Base Primer Extension method SNaPshot™ was used, based on multiplex PCR amplification (*Multiplex PCR Kit*, Qiagen, Hilden) of fragments with the SNP of interest. Primers, sized between 18 and 55 bp were designed. These bind in 5' → 3' direction to the multiplex PCR amplification with the 3'-terminus adjacent to the targeted SNP.

For the single nucleotide extension fluorescently labeled dideoxyribonucleotide triphosphates (ddNTPs) are used in a SNaPshot PCR reaction (SNaPshot reaction mixture, ABI PRISM® SNaPshot™ Multiplex Kit, Applied Biosystems). Due to the missing (-OH) group of ddNTPs at the 3'-terminus further DNA amplification is not possible. This leads to the single nucleotide base extension generated by the fluorescently tagged ddNTPs detected by a special laser detector after fragment separation via capillary electrophoresis. A DNA size standard (*GeneScan™ 120LIZ™* Size standard, Applied Biosystems) was used to determine the fragment size. The resulting electropherogram shows differently coloured peaks for each of the four ddNTPs, representing the genotype of the analyzed SNP: Adenine - green, (FS (fluorescent stain) = dR6G), Cytosine - black (FS = dTAMRA™), Guanine - blue (FS = dR110) and Thymine - red (FS = dROX™).

First, DNA was amplified by Multiplex PCR (*Multiplex PCR Kit,* see Table 14, Table 15 and Table 16).

Table 14: Reaction mixture for Multiplex PCR

Reagent	Volume [μl] per sample
2x Qiagen Multiplex PCR Master Mix	6
(Comprising Taq Polymerase, dNTP mix and MgCl$_2$)	
10x Primer Mix (see Table 15)	1.2
Q-Solution	1.2
RNAse-free water	1.6
Genomic DNA	2
In total	**12**

Table 15: 10x primer mix for Multiplex-PCR

Gene	Forward Primer sequence (5′ → 3′)	Reverse Primer sequence (5′ → 3′)
IL17F	GCACTGGGTAAGGAGTGGCATTTCTAC	TTGGAGAAGGTGCTGGTGACTGTTG
BTRC	GGGGCATTTGGGTGTGTGTCAG	GCCCTGCACTAAGGGTCAAACAGGTAC
RRM2	CGGGAGATTTAAAGGCTGCTGGAG	GACACGGAGGGAGAGCATAGTGG
PRB2	CAGCTTCACAGATGGTGGCTGATGAG	CCTGCTCATGATGCCCAGAATCAAG
DCP1B	AAGGAAAGCAAATTAATTAGGCTTGTGCTA	GAATGGAGAGTGGGGAGTTATCTTCTAATG
WWOX	CTAGGTGGCTTCAGTCAGCAGAACTG	TGCCTTCTGTTCTCATGCAACTTCAC

Table 16: Multiplex PCR conditions

Phase	Duration	Temperature	
Initial Denaturation	15 min	95 °C	
Denaturation	30 sec	94 °C	
Annealing	1:30 min	64.8 °C	**39 x**
Elongation	1:30 min	72 °C	
Terminal elongation	10 min	72 °C	
Cooling down	for ever	8 °C	

Afterwards, the PCR product was purified with *Fas*t-AP (Thermosensitive alkaline phosphatase, Life Technologies, Darmstadt, Table 17) and Exonuclease I (*Exo*I, Fermentas, St. Leon-Roth) to eliminate unincorporated PCR primers and dNTPs. The purification procedure was performed for 3 hours at 37 °C, then the enzymatic reaction was inactivated for 15 minutes at 80 °C.

Table 17: Reaction mixture for the first purification step

Reagent	Volume [µl] per sample
*Fas*t-AP buffer (10x)	0.95
*Fas*t-AP (1U/µl)	1.695
*Exo*I (20U/µl)	0.35
PCR product	3
In total	**6**

The SNaPshot PCR (Table 18) was run in a 384-well plate (FrameStar®, 4titude, Wotton, UK), under conditions listed in Table 19. The PCR mixture was prepared on ice. Used SNaPshot primers are displayed in Table 20.

Table 18: SNaPshot PCR mixture

Reagent	Volume [µl] per sample
SNaPshot™-Master Mix	0.35
Primer Mix (2 - 12 µM)	0.5
ddH$_2$O	2.15
Purified PCR product	2
In total	**5**

Table 19: PCR conditions for SNaPshot PCR

Phase	Duration	Temperature	
Initial Denaturation	2 min	94 °C	
Denaturation	10 sec	96 °C	
Annealing	5 sec	50 °C	**26 x**
Elongation	30 sec	60 °C	
Cooling down	for ever	8 °C	

Table 20: SNaPshot Primers

Gene	Sequence (5' → 3')
IL17F (rs763780)	GCACCTCTTACTGCACA
BTRC (rs10883617)	CTTTGGCCTGAAAAGGTACA
RRM2 (rs1130609)	GACACGGAGGGAGAGCATAGTGG
PRB2 (rs2900174)	$(CTGA)_2$CTCCTTACAAGACTCACAAGTGTTCT
DCP1B (rs11062040)	$(TGAC)_4$AATTAATTAGGCTTGTGCTA
WWOX (rs11644322)	$(GACT)_6$GATGTGATTACAGTGAATTAGGGTGG

A second purification step was conducted (Table 21) for 30 minutes at 37 °C to remove unincorporated fluorescently labeled ddNTPs which would affect the data analysis, followed by an incubation time of 15 minutes at 80 °C for enzyme deactivation.

Table 21: Reaction mixture for the second purification step

Reagent	Volume [µl] per sample
*Fas*t-AP (1U/µl)	0.5
*Fas*t-AP buffer (10x)	0.5
SNaPshot PCR product	5
In total	**6**

Next, 1 µl of the purified product was added to a 96-well sequencing plate, containing 10 µl of the sequencing mixture (Table 22), which was then incubated for 5 minutes at 95 °C and was placed on ice directly afterwards. Finally, the samples were analyzed with the *3130xl Genetic Analyser* (Applied Biosystems, Darmstadt) and data analysis was performed by using the *Gene mapper v3.7* software® (Applied Biosystems, Darmstadt).

Table 22: Sequencing mixture for SNaPshot™

Reagent	Volume [µl] per sample
Formamid	10
(*Hi-Di™ Formamid*, Applied Biosystems)	
GeneScan™ 120LIZ™ (Size standard)	0.05
Purified sample	1
In total	**11.05**

3.5   Generation of DNA constructs

3.5.1 Cloning of *WWOX* cDNA

For overexpression of *WWOX* in pancreatic cancer cell lines a genetic construct was generated, based on the pcDNA3 vector (Invitrogen, Karlsruhe). First, *WWOX* cDNA was engineered from total RNA of the LCL sample with the number 238. Using the *GoScript™ Reverse Transcription system* (Promega, Mannheim) with $(T)_{20}VN$ (Eurofins MWG, Ebersberg) as anchored primer, total mRNA was reversely transcribed. Afterwards, a specific PCR-based amplification of *WWOX* cDNA (using KOD-Polymerase and Q-Solution, see section 3.2.4, annealing temperature 63.4 °C), containing the exons 1 – 9, was carried out with the following primer pair (Table 23):

Table 23: Primers for *WWOX* cDNA amplification

Name of primer	Sequence (5' → 3')
***WWOX*comp_*Eco*RI-forward**	CTGACT*<u>GAATTC</u>*CCAGGTGCCTCCACAGTCA
***WWOX*comp_*Xho*I-reverse**	CTGACT*<u>CTCGAG</u>*CATCCGCTCTGAGCTCCACTTAG

Restriction sites are <u>underlined</u> and *italic*.

A restriction site for *Eco*RI was added to the forward, and for *Xho*I to the reverse primer. After *WWOX* amplification, both, the pcDNA3 plasmid DNA and the generated *WWOX* cDNA were cut with the named restriction enzymes in double digestion fashion (see chapter 3.2.9.2), followed by gel electrophoresis (see chapter 3.2.7) and agarose gel purification (see chapter 3.2.8). Next, the *WWOX* fragment was inserted between the restriction sites of *Eco*RI and *Xho*I of the pcDNA3 vector (see 3.2.10 and 3.2.11 and Figure 6), which then was transformed into *E. coli* (see chapter 3.2.11 and 3.7.2).
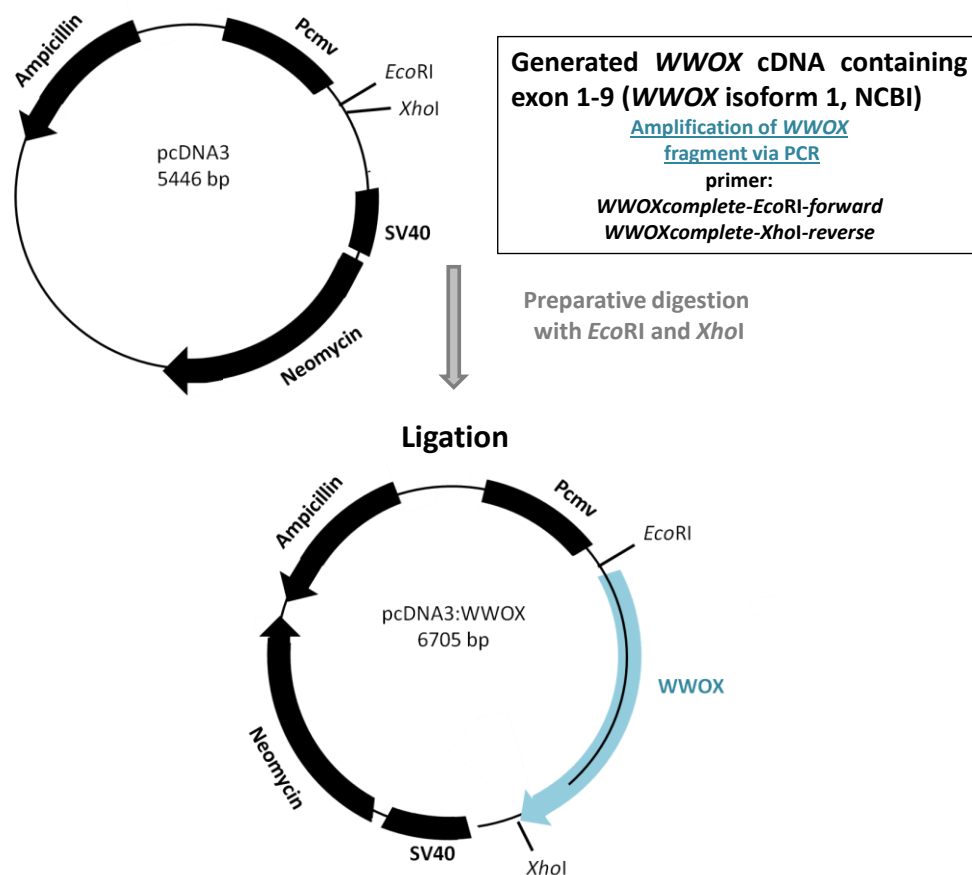
Figure 6: Cloning procedure: Generation of a pcDNA3:*WWOX* construct

Finally, the mini- and midi-preparation (see sections 3.7.5.1 and 3.7.5.2) of single clone cultures were performed to obtain purified plasmid DNA. To verify cloning of the whole *WWOX* coding region into the pcDNA3 vector Sanger-based direct sequencing (see 3.3) was conducted with the sequencing primers listed below (Table 24).

Table 24: Sequencing primers to verify the pcDNA3-*WWOX* construct

Name of primer	Sequence (5' → 3')
***WWOX*-Seq-F1**	CTCTGGCTAACTAGAGAACCCACTGCTTAC
***WWOX*-Seq-F2**	CCAACCACCCGGCAAAGATA
***WWOX*-Seq-F3**	AATGCTGCACGCTACGGAG
***WWOX*-Seq-F4**	ATGTACTCCAACATTCATCGCAG
***WWOX*-Seq-F5**	GTCTCTTCGCTCTGAGCTTCT
***WWOX*-Seq-F6**	CGAAACCGCCAAGTCT
***WWOX*-Seq-F7**	AGAGTCCCATCGATTTACAG
***WWOX*-Seq-F8**	ATGGCTGGCAACTAGAAG

This construct served as reference for absolute quantification of the expression ratios between *WWOX* mRNA of exon 4-6 (core region) and of exon 8-9 (last exon), obtained from LCLs.

3.5.2 Cloning of *SP1* into the pcDNA3 vector

To analyse the effect of the transcription factor SP1 (specifity protein 1) on pancreatic cancer cells, a *SP1* construct was generated. Therefore, a pOTB7:*SP1* construct was purchased from SourceBioscience (IRAU97D03, Nottingham, UK). The aim was to introduce *SP1* into the pcDNA3 vector. For that reason, the pOTB7:*SP1* and pcDNA3 plasmids were digested with *Eco*RI and *Xho*I in a double digestion fashion (3.2.9.2). Afterwards gel electrophoresis (see section 3.2.7) and gel purification (3.2.8) were performed, followed by the insertion of the *SP1* fragment into the pcDNA3 vector (see sections 3.2.10 and 3.2.11, Figure 7).
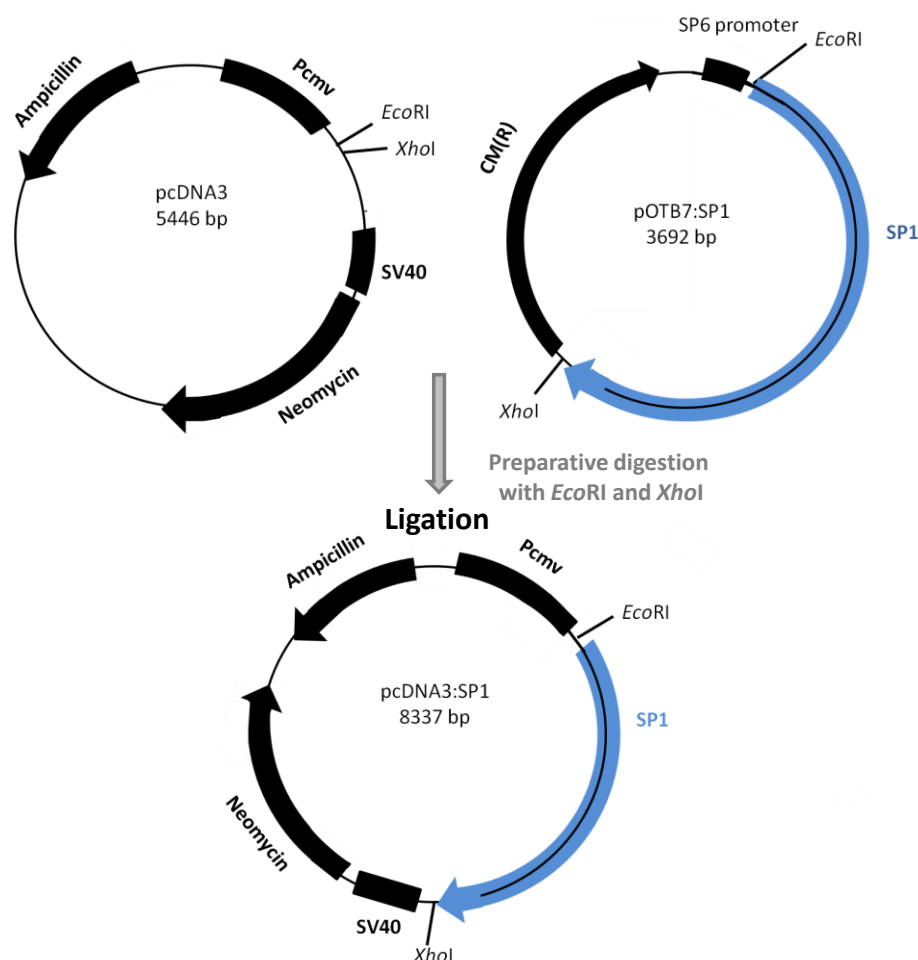
Figure 7: Cloning procedure: Generation of a pcDNA3:*SP1* construct

Finally, the newly generated construct was transformed into *E. coli* (see chapter 3.7.2) and mini- and midi-preparation were performed using single clone cultures (3.7.5.1, 3.7.5.2). Complete and error-free cloning of the entire *SP1* coding region was controlled by DNA sequencing analysis (see 3.3) with the next listed primers (Table 25).

Table 25: Sequencing primers for the construct pcDNA3:*SP1*

Name of primer	Sequence (5' → 3')
SP1-Seq-F1	CTCTGGCTAACTAGAGAACCCACTGCTTAC
SP1-Seq-F2	GTTTGGCATAGCAGCAATGATGTTG
SP1-Seq-F3	TTGATGGGCAACAGCTGCAGT
SP1-Seq-F4	CATTGGGGCTAAGGTGATTGTTTG
SP1-Seq-F5	TGGACAGGTCAGTTGGCAGACTCTAC
SP1-Seq-F6	GGTGAGAGGTCTTGCCATACACTTTC
SP1-Seq-F7	CCTGCCCCTACTGTAAAGACAGTGAAG
SP1-Seq-F8	GGCCTCCATGGCTACCATATTG
SP1-Seq-F9	GGACAGTGGGGCAGGTTCAG
SP1-Seq-F10	GAATCCATCATGGAAGAGCTGAGAA
SP1-Seq-F11	CCATGAGCGACCAAGATCA
SP1-Seq-F12	GGGTGTGAGAGTGGTGTTG
SP1-Seq-F13	CTGGTGGTGATGGAATACATGA
SP1-Seq-F14	GCACCCTGTGAAAGTTGTGT

3.5.3 Cloning of eGFP-tagged *RRM2* into the pcDNA5 vector

For cloning of the *RRM2* (*Ribonucleotide reductase subunit M2*) coding region into the pcDNA5 vector, the full length cDNA clone pOTB7:*RRM2* (Clone3528619, IRAUp969F0415D) was purchased from SourceBioscience (Nottingham, UK). The *RRM2* fragment was amplified out of the primary pOTB7:*RRM2* vector by using following primers, comprising restriction sites for *Hin*dIII and *Not*I (Table 26), under conditions described in section 3.2.4 (with Q-Solution, annealing temperature 63.4 °C).

Table 26: Primers to amplify RRM2 out of the pOTB7:*RRM2* construct

Name of primer	Sequence (5' → 3')
***RRM2-Hin*dIII-forward**	CTGACT*AAGCTT*CGCCGCCACTATGCTCTC
***RRM2-Not*I-reverse**	CTGACT*GCGGCCGC*GAAGTCAGCATCCAAGGTAAAAGAATTCTC

Restriction sites are underlined and *italic*.

After gel electrophoresis (see 3.2.7) and the agarose gel clean up process (3.2.8), preparative digestion (see 3.2.9.2) of the resulting *RRM2* fragment and of the pcDNA5 vector were conducted, first with *Hin*dIII, thereafter with *Not*I. Again, gel electrophoresis and the agarose gel purification were carried out, before integrating the *RRM2* DNA fragment between the restriction sites of the mentioned enymes of the pcDNA5 vector (see 3.2.10, 3.2.11, Figure 8).
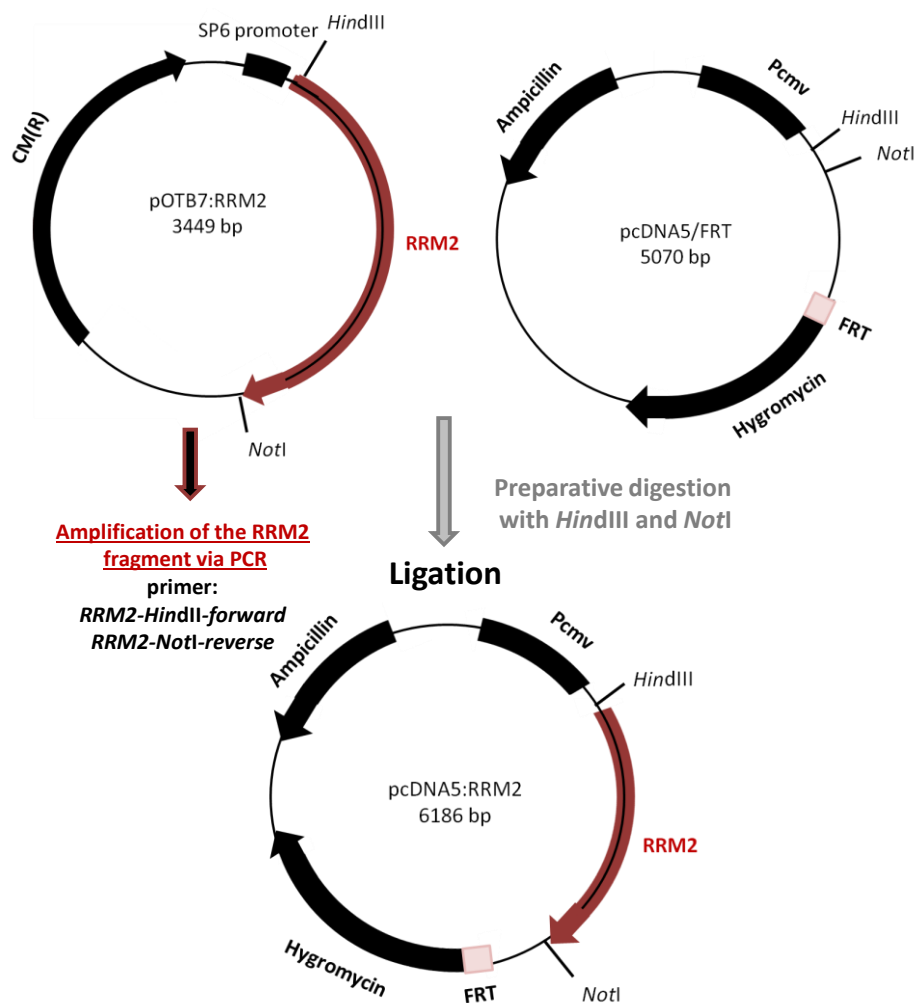
Figure 8: Cloning procedure: Generation of a pcDNA5:*RRM2* construct

For *RRM2* detection on translational level (see 3.8.4) *RRM2* was tagged with an eGFP (enhanced green fluorescent protein, see Figure 9). Therefore, a pcDNA5/FRT/TO GFP construct was bought from Addgene (Plasmid 19444, Cambridge, UK). Similar to the *RRM2* amplification procedure before, specific primers with artificial inserted restriction sites (Table 27) were ordered to amplify the eGFP out of the purchased construct (PCR as described in 3.2.4, with Q-Solution, annealing temperature 63.4 °C).

Table 27: Primers to amplify eGFP out of the pcDNA5/FRT/TO GFP construct

Name of primer	Sequence (5' → 3')
eGFP-*Not*I-forward	CTGACT*GCGGCCGC*TATGGTGAGCAAGGGCGAGGAGC
eGFP-*Xho*I-reverse	CTGACT*CTCGAG*TTACTTGTACAGCTCGTCCATGCCGAGAGT

Restriction sites are <u>underlined</u> and *italic*.

After gel electrophoresis and agarose gel purification, preparative digestion of the eGFP fragment and of the pcDNA5-*RRM2* construct was conducted, first with *Not*I then with *Xho*I. Then, eGFP was ligated into the pcDNA5-*RRM2* construct (see Figure 9), which then was transformed into *E. coli* TOP10. Single clones were cultivated (see 3.7.4) and the mini-preparation (see 3.7.5.1) was undertaken. Finally, a mutation at the position of a 5' single nucleotide polymorphism (SNP) rs1130609 of *RRM2* (located in the Kozak sequence) from G > T was inserted by mutagenesis PCR with specific mutagenesis primers (see section 3.2.6, annealing temperature 65.2 °C with Q-Solution) to have an additional construct carrying the variant allele for further analysis.
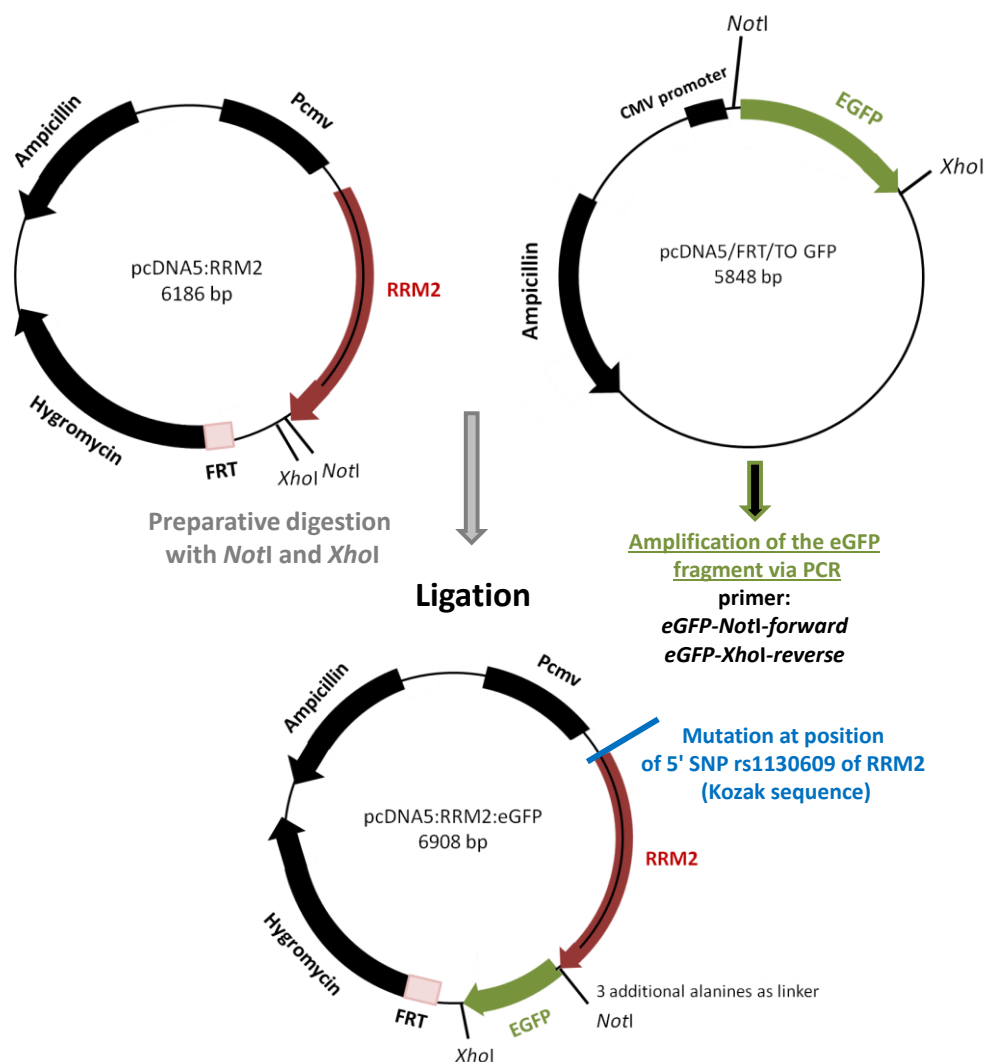
Figure 9: Cloning procedure: Generation of a pcDNA5:*RRM2*:eGFP construct

3.6 RNA workflow

When working with RNA, the existence of a ribonuclease-free environment should be ensured. For that reason, RNA work was performed under a fume hood, using materials, which were protected with an anti-RNase spray (*RNaseZap*, Sigma-Aldrich, Deisenhofen). Moreover, RNase-free filter tips were used.

3.6.1 RNA isolation

For RNA isolation 1×10^6 cells were harvested and transferred into a 50 ml falcon tube. The cell suspension was centrifuged at 500 g for 5 minutes at RT. The supernatant was removed and a washing step with 3 - 4 ml of PBS buffer was performed. Afterwards, the centrifugation step was repeated and the supernatant was discarded completely. Then,

the pellet was dissolved in 350 µl of *RLT Plus buffer* (Qiagen, Hilden). The solution was pipetted into a 2 ml reaction tube for the further RNA isolation process in the *QiaCube* robot (Qiagen, Hilden), using the *RNeasy Plus Mini Kit* (protocol with miRNA, Qiagen, Hilden) according to the manufacturer's instructions. After this procedure, the samples were put on ice directly and the RNA concentration was measured photometrically (see 3.6.2). Finally, the samples were stored at -80 °C.

3.6.2 Quantification of RNA

RNA quantification was performed photometrically, analog to DNA quantification (see section 3.2.3). For RNA an extinction of 1 at 260 nm (E_{260}) equates to 40 µg RNA per µl.

3.6.3 Reverse Transcription

For the analysis of gene expression (performed by quantitative RT-PCR, see section 3.6.4) isolated RNA had to be converted into cDNA (copy or complementary DNA) by reverse transcription (RT), performed by the *Super Script II* reverse transcriptase (Invitrogen, Karlsruhe). This polymerase uses dN6 random hexamer oligonucleotide primers (six randomly combined nucleotides, Roche, Mannheim) to generate cDNA. In comparison to the usual eukaryotic DNA the newly synthesized cDNA had no introns, due to the fact that the mRNA template is already spliced. For primer annealing 1 µg of RNA was incubated with 2 µl of the dN6-primers diluted in ddH$_2$O in a total volume of 18.5 µl for 5 minutes at 70 °C. Then, the samples were put on ice directly and were cooled down for 10 minutes. During that time the reverse transcription master mix was pipetted as shown in Table 28, from which 11.5 µl were added to each RNA-primer-mixture. The reverse transcription was run under 42 °C for 1 hour, followed by an inactivation step at 70 °C for 15 minutes.

Table 28: Reaction mixture for the reverse transcription

Reagent	Volume [μl] per sample
5x Superscript RT buffer	6
DTT (0.1 M)	3.5
dNTPs (10 mM)	1.5
RNase Inhibitor P/N (40 U/μl)	0.5
Super Script™ II (200 U/μl)	0.25
In total	**11.75**

Finally, the cDNA was diluted with 0.1 mM TE-buffer to a concentration of 2 ng/μl, except for cDNA pools (used for qRT-PCR standard curve), which were adjusted to 10 ng/μl.

3.6.4 Quantitative real-time PCR (qRT-PCR)

The quantitative real-time PCR is a technique to assess gene expression, which combines the amplification and quantitative detection of cDNA transcripts. The used cDNA was synthesized from total RNA during reverse transcription (see section 3.6.3). For quantification of the amounts of DNA products at each cycle the fluorescent DNA intercalating dye *eva green* (excitation 500 nm, emission 530 nm), included in the *5x HOT FIREPol®EvaGreen®qPCR Mix Plus* (Solis BioDyne, Estonia), was used. The measured fluorescent signal is proportional to the amount of amplified cDNA. A low cycle number implies a higher gene expression, because less cycles are needed to reach a specific threshold (Cycle threshold (Ct)) of DNA amount. The Ct value represents the number of cycles needed for the fluorescent signal to cross a threshold, which exceeds the background level. Additional to the gene of interest, at least three housekeeping genes (*36b4*, *HPRT1* and *UBC*, for primer sequences see Table 31 below) were measured to normalize the expression results. For this normalization process the ΔΔCt method was used. All samples, which were pipetted in duplicate, were averaged first. Then, the values of the intern control (housekeeping genes) were subtracted from the samples (ΔCt). And finally, the normalized control samples (treated with PBS) were subtracted from the normalized samples (ΔΔCt). To have the fold-change of expression, relative to the basal expression, the following equation (Equation 2) was used:

<div align="center">**Equation 2: Formula to calculate relative gene expression**</div>

$$\textit{Relative expression} = 2^{-[Ct - Ct\ housekeeping\ gene) - (Ct\ control - Ct\ housekeeping\ control)]}$$
$$= 2^{-[\Delta\Delta Ct]}$$

The qRT-PCR mixture was prepared (see Table 29) in a 348 well-plate (*Thermo Fast Plate 384 PCR*, ABgene), which was covered with an optical clear film. Furthermore, on every qRT-PCR plate a standard curve with six concentrations of a cDNA pool (pooled from cDNA of the measured cell lines, 1:5 dilutions) was pipetted to evaluate the amplification. For the performance of the quantitative RT-PCR under conditions shown in Table 30, the *TaqMan 7900HT* (Applied Biosystems) machine was used. Data analysis was performed with the *SDS 1.2 software* (Applied Biosystems).

Table 29: qRT-PCR master mix

Reagent	Volume [µl] per sample
qRT-PCR master mix	2
Primer (1:10)	0.2
ddH$_2$O	4.8
cDNA	3
In total	**10**

Table 30: qRT-PCR conditions

Phase	Duration	Temperature	
Initial Denaturation	15 min	95 °C	
Denaturation	15 sec	95 °C	
Annealing	20 sec	60 °C	**45 x**
Elongation	40 sec	72 °C	
Dissociation Step	15 sec	95 °C	
	15 sec	60 °C	
	15 sec	95 °C	

Table 31: Primers for qRT-PCR

Gene	Forward Primer sequence (5′ → 3′)	Reverse Primer sequence (5′ → 3′)
Reference genes		
36b4	GCAGATCCGCATGTCCCTT	TGTTTTCCAGGTGCCCTCG
B2MG	CCAGCAGAGAATGGAAAGTC	CATGTCTCGATCCCACTTAAC
GAPDH	CCCTTCATTGACCTCAACTACAT	ACGATACCAAAGTTGTCATGGAT
HPRT1	TGACACTGGCAAAACAATGCA	GGTCCTTTTCACCAGCAAGCT
UBC	CGGTGAACGCCGATGATTAT	ATCTGCATTGTCAAGTGACGA
***RRM2* related primer**		
RRM2	CACGGAGCCGAAAACTAAAGC	TCTGCCTTCTTATACATCTGCCA
RRM2v1	GGAGATTTAAAGGCTGCTGGAGT	CACGGAGGGAGAGCATAGTG
***WWOX* related primer**		
WWOX exon 4-6	CCAACCACCCGGCAAAGATA	AATGCTGCACGCTACGGAG
WWOX exon 8-9	ATGTACTCCAACATTCATCGCAG	GTCTCTTCGCTCTGAGCTTCT
Other primer		
BCL2	ACATCGCCCTGTGGATGACT	GGGCCGTACAGTTCCACAAA
GADD45A	GCTCAGCAAAGCCCTGAGT	GTTATCGGGGTCGACGTTGA
TP53	AGCTTTGAGGTGCGTGTTTG	TTGGGCAGTGCTCGCTTAG
SP1	CAGGCCTCCAGACCATTAAC	CAAGCTGAGCTCCATGATCAC
RNA5-8SP2	ACTGGGCTTCTGTGTGTCGATG	TGCAATTGCGTTCGAAGTGTC

3.6.5 RNA sequencing (RNAseq)

The RNA sequencing method (whole expressome analysis) is based on next generation sequencing and was used to investigate RNA transcripts vicinal to the *WWOX* index SNP (rs11644322). This procedure was performed by the Transcriptome and Genome Analysis Laboratory (TAL) of the Göttingen University Medical Center, headed by Dr. rer. nat. Gabriela Salinas-Riester. The analyzed samples were two pooled RNA probes from LCLs, whereof one sample was obtained from five cell lines carrying the wild type allele (Cell identifiers at the Coriell institute: HG00096, HG00109, HG00120, HG00244, and HG00258) and the other sample from five cell lines carrying the variant allele (Cell identifiers: HG00100, HG00108, HG00122, HG00245, and HG00265), respectively. Besides, RNA of the pancreatic cancer cell lines AsPC1 and MiaPaca-II, which were *SP1-*overexpressed and exposed to PBS or 30 nM of gemcitabine, were examined.

52

Furthermore, RNA (from three different clones) of the pancreatic cancer cell line PaTu8988t, stably transfected with shRNA plasmids for *WWOX* knock-down reason, was analysed, compared to control samples transfected with a negative control shRNA plasmid.

For RNA sequencing the Illumina *TruSeq* technology was used, comprising the following workflow steps: Sample preparation, Cluster generation, Sequencing chemistry, and data analysis. All working steps were performed according to the TruSeq® Stranded Total RNA Sample LS (Low Sample) Preparation Guide (Illumina, San Diego, CA, USA).

The typical RNAseq workflow implies the generation of cDNA fragments, which are flanked by multiple indexing adapters with constant sequences (Figure 10). This pool of cDNA fragments is called DNA library and is needed for sequencing with the *HiSeq® 2000* sequencer (Illumina, San Diego, CA, USA) where millions of short sequence reads are generated, corresponding to individual cDNA pieces.
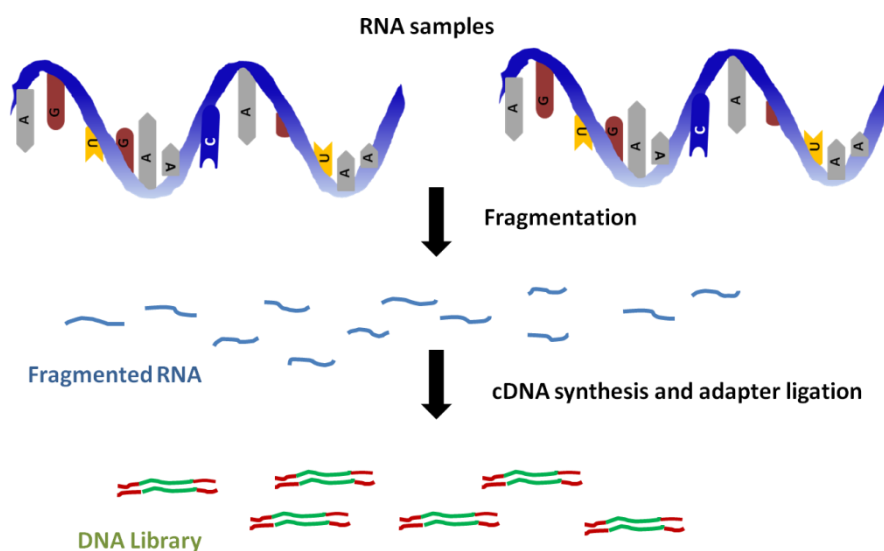
Figure 10: Workflow of RNA sequencing

The first step of sample preparation was the depletion of ribosomal RNA from total RNA. Afterwards, the remaining RNA was purified, fragmented and primed (with random hexamers) for cDNA synthesis. This cleaved RNA fragments were reversely transcribed to first strand cDNA by using reverse transcriptase and random primers, followed by second strand cDNA synthesis, where RNA templates were removed and a substitution strand was synthesized, incorporating dUTP instead of dTTP to generate dsDNA. To obtain blunt-ended cDNA, the dscDNA was separated from the second strand reaction

mixture by usage of *AMPure XP beads* (Agencourt Bioscience Corporation, Beverly, Massachusetts). Next, the 3' ends had to be adenylated. This means that a single adenine nucleotide was added to the 3' end of the generated blunt fragments to prevent ligation with each other during the following adapter (specific constant sequence) ligation. The adapter sequence contains a corresponding, complementary overhang of a single thymine nucleotide allowing its ligation to the cDNA fragment. The adapter ligation process to the end of the cDNA fragments is needed for the further hybridization step onto a flow cell, used for simultaneous analysis. Afterwards, DNA fragments carrying adapter molecules at both ends were selectively enriched by PCR with a primer cocktail, that can anneal to the adapter ends. For providing an optimal cluster density of every flow cell, the DNA library templates were quantified, using the *QuantiFluor™ Dye System* (Promega, Mannheim) containing a fluorescent DNA-binding dye, which was measured via Glomax® Fluorometer (Promega, Mannheim). Besides, the sample quality (size and purity) was determined with the *Bioanalyzer 2100*. This analyzer provides an automated capillary gel electrophoresis system (Agilent, Santa Clara, USA), using a DNA specific chip (*Chip DNA 1000*), allowing DNA fragment separation by size. Prior to sequencing, the cluster generation was performed using a *cBOT* instrument (Illumina, San Diego, CA, USA), where the library samples were bound to a flow cell by hybridization to oligonucleotides that are complementary to the adapter sequence and that are immobilized on the flow cell surface. Following steps are involved in this process: Immobilization, 3' extension, bridge amplification, linearization and hybridization.

In detail, the templates are copied by hybridized primers by 3' extension using a DNA polymerase. Only the copied immobilized template remains on the flow cell and was amplified via bridge amplification, where the template makes a loop to hybridize to a nearby oligonucleotide. The new template was duplicated by polymerase, forming a dsDNA bridge, which was denaturated afterwards to form single DNA strands. These strands loop over to adjacent oligonucleotides again and the procedure goes on as described, so that millions of individual, clonal cluster are created. Finally, each dsDNA bridge cluster was denaturated and the reverse strand was eliminated by specific base cleavage, so that the forward DNA strand is present. The 3' end of this forward strand and flow-cell bound oligonucleotides were blocked, preventing interference with the sequencing reaction. Then, the sequencing primer was hybridized to the complementary sequence on the illumina adapter on unbound ends of templates in the clusters,

whereafter the flow cell contained > 200 million clusters with ~ 1000 molecules per cluster and was ready to be sequenced (read lenght 50 bp).

3.7 Working with bacteria

To work with bacteria in an aseptic way, all working steps were peformed close to a Bunsen burner flame.

3.7.1 Bacteria growth and storage conditions

The *Escherichia coli* bacteria strain *One Shot® TOP10 Electrocomp™ E. coli* (Invitrogen, Karlsruhe) was used, which was grown in Luria-Bertani (LB) medium. The LB medium was prepared as follows (Table 32):

Table 32: LB medium

Reagent	Amount [g]
Tryptone	10
Yeast extract	5
NaCl	5
ddH$_2$O	**Add to 1000 ml**

This solution was autoclaved and stored at 4 °C. For the preparation of solid LB agar plates, 14 g of Agar (AppliChem, Darmstadt) was added additionally prior to the autoclaving step. Afterwards, the solution was cooled down to ~ 50 °C and the required antibiotic (e.g. Ampicillin 100 µg/ml, Chloramphenicol 170 µg/ml, Kanamycin 20 µg/ml) was added. Then, the prepared solution was poured into 92 mm petri dishes under the fume hood, which were placed there till they became dry. To store generated bacterial cultures for a long time, these were mixed at a ratio of 1:1 with a 50 % glycerol solution in a 2 ml reaction tube, and were frozen at -80 °C directly after.

3.7.2 Transformation by electroporation

This method is used to insert plasmids into bacteria cells. Bacteria can increase the amount of plasmids, so that a high amount can be harvested by mini- or midi-preparation (see 3.7.5.1, 3.7.5.2). An electric shock (~ 2500 volt/cm) increases the permeability of the cell membrane, allowing plasmid DNA to get inside the cell. The

electroporation mixture contained 30 µl of ddH$_2$O and 10 µl of the electrocompetent *E. coli,* which was transferred into a pre-cooled 2 mm electroporation cuvette. Then, 1 µl of dialyzed plasmid DNA (see 3.2.11) was added. For the electroporation process the *Gene Pulser II* (Biorad, Herkules USA) with the conditions of 2.5 kV, 25 µF and 200 Ω for five milliseconds was used. Directly afterwards, 800 µl of LB medium (at 37 °C) was added to the cuvette, which was then incubated for 1 hour at 37 °C. Finally, 50 and 200 µl of this solution were struck on agar plates containing the required antibiotic as selection marker, allowing growth only for successfully transformed bacteria.

3.7.3 Cultivation of bacteria on agar plates

To get single clones after the transformation process or to prepare a backup plate of a liquid bacteria solution prepared for mini-preparation, bacteria were cultivated on agar plates with the required antibiotic. The bacteria solution was distributed on agar plates with a pre-flamed arcuate *Pasteur* pipette. Then, the plates were incubated at 37 °C in the incubator *Incudrive* (Schütt, Göttingen) with the upside down overnight. These plates could be kept at 4 °C for approximately one month, if sealed with Parafilm® (Brand, Wertheim).

3.7.4 Cultivation of bacteria in solution

To generate a bacteria suspension for the mini preparation (see 3.7.5.1), in which the amount of a single bacteria clone can be highly increased overnight, 5 ml of LB medium were supplemented with the needed antibiotic (selection marker) in a 15 ml tube. Then, a picked clone from the agar plate was resuspended in this mixture, followed by a shaking period at 37 °C on the *K2 260 basic shaker* for bacteria (Ika, Staufen) at 250 rpm overnight. The tubes (lid not closed completely) were placed on a stand in an angular way to provide a larger surface for oxygen exchange. For the midi-preparation (see 3.7.5.2) 30 ml of LB medium (supplemented with the appropriate antibiotic) was filled in an autoclaved 500 ml glass bottle. Then, 30 - 80 µl of a pre-shaken 5 ml bacteria solution (as described before) was added to the bottle, which then was shaken at 37 °C overnight with the lid not attached in a tight way.

3.7.5 DNA isolation from bacteria

Plasmid DNA was isolated in two different ways. For the first analysis of new bacteria clones or as starting material for subcloning the mini-preparation method was performed. For later transfection experiments into mammalian cells a larger amount of plasmid DNA (300 - 3000 ng/µl) with high purity is needed, which can be isolated by plasmid midi-preparation extraction.

3.7.5.1 Isolation of Plasmid DNA by chloroform extraction (Plasmid mini-preparation)

For this procedure, single clones, which were grown on agar plates, were picked and mixed with 5 ml LB-media supplemented with the required antibiotic. This mixture was shaken for 12 - 16 hours at 37 °C. For having an inoculum for further experiments, 5 µl of this solution were plated on an agar plate with the required antibiotic. The 5 ml bacteria solution was centrifuged for 10 minutes at 4000 rpm (Centrifuge 5810 R; Eppendorf) at room temperature. The supernatant was discarded, then the pellet was resuspended in 250 µl of resuspension buffer (see Table 33) and transferred into a 1.5 ml reaction tube. Thereafter, the cells were lysed with 250 µl of Alkaline lysis buffer (Table 34) and shaken well. For the neutralization process, 350 µl of Neutralization buffer (Table 35) was added and the sample was inverted 6 to 8 times. The precipitation of proteins was seen as white smear. Then, the sample was centrifuged at 13000 rpm for 10 minutes (Biofuge pico, Heraeus) at 4 °C. The clear supernatant, containing the plasmid DNA, was pipetted into a new 1.5 ml reaction tube and was mixed with 500 µl of a chloroform-isoamylalcohol (24:1) solution. The solution was inverted and shaken well, so that no phase boundary could be seen before the next centrifugation step at 13000 rpm for 5 minutes at RT. The upper phase was transferred in a new 1.5 ml reaction tube and 650 µl of pre-cooled isopropanol (-20 °C) was added, followed by 15 minutes of centrifugation at 13000 rpm at 4 °C. Thereafter, the supernatant was discarded and the sample was washed with 800 µl of 70 % ethanol (-20 °C). Again, a centrifugation step was conducted at 13000 rpm for 4 minutes at 4 °C and the supernatant was removed, followed by a repeated washing and centrifugation step. Next, supernatant removal was performed, even discarding the last drop, and the opened reaction tube was put on a heating block at 37 °C till the pellet appeared transparent and dry. Then, 50 µl of TE

buffer (Table 36) was added and the sample was put on a heating block (37 °C) for further 30 minutes, shaking. At the end, DNA was quantified photometrically (see 3.2.3).

Table 33: Resuspension buffer

Reagent (pH = 8, at 4 °C)	Concentration
Tris-HCl	50 mM
EDTA	10 mM
RNAse A (added after autoclaving process)	100 µg/ml

Table 34: Alkaline Lysis buffer

Reagent (pH = 8, at RT)	Concentration
NaOH	200 mM
SDS	1 % (w/v)

Table 35: Neutralization buffer

Reagent (pH = 5.5, at RT)	Concentration
Potassium acetate	3 M

Table 36: TE buffer

Reagent	Concentration
Tris	10 mM
EDTA	0.1 mM

3.7.5.2 Isolation of plasmid DNA by solid extraction

(Plasmid midi-preparation)

The Plasmd midi-preparation was performed via the *Plasmid Plus Midi Kit* (Qiagen, Hilden) according to the manufacturer's instructions. This DNA, with a high purity, was used for later transfection experiments in mammalian cells.

3.8 Protein analysis

3.8.1 Preparation of cell lysates for Western Blots

To isolate proteins for Western Blot analysis, pancreatic cancer cells, cultivated in a 6-well plate, were trypsinized with 500 µl of trypsin per well for 2 - 3 minutes at 37 °C. Afterwards, the cell suspension was transferred in a 15 ml falcon tube already containing the doubled amount of DMEM medium (15 % FCS, 1 % PS) for trypsin deactivation and was centrifuged for 5 minutes at 500 g. The supernatant was removed and the cell pellet was washed with 3 ml of PBS. The centrifugation step was performed again, then 50 - 100 µl of RIPA buffer (supplemented with protease and phosphatase inhibitors, Roche, Mannheim) was added. Afterwards, three repetitions of freeze-thaw cycles in liquid nitrogen and on a heating block at 37 °C, respectively were performed to ensure cell disruption, followed by centrifugation at 13000 rpm for 10 minutes at 4 °C. Finally, the supernatant was transferred into a new reaction tube and was stored at minus 20 °C.

Table 37: RIPA buffer

Reagent	Concentration [mM] or percentage
Tris-HCl	50
NaCl	150
EDTA	1
NP-40	1 % (v/v)
Na-deoxycholate	0.25 % (v/v)
SDS	0.1 %

3.8.2 Determination of protein content via Bicinchoninic acid assay

For quantitation of total protein, the *Pierce™ BCA Protein Assay Kit* (Life Technologies, Darmstadt) was used. This method is a combination of the reduction of Cu^{+2} (cupric ion) to Cu^{+1} (cuprous ion) by protein in an alkaline environment (called biuret reaction) and a highly sensitive and selective colorimetric detection of the cuprous cation (Cu^{+1}) by usage of a special reagent comprising bicinchoninic acid. The chelation of two BCA (bicinchoninic acid) molecules with one Cu^{1+} ion forms a purple, water-soluble reaction product. This complex shows a strong absorbance at 562 nm, which is almost linear with increasing protein concentrations over a working range of 20 - 2000 µg/ml. This assay was performed as follows: First, a BCA working reagent solution was prepared (50 parts of Bicinchoninic acid solution, 1 part of 4 % cupric sulfate solution). Then, 25 µl of a standard solution (standard bovine serum albumin (BSA), range of 0 - 1500 µg/ml) or of the sample, as well as 200 µl of the BCA working reagent solution was pipetted in each well of a 96-well plate, which was shaken for 30 seconds. Afterwards the plate was incubated for 30 minutes at 37 °C and the absorbance was measured with a Victor X4 Light Multilabel Reader (PerkinElmer, Wiesbaden) at 562 nm.

3.8.3 Western Blot

The Western Blot technique is used for the identification of specific proteins out of a protein mixture, which was extracted from cells. This mixture was applied to gel electrophoresis for protein separation by size. Afterwards, the resulting protein bands were transferred to a membrane, where the proteins were accessible for specific antibody binding for detection. In this thesis siRNA targeted gene knock-down of the *WWOX* tumor supressor gene was conducted (see chapter 3.10.1) in the two pancreatic cancer cell lines PaTu8988t and L3.6. To evaluate this knock-down, Western Blotting was performed with transfected and control samples.

3.8.3.1 SDS-polyacrylamide gel electrophoresis (SDS-PAGE)

Using SDS-PAGE, proteins can be separated corresponding to their size. For that reason, samples were mixed and denatured at 95 °C for 5 minutes in a 4x *Bromphenol Blue* loading buffer (NuPage LDS Sample Buffer, 3 parts of loading buffer, 1 part of lysate), containing SDS (amphipathic surfactant), which charges the proteins proportionally to

their mass. This ensures that the separation step during electrophoresis was solely dependent on the molecular weight. Following to denaturation, samples were put on ice for 5 minutes.

The polyacrylamide gel consists of two parts, a separating and a stacking gel. First, the separating gel was prepared as follows (Table 38):

Table 38: 10 % Separating Gel, mixture for two mini gels

Reagent	Added Volume
ddH$_2$O	7.9 ml
30 % AB (Acrylamide/Bis-acrylamide) (Rotiphorese®)	6.7 ml
Tris (1.5 M, pH = 8.8, separating gel buffer)	5 ml
10 % SDS Solution	200 µl
10 % APS Solution	200 µl
TEMED	20 µl
In total	**20 ml**

The gel was poured into a gel electrophoresis chamber (Biometra, Göttingen) until 1.5 cm of the chamber top. The rest of the gel chamber was filled up with water. Then, the gel was incubated at RT for 30 minutes till the gel was polymerized. During that time the stacking gel was prepared as follows (Table 39):

Table 39: 5 % Stacking Gel

Reagent	Added Volume
ddH$_2$O	3.4 ml
30 % AB (Acrylamide/Bis-acrylamide) (Rotiphorese®)	0.83 ml
Tris (1M, pH = 6.8, stacking gel buffer)	0.63 ml
10 % SDS Solution	50 µl
10 % APS Solution	50 µl
TEMED	5 µl
In total	**5 ml**

The water on top of the separating gel was removed and the prepared stacking gel was poured instead, which was incubated for 30 - 40 minutes at RT to polymerize.

3.8.3.2 Gel electrophoresis

The gel was placed into an electrophoresis chamber, which was filled with 1x SDS running buffer (dilution of 10x buffer, see Table 40). Then, 1x SDS buffer was put on top of the gel, to cover the wells of the gel.

Table 40: SDS Running Buffer (10x)

Reagent (pH = 8.3)	Concentration [mM] or percentage
Tris	250
Glycin	1920
SDS	1 %
ddH$_2$O	**Ad 1000 ml**

The wells of the gel were flushed with a syringe shortly before loading. Thereafter, an amount of 20 µg of each denaturated sample was loaded on the gel, which was run for 3 - 4 hours at 20 mA. Two different molecular weight marker were used, 1 µl of the *MagicMark^{TM} XP Western Protein Standard* (LifeTechnologies), which is visible upon detection and 2 µl of a *Prestained Marker* (10 - 180 kDa, biofroxx), which is visible on the gel and the PVDF membrane.

3.8.3.3 Blotting

To transfer the gel on a blotting membrane (PVDF, polyvinylidene difluoride), the semidry transfer method was used. The gel and the blotting membrane were arranged like a sandwich between filter papers. First, the blotting membrane was activated with methanol (100 %) for 10 seconds, washed with water for 3 minutes and then incubated in 1x transfer buffer (dilution of 10x buffer, see Table 41) for 15 minutes. The transfer buffer is used to facilitate the binding of proteins to the blot. The gel was detached from the gel chamber plates, the stacking gel was cut and then the separating gel was incubated for 15 minutes in transfer buffer as well.

Table 41: Western Blot Transfer Buffer (10x)

Reagent	Concentration [mM]
Tris	48
Glycin	39
10 % SDS solution	0.037 %
Methanol	20 %

Diluted in ddH$_2$O

Six thick Whatman filter papers (for one gel) were also soaked in transfer buffer for 5 to 10 minutes. Then, the gel sandwich arrangement was performed on a Semi-Dry-Electroblotter (peqlab). First, three soaked filter papers were put on the Electroblotter, then the blotting membrane followed by the gel, was added. Air bubbles under the gel were erased by adding some transfer buffer on top of the gel. The bubbles were pushed by hand to the border of the gel. Three further filter papers (soaked in transfer buffer) were placed on top of the gel. Afterwards, the sandwich-complex was compressed with a little roll. The blotting process was performed at 100 mA (for one gel) for 1 hour at RT. Following to this, the blotting membrane was cut near the desired kDa number of the protein of interest (WWOX, 46 kDa) and of the control protein (Actin, 42 kDa), which can be estimated from the Prestained marker. The cut membrane pieces were washed with TBS-T (0.1 % Tween20, see Table 42 and Table 43) for 5 minutes at RT.

Table 42: Tris buffered saline (TBS) Buffer

Reagent (pH = 7.5)	Concentration [mM]
NaCl	150
Tris	50

Table 43: TBS-Tween

Reagent	Concentration
Tween20, dissolved in TBS buffer	0.1 %

3.8.3.4 Blocking

To avoid unspecific binding of the antibody to the membrane, the membrane pieces with the transferred protein bands were blocked by adding 5 % milk dissolved in TBS-T (0.1 % Tween20, see Table 44) for 1 hour at RT.

Table 44: Blocking Buffer for the Western Blot membrane

Reagent	Final concentration	100 ml
Non-fat blotting grade milk powder, dissolved in 0.1 % TBS-Tween	5 %	5 g

3.8.3.5 Incubation with antibodies

After the blocking procedure, 4 - 5 ml of the primary antibody (see Table 45), diluted for actin in 5 % milk-TBST (1:4000) and for WWOX in 5 % BSA-TBST (1:200), were added to the blot overnight at 4 °C.

Table 45: First Antibody Information

Membrane	Antibody	Host	Company	Protein size	Dilution	Buffer
A	WWOX (N-19): sc-20528	goat	Santa Cruz	46	1:200	5 % BSA-TBST
B (For normalization)	Actin	rabbit	Acris	42	1:4000	5 % milk-TBST

On the next day, the membranes were washed three times for 5 minutes with TBST (0.1 % Tween20) and the second antibody (Table 46), diluted in 5 % milk-TBST, was added (2 - 3ml) for 2 hours shaking at RT. Afterwards, the blot was washed three times with TBST (0.1 % Tween20) again.

Table 46: Second Antibody Information

Membrane	Antibody	Host	Company	Dilution	Buffer
A	**Anti-goat IgG HRP** (Horseradish peroxidase)	rabbit	Acris	1:30000	5 % milk-TBST
B (For normalization)	**Anti-rabbit IgG HRP** (Horseradish peroxidase)	goat	Acris	1:30000	5 % milk-TBST

3.8.3.6 Detection with HRP substrate

The HRP (Horseradish peroxidase), contained in the second antibody, can be detected by an enhanced chemiluminescent solution (*ECL, Luminata™ Forte Western HRP Substrate*, MerckMillipore, Darmstadt). The membranes were covered with the ECL solution and were placed in a Luminescent Image Analyzer (*Image Quant™ LAS 4000 Mini*). The chemiluminescent signals were determined with the corresponding *Image Quant LAS 4000 Mini Control software v1.2*.

3.8.4 *In vitro* translation via TNT Assay

Using the *in vitro TNT® Coupled Transcription/Translation System* (Promega, Mannheim) allows analysis of protein expression without using cells. The delivered master mix contains all essential components like RNA polymerase, nucleotides, salts, ribonucleotide inhibitor and reticilocyte-solution to generate complex proteins, based on plasmid DNA. Used plasmid DNA requires a T7 promoter located upstream of the expressed gene. For information about the used pcDNA5:*RRM2*:eGFP construct see section 3.5.3.

The reaction mixture was pipetted on ice as described in Table 47, followed by an incubation time of 90 minutes at 30 °C. Thereafter, the reaction was stopped on ice and was diluted (1:2) with ddH$_2$0. These mixtures (100 µl) were transferred into a black 96-well plate with a transparent bottom (Greiner, Frickenhausen) for fluorescence measurement (of eGFP) with the Tecan reader (excitation 485 nm, emission 535 nm).

Table 47: Reaction mixture for the TNT® Assay

Reagent	Added volume [µl]
TNT® T7 Quick Master Mix	40
Methionin [1mM]	2
Plasmid-DNA [0.5 µg/µl]	2
T7 TNT® PCR Enhancer	1
ddH$_2$0	**Add to 50**

3.9   Mammalian cell culturing

All cell culture work was performed under the sterile bench. The used cell lines were cultured in an incubator at 37 °C under 5 % CO$_2$ and 95 % humidity. To avoid microbial contamination and to check the growth status, all cells were controlled via microscope (Microscope TELAVAL 31, Zeiss, Jena) regularly. The culture media was pre-warmed at 37 °C before use and was supplemented with 1 % Penicillin-Streptomycin (PS) to prevent bacterial contamination. Besides, fetal calf serum (FCS) was added, which contains proteins that are necessary for cell growth. The subculturing of cells was performed twice a week in a cell specific split ratio, which was dependent on the proliferation rate and the specific conditions needed for the experiments. The general cell number for suspension cells should be between 3 x 10^5 - 8 x 10^5 cells per milliliter of media. Adherent cells should not exceed a confluence of 80 %. For detaching adherent cells from the culture flask bottom, these were washed with PBS buffer (see Table 48) and were trypsinized with 5 ml of trypsin (TrypLE™ Express, Gibco/Invitrogen) for a 75 cm^2 flask and 3 ml of trypsin for a 25 cm^2 flask, followed by an incubation time of approximately 3 minutes at 37 °C. For the deactivation of trypsin, the doubled volume of culture media (supplemented with FCS) was added. Afterwards, the cells were transferred to a 50 ml falcon tube and centrifuged at 500 g for 5 minutes at room temperature. The supernatant was removed and the pellet was resuspended in culture media. Then, cell counting was conducted (see section 3.9.3) and the required volume was seeded on plates and/or transferred into a new cell culture flask for subculturing.

Table 48: PBS Buffer

Reagent (pH = 7.4)	Concentration [mM]
NaCl	128.5
KCl	2.8
Na_2HPO_4	8.1
KH_2PO_4	1.5

3.9.1 Freezing cultured cells

For long-time preservation of cells for later studies, cell lines were stored in liquid nitrogen. It is advised to cryopreserve cells with a low passage number and when a confluence of 80 % is reached. The cells were harvested and transferred into a 50 ml falcon tube, followed by centrifugation at 500 g for 5 minutes at RT. The supernatant was removed and the pellet was resuspended in 7.5 ml of a pre-cooled freezing solution, consisting of 90 % pure FCS and 10 % of sterile DMSO (Dimethylsulfoxide, AppliChem, Darmstadt). DMSO is used as antifreezing agent, which prohibits the generation of ice crystals, which can lead to cell death. Further steps were performed on ice. Afterwards, the cells (1.5 ml) were pipetted in 1.8 ml *Cryo tubes* (Nunc, Thermo Scientific, Denmark) and were stored in a pre-cooled *Mr. Frosty freezing box* (Sigma-Aldrich, Deisenhofen) at -80 °C overnight, allowing cells to cool down with a speed of 1 °C/min. The next day, the frozen cells were transferred into a liquid nitrogen storage container at around -170 °C.

3.9.2 Defreezing cultured cells

Cryopreserved cell lines that were stored in liquid nitrogen were thawed quickly and transferred into a 50 ml falcon tube for centrifugation (5 minutes, 500 g, RT), which already contained 20 ml of cell culture media (1 % PS). It is important to relieve the cells from the toxic DMSO. Afterwards, the supernatant was removed, the pellet was resuspended in 10 ml of media (1 % PS, 10 - 15 % FCS (depending on the cell line)) and the cell suspension was pipetted into a 25 cm² Tissue Culture Flask. After a cultivation time of 1 - 2 days at 37 °C and 5 % CO_2, cells were transferred to a 75 cm² flask (20 ml) for increased growth.

3.9.3 Counting cells with the Neubauer-Cell Chamber

The number of cells in a cell suspension was determined via Neubauer-Cell Chamber. To distinguish between living and dead cells, the cell suspension was mixed with the vital stain *Trypan Blue* (Sigma-Aldrich, Deisenhofen) in a ratio of 1:1. Afterwards, 15 µl of the staining solution were pipetted on the counting chamber, which was covered with a cover slip. Living cells do not absorbe *Trypan Blue,* while dead cells do. Via microscopy the living cells appear in a more bright colour, in comparison to the blue background media and the dead cells. All living cells in each of four squares were counted. The cell concentration per ml was calculated as follows (see Equation 3):

Equation 3: Calculation of cell concentration per milliliter

$$Cell\ concentration/ml = \frac{Sum\ of\ all\ living\ cells\ in\ all\ four\ squares * 2 * 1000}{4 * 0.1\ µl/square}$$

$$Cell\ concentration/ml = Sum\ of\ all\ living\ cells\ in\ all\ four\ squares * 5000$$

The average of all four squares is calculated at first. The dilution factor of the cell suspension, which was 2, has to be considered. The area of each square is 1 mm² and the chamber hight is 0.1 mm. This results in a volume of 0.1 µl/square. To sustain the concentration of cells per milliliter, a factor of 1000 has to be included into the equation.

3.9.4 Lymphoblastoid cell lines

The lymphoblastoid cell lines (LCLs), which are donated by Britain Caucasian, are non adherent cells, which were obtained from the NIGMS Human Genetic Cell Repository at the Coriell Institute for Medical Research. These were established by Epstein-Barr Virus transformation of peripheral blood mononuclear cells using phytohemagglutinin as a mitogen. All cell lines are free of bacterial, fungal or mycoplasma contamination. Cultivation of these cells was carried out in 75 cm² Tissue Culture Flasks. The used media was RPMI media (2 mM L-glutamine, 15 % FCS, 1 % PS). The passaging of cells was performed twice a week at a ratio of 1:7. For experiments only cells with a passage number < 10 were used. All LCLs from Coriell Cell Repositories, I used as an ethnically homogenous sample set, are listed in Table 49.

Table 49: ID numbers of lymphoblastoid cell lines from Coriell Cell Repositories (http://ccr.coriell.org).

HG00096	HG00097	HG00099	HG00100	HG00101	HG00102	HG00103	HG00104	HG00106
HG00108	HG00109	HG00110	HG00111	HG00112	HG00113	HG00114	HG00116	HG00117
HG00118	HG00119	HG00120	HG00121	HG00122	HG00123	HG00124	HG00125	HG00126
HG00127	HG00128	HG00129	HG00130	HG00131	HG00133	HG00134	HG00135	HG00136
HG00137	HG00138	HG00139	HG00140	HG00141	HG00142	HG00143	HG00146	HG00148
HG00149	HG00150	HG00151	HG00152	HG00154	HG00155	HG00156	HG00158	HG00159
HG00160	HG00231	HG00232	HG00233	HG00234	HG00235	HG00236	HG00237	HG00238
HG00239	HG00240	HG00242	HG00243	HG00244	HG00245	HG00246	HG00247	HG00249
HG00250	HG00251	HG00252	HG00253	HG00254	HG00255	HG00256	HG00257	HG00258
HG00259	HG00260	HG00261	HG00262	HG00263	HG00264	HG00265	HG01334	

3.9.5 Pancreatic cancer cell lines

Pancreatic cancer cell lines I used for experiments during my PhD program were MiaPaca-II, AsPC1, CFPac, L3.6, PaTu8988t and PancI. These cell lines were purchased from the ATCC company (Wesel, www.atcc.org). The cultivation of these cells was performed according to their recommendation (http://www.lgcstandards-atcc.org). The split ratio was 1:8.

3.9.6 HEK-293 cells

HEK-239 cells are human embryonic kidney cells which grow in an adherent manner and were cultivated in DMEM media supplemented with 10 % FCS and 1 % PS. The passaging was performed at a ratio of 1:10.

3.9.7 PaTu8988t cells stably transfected with shRNA plasmids against *WWOX*

The pancreatic cancer cell line PaTu8988t was stably transfected with *SureSilencing shRNA plasmids* (linearized pGeneClip™ Hygromycin Vector with specific sequences targeting WWOX, Qiagen, Hilden, see 3.10.2). The used culture media was DMEM supplemented with 10 % FCS, 1 % PS and 100 µg/ml Hygromycin B. The passaging was performed at a ratio of 1:8.

3.10 Transfection of mammalian cells

The transfection process allows the injection of plasmid DNA into cells for overexpression or knock-down reason of genes. In this work the liposome transfection method was used, where a positively charged lipid reagent surrounds the negatively charged plasmid DNA and forms an aggregate, which can permeate the cell membrane. Inside the nucleus the inserted DNA is then released and can be expressed. Two different transfection ways were conducted. Performing a transient transfection implies that the DNA is not inserted into the nuclear genome, and therefore is just temporarily expressed. Stably transfected cells exhibit persistence of the inserted gene in the genome of the cell and their daughter cells. For transient overexpression of genes, the *X-tremeGene HP DNA Transfection Reagent* (Roche, Mannheim) was used. Transient transfection of siRNA (small interfering RNA) used for gene silencing was performed by usage of *RNAiMAX Transfection reagent* (Invitrogen, Karlsruhe). For the stable gene knock-down via shRNA (short-hairpin RNA) the *Attractene Transfection reagent* (Qiagen, Hilden) was employed.

3.10.1 Transient *WWOX* knock-down by siRNA

The pancreatic cancer cell lines L3.6 and PaTu8988t were used to assess the consequences of targeted *WWOX* knock-down by transient siRNA (20 - 25 bp long, doublestranded) transfection. SiRNA can affect the expression of genes, with a complementary nucleotide sequence, by cracking the mRNA after transcription, so that translation is impaired. The transfection was carried out on six-well plates, three wells per condition, in a fast-forward fashion. First, the cells were freshly seeded at a density of 250,000 cells/2 ml in DMEM medium (10 % FCS) without Penicillin-Streptomycin. The transfection mixture, containing 30 pmol of a predesigned panel of four siRNAs to target *WWOX* (Dharmacon/GE Healthcare Cat-Nº M-003961-03-0005, Lafayette, CO, USA), OptimMem® medium and the transfection reagent *RNAiMAX* (both from Invitrogen, Karlsruhe) was prepared as listed in Table 50 and incubated for 20 minutes at RT. Thereafter, 500 µl of the mixture was added in a dropwise manner per well. A scrambled panel of siRNAs (ON-TARGETplus Non-targeting siRNA #1, Dharmacon Cat-Nº D-001810-01) was transfected the same way serving as negative control. After transfection, the cells were cultured for 24 h at 37 °C before being treated with gemcitabine or 5-FU (see chapter 3.10.4).

Table 50: siRNA transfection mixture

Reagent	Volume [µl] per well
OptiMem®	500
siRNA	1.5 (20 µM stock)
Lipofectamine® RNAiMAX	5

3.10.2 Stable *WWOX* knock-down by shRNA

Another technique for *WWOX* gene knock-down is plasmid-based RNA interference, where plasmids carrying a shRNA (short-hairpin RNA, artificial RNA that exhibts a tight hairpin turn) are stably transfected into cells. For this purpose, I used the *SureSilencing shRNA Plasmid Kit* from Qiagen (Hilden), containing four gene-specific shRNA plasmids and one negative control plasmid (21 bp long). The Kit used the pGeneClip™ vector (4989 bp, obtained from Promega Corporation, Madison, WI, see Figure 11, for sequence see appendix), which expresses a shRNA under control of the U1 promoter and the hygromycin resistance gene. The selection of stably transfected cells is allowed due to the hygromycin resistance.
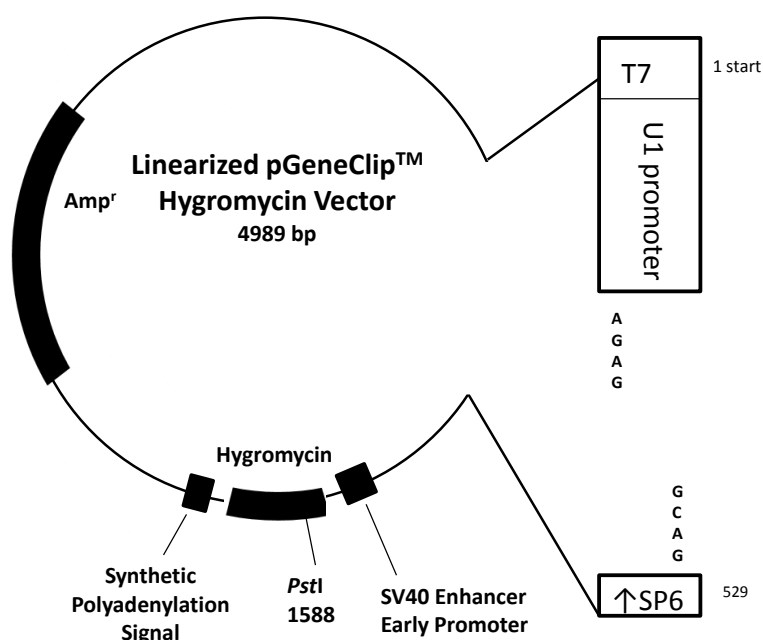
Figure 11: Scheme of the pGeneClip™ Hygomycin Vector. Modified according to SureSilencing ShRNA Plasmid Handbook, Qiagen)

The specific shRNA sequences (see Table 51) are inserted between position 438 and 439 of the plasmid sequence.

Table 51: SureSilencing shRNA (*WWOX*) Plasmid details

Clone ID	Insert Sequence
1	AGTGCATCCTGGAAATATGAT
2	GAGACCACCTTTCAAGTGAAT
3	CAGCACCACTGCCATGGAAAT
4	GTGAAGCAGTGTCACGCATTT
Negative control	GGAATCTCATTCAATGCATAC

First, the delivered shRNA plasmids were transformed into *E. coli* via electroporation (see section 3.7.2), then the bacteria solution was distributed on agar plates containing ampicillin as selection marker. The next day, clones were picked and single clone culturing was performed, followed by the isolation of plasmid DNA via mini-preparation (see section 3.7.5.1). For qualitiy control, a successful *Pst*I restriction enzyme digestion was conducted. Thereafter, midi-preparation (see section 3.7.5.2) was performed.

Next, the appropriate hygromycin B concentration (for selection process) had to be identified by testing of seven different concentrations (0, 100, 200, 400, 600, 800 and 1000 µg/ml). For this, PaTu8988t cells were plated at a density of 5000 cells/ml (24-well plate), cultured at 37 °C at 5 % CO_2 till a confluence of < 10 % was reached, before being exposed to hygromycin B. When the "0" concentration point reached confluence, the medium containing hygromycin B was changed every two days till confluence was seen. Then, cell viability analysis of these cells (in quadruplicates), referred to a drug-free condition, was conducted via *PrestoBlue*® staining and fluorescence measurement with the Tecan reader (see 3.10.4). For an increased likelihood of integration and a shorter time to get stable transfectants, the plasmid was linearized with the enzyme *Bsa*I-HF (see 3.2.9.2).

Then, the shRNA plasmids were transfected into the cells. For this purpose, 59.5 µl of OptiMem® medium were dispensed into a 24-well plate. Afterwards, 0.4 µg of the shRNA plasmids was added per well and mixed by gently rocking the plate for several times, before adding 3 µl of the *Attractene Transfection Reagent* (Qiagen, Hilden) per well. Again, the plate was shaken for some time. Then, the plate was incubated for 15 minutes at RT to allow the formation of the transfection complex. During that time, cells were prepared by washing twice with PBS, trypsinization with 150 µl of trypsin and cell harvesting by centrifugation at 500 g for 5 minutes in a falcon already containing 300 µl

of DMEM medium. Afterwards, the pellet was washed once with medium by resuspension and recentrifugation. Then, the pellet was resuspended in fresh growth medium (10 % FCS, 1 % PS). After cell counting, 125,000 cells/500 µl were added to the well containing the *Attractene*-plasmid-complexes, when 15 minutes of transfection complex formation were over. Moreover, untransfected cells were seeded on the same plate to have another control. Again, the plate was mixes gently by rocking back and forth and was incubated at 37 °C for 48 hours.

Thereafter, cells were harvested as described before and 2500 cells/500 µl (< 10 % confluence) were seeded again on a 24-well plate, 4 wells per condition in DMEM medium without hygromycin B. Cell growing without hygromycin B was carried out for 5 hours, before the effective hygromycin B concentration was added again. The hygromycin medium was renewed every 2 - 3 days for a time range of 7 days. Afterwards no hygromycin was added anymore till cell growing was seen. Then, hygromycin B was supplemented again, but in a reduced concentration of 100 µg/ml. The grown single clones were picked with a 10 µl pipette tip by pipetting 5 µl of DMEM medium 5 - 6 times on the place of clone growing. The pipetted volume was transferred into a 12-well plate, filled with 500 µl of DMEM medium (supplemented with 100 µg/ml of hygromycin B). Again, cell cultivation was performed, till clones were seen and transferred to a new 24-well plate. When 50 % of confluence was reached, cells were trypsinized and pipetted first into a 25 cm^2 cell culture flask with 5 ml of DMEM medium, containing 100 µg/ml of hygromycin B, followed by a later transfer into a 75 cm^2 culture flask comprising hygromycin medium as well.

Finally, gemcitabine sensitivity (10 - 1000 nM) was tested for this stably shRNA-transfected cells, according to the Viability Assay described in section 3.10.4.

3.10.3 Transient overexpression of genes

Pancreatic cancer and HEK-293 cells were plated at a density of 2×10^5 - 4×10^5 cells/2ml (depending on the cell line and the purpose) on a six-well plate (three wells per condition) and were cultured at 37 °C and 5 % CO_2 till a confluence of 80 % was reached. In this work following plasmids were transfected into cells: pcDNA3-*SP1* and pcDNA3-*WWOX*.

The transient transfection was performed as follows: First, 200 µl of DMEM medium

(without FCS and PS) were mixed with 3.6 µg of plasmid DNA. Then 10.8 µl (Ratio 1:3, µg DNA : µl transfection reagent) of the *X-tremeGene Transfection Reagent* was added and mixed carefully. This mixture was incubated for 15 minutes at RT. During that time the culture medium of the wells was renewed (without PS). Finally, 200 µl of the transfection mixture was added in a dropwise manner and the plate was shaken slightly and incubated for four hours at 37 °C and 5 % CO_2. Next, the readout of the transfection procedure was performed. Cells, overexpressed with pcDNA3-*WWOX* were exposed to gemcitabine as follows: After the mentioned four hours, cells were harvested and transferred into a 50 ml falcon tube, which already contained 12 ml of DMEM medium, followed by centrifugation at 500 g for 5 minutes. Then, supernatant removal was conducted and the pellet was resuspended in 700 µl of media. After cell counting, cells (3000 cells/100µl) were seeded on a black 96-well plate with a transparent bottom (Greiner, Frickenhausen) and were cultured for 24 hours (37 °C, 5 % CO_2), before being treated with gemcitabine in quadruplicates. After further 72 hours, cell viability was analyzed via *PrestoBlue®* staining (see section 3.10.4).

In case of *SP1*-transfection, four hours after transfection, transfected wells were pooled in the doubled amount of cell culture medium, centrifuged (500 g, 5 minutes) and resuspended in 12.5 ml of medium. Afterwards, 1 ml of this suspension was plated per well of a 12-well plate. Then, 48 hours after transfection, cells were treated with gemcitabine, 5-FU or irinotecan in duplicates. After further 24 hours, RNA samples were collected (3.6.1), which were used for future expression analysis (see Methods sections 3.6.3 and 3.6.4.)

3.10.4 Viability Assay of cytostatic-treated cells

To assess gemcitabine and 5-FU sensitivity of cells with RNAi-mediated *WWOX* knock-down (see 3.10.1, 3.10.2) or *WWOX* overexpression (see 3.10.3) cell viability testing was performed. Therefore, cells were trypsinized 24 hours after transfection and were seeded at a density of 3,000 cells/100 µl on a black 96-well plate with a transparent bottom (Greiner, Frickenhausen). Afterwards, gemcitabine or 5-FU was applied on the 96-well plate at ten concentrations (for each cell line concentration ranges tested in concentration tests before, but identical distances on a log_{10}-scale, for gemcitabine from 10 to 1000 nM for PaTu8988t and from 4 to 400 nM for L3.6; for 5-FU 250 - 50000 nM for both cell lines) and referred to a drug-free condition, each in quadruplicates. Upon a

further incubation time of 72 h at 37 °C and 5 % CO_2 the resazurin-based *PrestoBlue®*
Cell Viability reagent (Invitrogen, Karlsruhe) was added and fluorescence signals
(excitation 485 nm, emission 612 nm) were recorded after 4 hours. Viable cells are able
to reduce the blue resazurin to the red-fluorescent resorufin. The measured fluorescent
signal is proportional to the number of metabolically active cells, allowing
quantification. The read out was conducted with the *Tecan Ultra* Plate reader (Tecan,
Crailsheim, excitation 485 nm, emission 612 nm).

In addition, transfected cells were incubated for further 48 h on a 6-well plate (referred
to the time point when cells were removed from the six-well plate 24 h after
transfection) to evaluate WWOX knock-down on protein level (3.8.3).

3.11 Sensitivity of lymphoblastoid cells toward gemcitabine

Using a genome-wide approach, comprising 89 fully sequenced lymphoblastoid cell lines
(LCLs, see section 3.9.4), individual cell line's sensitivity toward gemcitabine was
assessed. Dose-effect curves for gemcitabine treatment were established and EC_{50} (half
maximal effective concentration) values were calculated and correlated in relation to the
cell vitality. The inhibition of cell proliferation was used as toxicity readout, which was
ascertained by Carboxyfluorescein succinimidyl ester (CFSE, eBioscience, Frankfurt)
staining, measured by flow cytometry. Gemcitabine was used at concentrations of 0, 1.9,
3.8, 6.4, 10.8, 18.1, 30.4, and 76.0 nM. This chosen concentration range was based on a
test phase, performed by a former student in our lab, Dr. rer. nat. Sebastian Roppel, who
executed this experiment for a another set of 111 LCLs.

First of all, the cell lines were cultured in 75 cm² culture flasks in a volume of 50 ml
RPMI medium (supplemented with 15 % of FCS, 1 % PS, flask stored in a vertical way) to
get a sufficient number of cells for the experiment (for cell counting see section 3.11.1).
Per week, around 8 - 14 cell lines were analyzed in parallel. The cell concentration was
kept between 3×10^6 and 6×10^6 cells per milliliter, to allow logarithmic growth.
Besides, 30 % of the cell lines were measured twice, to exclude unreliable results. Prior
to the gemcitabine treatment, the cells were stained with CFSE (see section 3.11.2),
which dilutes with each cell division allowing to assess the effect of gemcitabine on the
inhibition of cell proliferation. After the CFSE staining procedure cells were incubated at
37 °C and 5 % CO_2 for 24 h, prior to plating of 100,000 cells/ml per well, in duplicate for

each concentration, on a 24-well plate and the exposure to gemcitabine at the concentrations mentioned above. The treated cells were incubated for 72 h at 37 °C and 5 % CO_2, before the analysis via flow cytometry (see 3.11.3, 3.11.4) with excitation at 485 nm and emission at 517 nm was performed. PBS treated LCL control samples (in duplicate) were incubated for 48 hours, before being measured by flow cytometry. These control samples were needed to calculate the proliferation index by comparing these results of the control samples with those control samples measured after 72 hours.

In addition, LCLs were seeded on 6 well plates, treated with PBS (Control) and the gemcitabine concentrations 3.8 nM and 30.4 nM (three wells per condition, 3 ml per well) for DNA and RNA collection. After 24 hours three wells were pooled for each concentration, and the suspension was divided up into two 5 ml FACS tubes (BD Falcon), which were processed as described in chapter 3.2.1 and 3.6.1 dealing with DNA and RNA isolation, respectively.

The whole procedure was divided up into several parts as described before, which were conducted as follows:

3.11.1   Counting cells via flow cytometer

For counting cells, 150 µl of the well resuspended cell suspension (out of the 50 ml in the flask) were pipetted into 5 ml Falcon tubes. Afterwards, a special staining solution containing *Sytox Blue* and *Vybrant®DyeCycle™ Ruby stain* (both Life Technologies Corporation, Darmstadt) was prepared, which stains living and dead cells. Both dyes incorporate into the DNA of cells and can be detected via measurement of fluorescence. The *Vybrant Ruby* stains dead and living cells, whereas *Sytox Blue* merely represents a dead cell stain. This cell dyeing allows the differentiation of living cells from dead cells and cell debris by flow cytometry. To provide a consistent cell counting system, the number of cells per sample was determined by addition of *CountBright™ Absolute Counting Beads* (Invitrogen, Karlsruhe). The ratio of bead events (adjusted to 2500 beads) was compared to the ratio of cell events (adjusted to 100,000 events), which leads to the absolute number of cells per sample. The staining mixture per sample was composed as follows (Table 52):

Table 52: Mixture for vitality staining

Reagent	Volume per sample [µl]
RPMI medium (15 % FCS, 1 % PS)	150
Sytox Blue stain	0.3 (1:1000)
Vybrant Ruby stain	0.15 (1:2000)
Counting Beads	10

Then, 160 µl of the vitality staining solution was added to 150 µl of cell suspension and was mixed well, followed by 15 minutes of incubation at 37 °C. Afterwards, cell counting was conducted with the *Flow Cytometer BD LSRII* (Becton Dickinson). The cell number determination by *counting beads* was performed according to manufacturer's instruction and the cell concentration was calculated with the following Equation 4:

Equation 4: Calculation of the cell concentration in a cell suspension containing counting beads.

$$\frac{\textit{Counted cells x total number of beads in the solution x dilution factor}}{\textit{Counted beads x total volume of sample (cell suspension and volume of beads)}}$$

3.11.2 CFSE staining of LCLs for proliferation analysis

To assess the inhibition of cell proliferation, induced by gemcitabine, LCLs were loaded with CFSE (Carboxyfluorescein succinimidyl ester) stain. After cell division of these cells, the progeny contains half of the number of CFSE-tagged molecules. Therefore each cell division can be determined by measuring the corresponding decrease in cell fluorescence via flow cytometry. The diacetylated non-fluorescent CFDA, SE form (Carboxyfluorescein diacetate succinimidyl ester) can easily cross intact cell membranes. Esterases, which are present inside the cell, cleave the acetates. The deacetylated form is fluorescent and covalently binds to intracellular amines, so that fluorescent CFSE stays within the cell.

Prior to CFSE staining, the cells were counted (see chapter 3.11.1) and adjusted to the appropriate volume for 15×10^6 LCLs. The cell suspension was centrifuged at 250 g for 7 minutes at RT. Afterwards, the supernatant was discarded and the pellet was resuspended in 500 µl of PBS. Then, 500 µl of the staining solution, consisting of 40 µM

CFSE in PBS (550 µl PBS mixed with 2.2 µl of CFSE), was added and vortexed gently at 1400 rpm for 5 seconds, before this cell suspension was transferred directly to 37 °C for 2 minutes and 30 seconds. Immediately afterwards, the staining process was stopped with 10 ml of ice-cold cell culture medium (RPMI medium supplemented with 15 % FCS, 1 % PS) in complete darkness for 5 min on ice. Again centrifugation and supernatant removal was performed under the same conditions as before, followed by resuspension of the pellet in 25 ml of warm cell culture medium. Thereafter, the cell suspension was transferred into a new cell culture flask, which was incubated at 37 °C and 5 % CO_2 for 24 h.

3.11.3 Flow cytometry preparation

After an incubation time of 72 hours, cells were harvested by mixing the well, pipetting in circles. Then, a defined suspension volume (see Table 53) was transferred into 5 ml FACS tubes. Due to different cell growth behaviour upon different gemcitabine concentrations and the need for similar cell numbers for the following staining procedure, an adjustment of the cell number was performed by pipetting different volumes.

Table 53: Volume of gemcitabine treated samples measured by flow cytometry

Concentration of gemcitabine [nM]	Volume of cell suspension [µl]
Control	200
1.9	200
3.8	200
6.4	300
10.8	300
18.1	400
30.4	600
76.0	800

After cell washing with PBS, centrifugation at 250 g for 5 minutes and supernatant removal, 200 µl of the staining solution for vitality analysis (see Table 52 in chapter 3.11.1) was added. These solutions were mixed at 1400 rpm for 10 seconds and were incubated for 15 minutes at 37 °C, 5 % CO_2 before being measured with the flow cytometer. The data was analyzed by usage of the *Cyflogic 1.2.1* free software (www.cyflogic.com).

3.11.4 Flow cytometry and its measurement conditions

Flow cytometry allows the multiparametric analysis of individual cells in a cell suspension, passing a laser with high speed. Depending on the shape, structure and/or staining different effects can be seen, giving information about cellular characteristics. In this work the method was used to assess the impact of gemcitabine on vitality and proliferation of LCLs. To eliminate cell debris seen as small particles the particle size was analysed first in the FCS (forward scatter channel), which is dependent on the volume of the cell, and the SSC (sideward scatter channel), which is related to the granularity of particles. For vitality testing, the fluorescent DNA intercalating dye *Sytox Blue* (excitation 440 nm, emission 480 nm), assessed in the Pacific Blue (based on 6,8-difluoro-7 hydroxycoumarin fluorophore) channel, and the *Vybrant Ruby* dye (excitation 638 nm, emission 686 nm), assessed in the APC (Allophycocyanin, a photosynthetic pigment found in blue-green algea) channel, were used. To determine the proliferation rate under gemcitabine treatment, CFSE staining (excitation 492 nm, emission 517 nm, see chapter 3.11.2) was performed, which was detected in the FITC (fluorescein isothiocyanate) channel. For each channel different voltages were used, 170 volts for the FCS channel, 210 volts for the SSC channel, 685 volts for the APC channel, 215 volts for the FITC channel and 220 volts for the APC channel.

3.11.5 Data Analysis

Data analysis was performed by usage of the *Cyflogic 1.2.1* free software for academic use (www.cyflogic.com). To differentiate between living and dead cells, Dot-Plots were drawn, with the APC channel on the x-scale, and the Pacific Blue channel on the y-scale (see Figure 12 - Figure 14). This allows gating of living cells, so that their percentage compared to dead cells could be calculated. Besides, the geometric mean of the FITC channel detection for living cells was determined, which stands for the CFSE dye used

for proliferation analysis. These described values were needed for the statistical assessment of cellular sensitivity upon gemcitabine treatment and the calculation of EC_{50} values (EC_{50Vit}, $EC_{50Prolif}$). Two different EC_{50} values were computed: One for the impact of gemcitabine on cell vitality (EC_{50Vit}) by using the four-parametric MMF model (Multiple Multiplicative Factor Model), and one for the impact of gemcitabine on proliferation inhibition ($EC_{50Prolif}$) using the three-parametric Gompertz model. The choice of an adequate model was performed with the *Curve Expert Professional* software (www.curveexpert.net), which encompasses 80 models. The criteria for the chosen model was a r^2 value ≥ 0.95 for each cell line. For the determination of EC_{50} values for all cell lines, the Solver algorithm in EXCEL was used. Below, exemplary data generated via flow cytometer is presented, showing the detected living cell population under PBS and gemcitabine exposure (two concentrations).
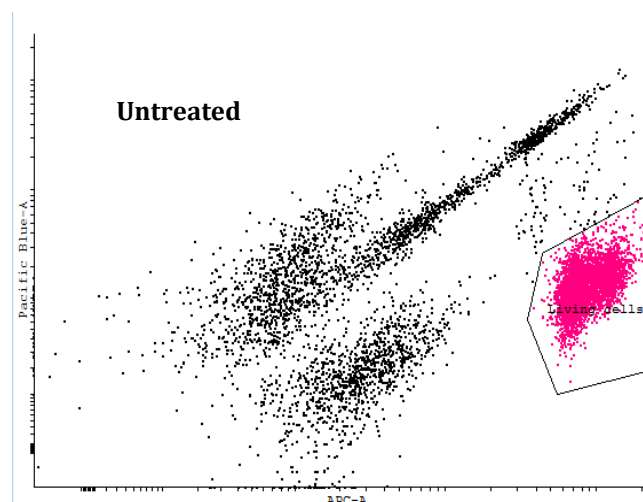
Figure 12: Flow cytometry data of untreated LCL number 240: The determination of living cells (red coloured gate) was performed via Vybrant Ruby and Sytox Blue staining.
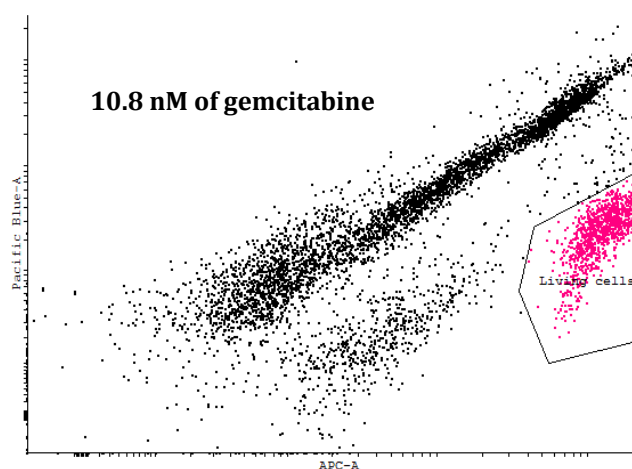
Figure 13: Flow cytometry data of LCL number 240, treated with 10.8 nM of gemcitabine for 72 h: The determination of living cells (red coloured gate) was performed via Vybrant Ruby and Sytox Blue staining.
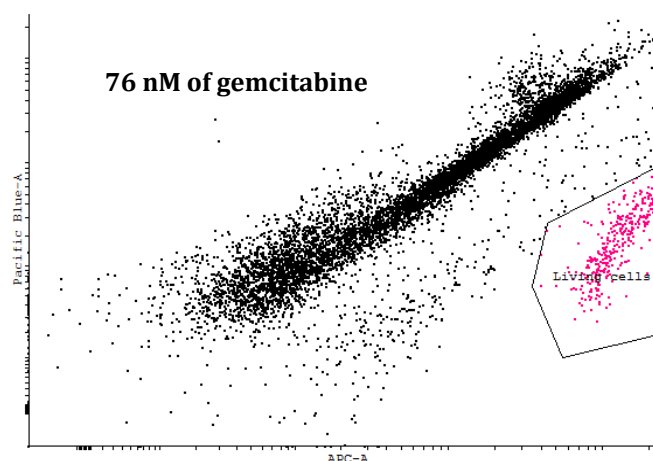
Figure 14: Flow cytometry data of LCL number 240, treated with 76 nM of gemcitabine for 72 h: The determination of living cells (red coloured gate) was performed via Vybrant Ruby and Sytox Blue staining.

3.12   Electrophoretic Mobility Shift Assay

The Electrophoretic Mobility Shift Assay (EMSA) is used for detecting sequence-specific binding of DNA to proteins (e.g. of transcription factors) from nuclear extracts of cells. For detecting the protein binding to the probe, the probe, which is a complementary oligonucleotide probe with a GATC-nucleotide overhang on the 5' terminus, was radioactively labeled with α-^{32}P-dCTP.

3.12.1   Isolation of Nuclear Protein Extracts

For the isolation of nuclear protein extracts from the pancreatic cancer cell lines CFPac, PancI, PaTu8988t and MiaPaca-II the protocol from the *CelLytic™ NuCLEAR™ Extraction Kit* (Sigma, Deisenhofen, Germany) was modified. First, cells were lysed by osmotic pressure so that the cytosolic components move out of the cells. The cytosolic components were separated from membranes and the nuclei by centrifugation steps. To prevent nuclear proteins from leaving the nucleus, sodium-ortho-vanadate (AppliChem, Darmstadt, Germany), an inhibitor of nuclear transporters, was added. At the end, the membrane was destroyed chemically and mechanically so that membrane fragments could be separated from the nuclear proteins by centrifugation. The detailed procedure, which was conducted on ice for the whole time, is described below.

A cell number of at least 1×10^7 was required for the isolation of nuclear protein extract. The cells were harvested and transferred into cooled 50 ml tubes. The tubes were centrifuged at 500 g for 10 minutes at 4 °C. Then, the supernatant was discarded and the

pellet was washed with 10 ml of ice-cold PBS containing sodium-ortho-vanadate to a final concentration of 1 mM. The tube was centrifuged at 500 g for 10 minutes at 4 °C. Again the supernatant was removed and the cells were resuspended with 1.5 ml of ice-cold PBS (containing sodium-ortho-vanadate to a final concentration of 1 mM) and pipetted into a 2 ml reaction tube. The reaction tube was centrifuged at 3000 rpm for 10 minutes at 4 °C. Supernatant removal was performed and the pellet was slowly resuspended in a five-fold packing volume of a buffer based on HEPES/KOH (pH 7.9 at 4 °C, Nuclear Extraction Buffer A, see Table 54), which was supplemented with DTT, PMSF and sodium-ortho-vanadate shortly before use (should not exceed a volume more than 500 µl). The formation of foam should be avoided. The mixture was incubated on ice for 15 minutes. The damage of cells was controlled with the microscope via cell staining with *Trypan blue*. Afterwards, the cells were destroyed mechanically in an oblong glass envelope by usage of a pestle. The mixture was compressed 30 times. Then 10 µl of a 10 % NP-40-solution (nonyl-phenoxypolyethoxylethanol, Sigma) was added per 100 µl of lysed sample and vortexed vigorously for 10 seconds. Thereafter, the sample was centrifuged at 10000 g for 30 seconds. The supernatant contains the cytoplasmic fraction which was discarded. The pellet was absorbed in 2/3 of packing volume (~ 70 µl) of a 20 mM HEPES/KOH buffer (pH 7.9 at 4 °C, Nuclear Extraction Buffer B, see Table 55), which was supplemented with DTT, PMSF and sodium-ortho-vanadate shortly before use. The reaction tube was shaken, fixed on a plate vortexer, at 1800 rpm for 30 minutes at 4 °C in the cooling room. Finally, the mixture was centrifuged at 17,000 g for 5 minutes at 4 °C and the supernatant containing the nuclear proteins was transferred into a new reaction tube, which was stored at -80 °C.

Table 54: Ingredients of Nuclear Extraction Buffer A

Reagent (pH = 7.9, at 4 °C)	Concentration of stock solution [M]	Concentration [mM]
Hepes/KOH	0.5	10
MgCl$_2$	1	1.5
KCl	1	10
DTT *(added shortly before use)*	0.1	0.5
PMSF *(added shortly before use)*		*1 ml of saturated solution*
Sodium-ortho vanadate *(added shortly before use)*	0.2	1
ddH$_2$O		**Ad 100 ml**

Table 55: Ingredients of Nuclear Extraction Buffer B

Reagent (pH = 7.9, at 4 °C)	Concentration of stock solution [M]	Concentration [mM]
Hepes/KOH	0.5	20
Glycerin 85 %		25 %
NaCl	5	420
MgCl2	1	1.5
EDTA	0.5	0.2
NP-40 *(= modification)*		*1 % final concentration*
Na-DOC *(= modification)*		*0.5 % final concentration*
DTT *(added shortly before use)*	0.1	0.5
PMSF *(added shortly before use)*		*1 ml of saturated solution*
Sodium-ortho vanadate *(added shortly before use)*	0.2	1
ddH$_2$O		**Ad 100 ml**

3.12.2 Labeling of probes

Before probe labeling with radioactive α-^{32}P-dCTP, they had to be annealed. The two complementary strands (complementary besides the GATC-nucleotide overhang) were mixed as follows in a 1.5 ml reaction tube (Table 56).

Table 56: Mixture for oligo-nucleotide annealing

Reagent	Added volume [μl]
Oligo_forward (100 μM)	1
Oligo_reverse (100 μM)	1
NaCl (0.5 M)	1
ddH$_2$O	**Ad 50 μl**

This mixture was incubated in one liter of heated water ($\sim$ 95 °C), which was stirred gently with a magnet stirrer with 100 rpm till the water reached room temperature and the oligonucleotides were annealed. Thereafter, the 5' overhang was filled via Klenow-enzyme. During this step, in addition to non-radioactive dATP, dGTP and dTTP-nucleotides, alpha-^{32}P-labeled dCTP was incorporated. The labeling process was performed in the radioactive labour where all safety rules and procedures were followed.

Before entering the radioactive area, the double-stranded oligonucleotides were mixed with dNTPs (A, G, T), a 10x Klenow-buffer and ddH$_2$O on ice (see Table 57). Afterwards, the Klenow-enzyme and α-^{32}P-dCTP were added in the radioactive room and the samples were incubated for 1 hour at 37 °C.

Table 57: Mixture for probe-labeling with alpha-^{32}P-dCTP

Reagent	Added volume [μl]
Double-stranded oligonucleotides (2 pmol/μl)	1
dNTPs (A, G, T each 1 mM)	1
10x Klenow-buffer	2
ddH$_2$O	12
α-^{32}P-dCTP (10 μCi/μl)	2 μl *(added in the radioactive area)*
Klenow-enzyme (1 U/μl)	2 μl *(added in the radioactive area)*
In total	**20 μl**

To separate the labeled oligonucleotides from the not incorporated radioactive and non-radioactive dNTPs, *mini Quick Spin Oligo Colums* (Roche) were used. The sephadex matrix of the columns was homogenized by shaking and vortexing. Thereafter, the lid and the bottom of the column were opened and the column was transferred into a 1.5 ml reaction tube for centrifugation at 3200 g for 2 minutes at room temperature (Biofuge 15 R, Heraeus). Then, the column was placed into a new 1.5 ml reaction tube and the radioactive probe (which was centrifuged before to avoid contamination) was pipetted into the middle of the column and centrifuged again for 4 minutes. The flow-through contained the purified α-^{32}P-dCTP labeled probe. To quantify the radioactivity, 4 ml of safety scintillator (Aquasafe 500 Plus, Zinsser Analytic) was mixed with 1 μl of the probe. This mixture was measured with the scintillation counter LS1801. The radioactivity was detected as *counts per minute* (cpm). For the EMSA experiment 30,000 cpm of the probe were needed to perform the binding reaction. The following table (Table 58) shows the primers, which I radioactively labeled and used for the EMSA experiment.

Table 58: Olionucleotides for the EMSA experiment (*RRM2*)

Name of primer	Sequence (5' → 3')
*RRM2*_v1_1130609-**G (WT)**	GATCCTCTGCTTCGCTGCGCC**G**CCACTATGCTCTCCCTC
*RRM2*_v1_1130609-**C (WT)**	GATCGAGGGAGAGCATAGTGG**C**GGCGCAGCGAAGCAGAG
*RRM2*_v1_1130609-**T (Var)**	GATCCTCTGCTTCGCTGCGCC**T**CCACTATGCTCTCCCTC
*RRM2*_v1_1130609-**A (Var)**	GATCGAGGGAGAGCATAGTGG**A**GGCGCAGCGAAGCAGAG

3.12.3 The binding reaction

An amount of 20 μg of the nuclear extract was mixed and incubated with a 4x binding buffer (see Table 59), poly dI-dC (poly deoxyinosinic-deoxycytidylic, unspecific competitor to avoid unspecific protein binding) and ddH_2O for 10 minutes on ice (see Table 60). Afterwards, the respective radioactive probe (30,000 cpm) was added to the binding reaction mixture (performed in the radioactive area).

Table 59: 4x Binding buffer

Reagent (pH = 7.9, at 4 °C)	Concentration [mM]
Hepes (pH 7.8)	80
EDTA (pH 8)	4
DTT	2
Glycerin	40 %
KCl	560

Table 60: Mixture for the binding reaction

Reagent	Added volume [μl] or amount [μg]
4x binding buffer	5
Nuclear protein extract	20
Poly dI-dC (1μg/μl)	2
ddH$_2$O	**Ad 18 μl**

After an incubation time of 15 minutes, 4 μl of a 6x loading dye (see Table 61) was added and the samples were loaded on a 5 % native non-denaturating polyacrylamide gel (see 3.12.4).

Table 61: 6x loading dye

Reagent (-20 °C)	Concentration [%]
Glycerol 87 %	30 (v/v)
Bromphenol blue	0.25 (w/v)
Xylene Cyanol FF	0.25 (w/v)

3.12.4 Non-Denaturating Polyacrylamide Gel Electrophoresis

The polyacrylamide gel was equilibrated in 0.5 % TBE-buffer (dilution of 5x buffer, see Table 63) for 1 hour with 180 V before usage. After sample loading, the gel was run for 1.5 hours with the same voltage. The polyacrylamide gel was prepared as follows (Table 62):

Table 62: 5 % Polyacrylamide Gel

Reagent	Added Volume [ml]
40 % (w/v) Acrylamide/Mix 27:5:1	4.4
5x TBE	3.5
ddH$_2$O	27
APS 10 % (w/v)	0.350 *(added in the end → gel forming process)*
TEMED	0.035 *(added in the end → gel forming process)*

Table 63: 5x TBE buffer

Reagent (pH = 8)	Concentration [mM]
Tris	450
Boric acid	450
EDTA	10

After electrophoresis, the gel was laid on two *Whatman* paper (Schleicher und Schüll, Dassel) and was covered with a wrapping film. The drying process was performed on a vacuum-gel-drying-system at 80 °C for one hour. For visualizing the bands the gel was placed in a cassette, covered with a Fujifilm BAS1500 plate overnight. The radioactive signals were detected in a PhosphorImager (Raytest, Sprockhövel) by using the software *BASreader* and *AIDA* (Version 4.15.025, Raytest, Sprockhövel). In addition, the gel was put in a cassette with an x-rayfilm (Hyperfilm MP (18 × 24 cm), GE Healthcare) for 7 - 10 days at -80 °C. To develop the x-rayfilm the x-ray-developer G150 und fixer G354 (AGFA, Leverkusen) were used in the darkroom. The signals were quantified by using the Fluor-STM MultiImager (BioRad, Hercules, CA, USA).

3.12.5 Cold Competition Experiment

To assess the specificity of a protein binding, cold competition experiments were conducted. Therefor, non-radioactive labeled samples were added with an excess (5- till 100-fold) to the mixture for the binding reaction (see chapter 3.12.3, Table 60), after the binding reaction was incubated for 10 minutes. Thereafter, this mixture was again incubated for 10 minutes before adding the radioactive probe in the radioactive area. Specific binding is indicated by loss of factor binding to the radioactively labeled probe.

The cold competition procedure was performed for investigation of binding specificity between the different alleles of the *RRM2* SNP rs1130609 located in the 5' region.

3.13 Statistical analysis

EC_{50} values for individual LCL proliferation inhibition by gemcitabine were calculated by a three-parameter Gompertz model based on dose-response effects for eight gemcitabine concentrations (0, 1.9, 3.8, 6.4, 10.8, 18.1, 30.4, and 76.0 nM). Suitability of this model fit was proven by r^2 values > 0.95 for 88 LCLs and $r^2 = 0.93$ for one LCL.

Descriptive statistics include data characterization by their distribution and visualization. Error bars and dot plots were used for parametric, box plots for non-parametric presentation of cumulative data. Single data point correlations were visualized by scatter plots.

All analytical testing was carried out two-sided. By default, threshold for statistical significance was set at $p < 0.05$ not accounting for multiplicity testing. Correction for multiple testing did not apply for the functional effects of the single investigated SNPs, for which clear hypotheses were deduced from clinical association data. However, in case of mechanistic studies apart from defined SNP effects the numbers of statistical tests according to the investigated parameters should be considered when interpreting the reported p-values. Applicability of parametric tests was assessed by compatibility of data with normal distribution (if $p > 0.05$ according to Shapiro-Wilk test). In some cases, this assumption could be matched by data log-transformation (e.g. EC_{50} values for gemcitabine in LCLs). If no compatibility with normal distribution could be achieved non-parametric testing was applied.

Regarding the presented correlation data, in each case normal distributions of the

respective two parameters could be assumed. Thus, correlation coefficients according to Pearson are reported. Differences between paired samples (e.g. RNA expression before and during chemotherapy) were assessed using the Wilcoxon signed rank test. Treatment effects between two groups in pancreatic cancer cell lines were evaluated by t-test without assuming equal variances. Genotype effects on functional parameters were assessed by Mann-Whitney U testing for two groups, and by Jonckheere-terpstra test for three group comparisons. Statistical testing was performed using SPSS, version 12.0 (IBM, IL, USA).

4 Results

An earlier analysis of our research group identified genetic single nucleotide polymorphisms in the *WWOX* and *RRM2* genes by genotyping germline DNA samples isolated from peripheral blood cells (Roppel 2013, Zimmer 2013)*. These SNPs were associated with the overall survival of patients treated with gemcitabine. Below, firstly all experimental data concerning the *WWOX* polymorphism are presented, followed by the data concerning the *RRM2* polymorphisms.

4.1 The SNP rs11644322 association with the overall survival suggesting relevance of *WWOX* in pancreatic cancer and gemcitabine treatment

The variant *A* allele at the *WWOX* SNP rs11644322 (G > A) site was found associated with a worse clinical outcome in patients treated with gemcitabine for PDAC (Roppel 2013). Therefore, I set out for detailed functional assessment of this SNP in my thesis. That included a presumed specific functional role of the *WWOX* rs11644322 SNP site, but also experiments aiming at elucidation of the role of *WWOX* in gemcitabine therapy in general.

4.1.1 Modulation of gemcitabine sensitivity by *WWOX* rs11644322

The hypothesis was tested whether the *WWOX* index SNP affects cellular sensitivity to cytostatic drugs. Therefore, dose-response effects were examined in a panel of 89 LCLs employing different concentrations of gemcitabine (0, 1.9, 3.8, 6.4, 10.8, 18.1, 30.4, and 76.0 nM). For each cell line, EC_{50} values were calculated as described in the Methods section (see section 3.11.5). Gemcitabine sensitivity was found to be modulated by rs11644322. The *A* allele was associated with increased resistance toward gemcitabine ($p = 0.002$, see Figure 15). This finding is accordant to the clinical observation in which carriers of this *A* allele experienced shortened overall survival (see section 1.5.2, Figure 5)*.
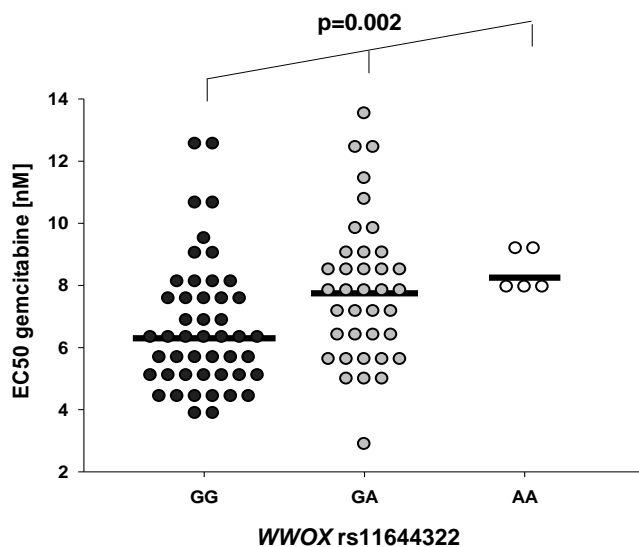
Figure 15: Impact of *WWOX* rs11644322 on cellular gemcitabine sensitivity of lymphoblastoid cell lines. EC_{50} values representing cellular sensitivity towards gemcitabine in relation to the three genotype configurations at rs11644322. Out of 89 LCLs, 47 harbored *GG* genotype, 37 *GA,* and 5 AA. EC_{50} data were calculated by a three-parameter Gompertz model for proliferation inhibition determined by flow cytometry-recorded CFSE staining based on dose-response effects of gemcitabine concentrations at 0, 1.9, 3.8, 6.4, 10.8, 18.1, 30.4, and 76.0 nM. Statistical differences were assessed by the non-parametric Jonckheere-Terpstra trend test with given p-value referring to two-sided testing. This figure was generated with Sigma Plot, version 12.

4.1.2 *WWOX* expression in relation to the rs11644322 SNP site

4.1.2.1 Location of the rs11644322 SNP site

The SNP *WWOX* rs11644322 with a minor allele frequency (MAF) of 26.1 % is located in the immense intron 8 (776656 bp long) separating exon 8 and 9 (see Figure 16 for full length transcript). GeneBank entries (http://www.ncbi.nlm.nih.gov/gene/) suggest several alternative transcripts of *WWOX* terminating within intron 8.
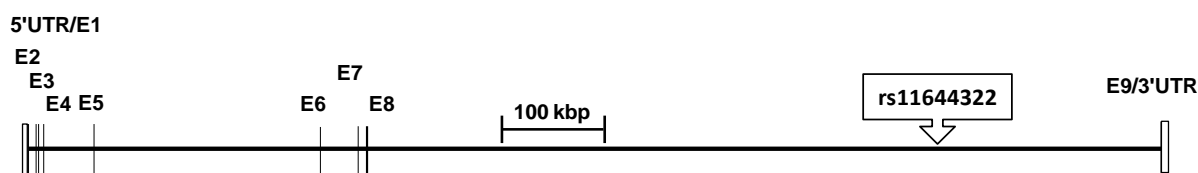
Figure 16: Genetic architecture at the *WWOX* locus. Information was taken from NCBI GeneBank (see assembly GRCh38.p2). The coding region contains 9 exons, the first and the last one flanked by the 5' and the 3'-untranslated region (UTR), respectively. The vertical lines represent the exons. The location of the index SNP rs11644322 in intron 8 is marked. Proportionality of sizes and distances are retained. The vertical lines denoted with E1 - E9 represent the protein coding exons.

4.1.2.2 *WWOX* expression of exons flanking the index SNP

As illustrated in Figure 16, rs11644322 is flanked by the exons 8 and 9 of *WWOX*. Transcription of this region was compared with that of exon 4-6, considered as core *WWOX* region. For absolute quantification of the expression ratios between these two *WWOX* coding regions a cDNA comprising entire *WWOX*, was cloned as reference (see

3.5.1). Expression analysis (see 3.6.4) in 88 LCLs (for one cell line reverse transcription failed) identified a mean transcription rate of 67 % for exon 8-9 compared to the core coding region (see Figure 17, bar plot), indicating the presence of the last exon in the majority of *WWOX* transcripts. In addition, a substantial intra-cell line correlation between the expression of these two *WWOX* regions was verified, which even increased upon gemcitabine exposure (Figure 17).
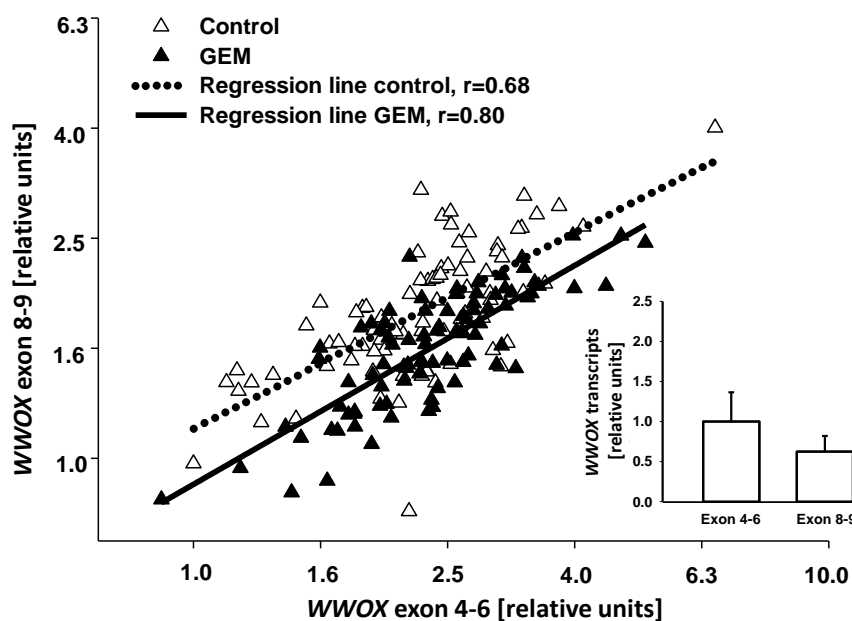
Figure 17: Expression of the last exon in relation to that of the core *WWOX* coding region. The mRNA expression of the terminal exon 9 (captured by an exon 8/exon 9-spanning primer pair) was compared with the major part of the coding region (represented by an exon 4/exon 5/exon 6-spanning primer pair). The graphs summarize the data obtained with 88 lymphoblastoid cell lines (for one cell line reverse transcription failed) treated either with PBS only (baseline) or with 30 nM of gemcitabine at 37 °C for 24 h. The scatter plot illustrates expression correlation between regions 4-6 and 8-9. Both axes are displayed in $\log_{10}$-scale, by which normal distributions of the data could be assumed. The respective regression lines with the Pearson correlation coefficient r are indicated. All expression data were referred to the cell line with the lowest transcript numbers for exon 4-6 under basal conditions (set to "1"). To account for inter-sample heterogeneity, expression data were normalized to a weighted mean of five reference genes (*B2MG, GAPDH, HPRT1, UBC, 36b4*). The lower right insert illustrates the quantitative transcript numbers of the last *WWOX* exon in relation to the core coding region of which the mean over the entire LCL cohort was set to "1" (error symbols denote one SD). This figure was generated with Sigma Plot version 12.

4.1.2.3 Impact of rs11644322 SNP on *WWOX* regional transcription

It should be delineated whether the *WWOX* SNP rs11644322 affects transcription of exon 4-6 and 8-9. Presence of the *AA* genotype at the index SNP site was accompanied by lower transcription of both *WWOX* regions, with and w/o gemcitabine (Figure 18). However, no significant change in *WWOX* gene expression could be detected between *GG* and *GA* genotypes in the present experimental setting with short-term incubation time of 24 h.
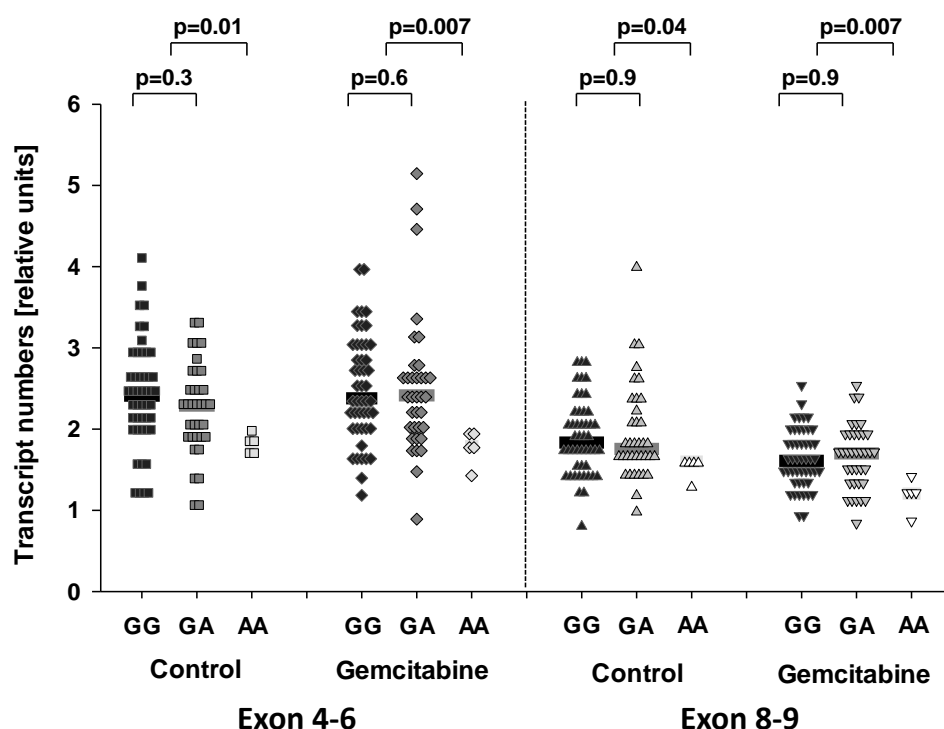
Figure 18: Impact of rs11644322 SNP on *WWOX* regional transcription (exon 4-6/8-9). The left side of the image refers to the central coding region (exon 4-6), the right to that of exon 8-9, each for baseline conditions and upon 30 nM gemcitabine incubation for 24 h at 37 °C. The median value for each group is highlighted by a horizontal grey-shaded line. Statistical differences between two groups were assessed by the non-parametric Mann-Whitney U test. The lower line of p-values refers to testing between *GG* and *GA* genotype, the upper one between combined *GG* and *GA* versus *AA* configuration. This figure was generated with Sigma Plot version 12.

4.1.2.4 Whole transcriptome analysis around the *WWOX* index SNP

As located far distant from exon 8 and 9, it was suggested that the rs11644322 site might be involved in regulation of non-coding RNA expression. To discover non-coding RNAs vicinal to the index SNP, whole transcriptome analysis (RNAseq, see 3.6.5) was undertaken. For two pooled RNA probes from LCLs, carrying the *GG* vs. *AA* genotype at rs11644322, there was no coverage around the index SNP site (see Figure 19).

This observation demonstrates that there are no transcripts encoded in the genetic vicinity of rs11644322.
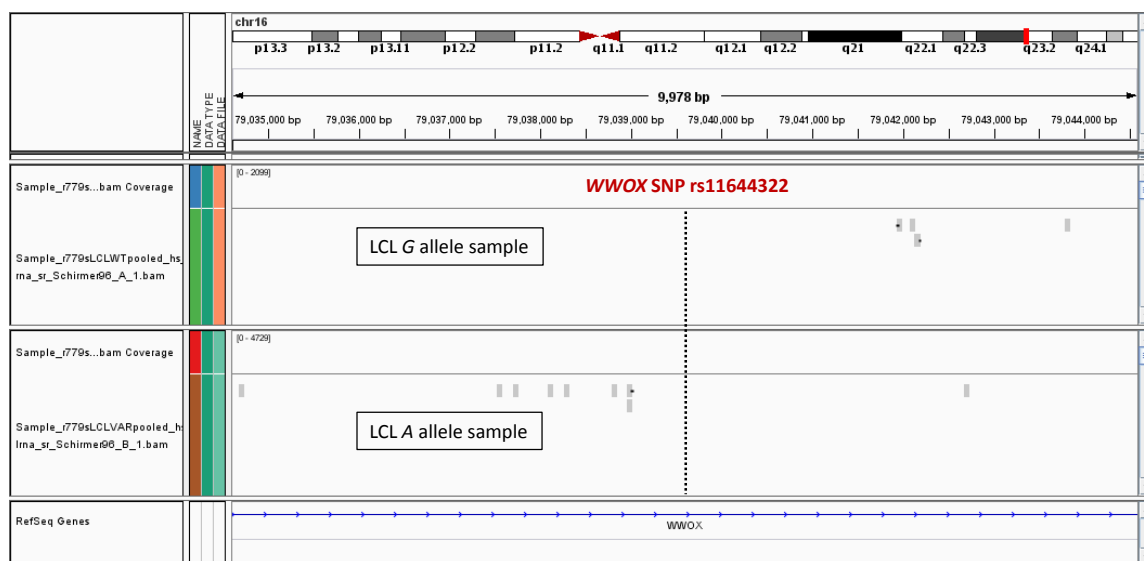
Figure 19: Whole transcriptome analysis around rs11644322. Data were analyzed by RNA sequencing of two pooled LCL samples containing the homozygous *G* (upper panel) or the *A* (lower panel) allele at rs11644322 with each pool consisting of RNA of five LCLs (cell identifiers at the Coriell institute for G allele: HG00096, HG00109, HG00120, HG00244, and HG00258; for A allele: HG00100, HG00108, HG00122, HG00245, and HG00265). Genomic sequences ± 5000 bp around the index SNP (marked with a dashed line) are shown.

Likewise, in the pancreatic cancer cell lines PaTu8988t, MiaPaca-II, and AsPC1 no reads or only reads at very low amounts, not distinguishable from technical noise (< 0.5 reads/kilobase of transcript/per million mapped reads), could be observed within a range of ±1 Mbp referred to the index SNP rs11644322.

4.1.2.5 Global transcriptome stratified for rs11644322

Five pooled LCLs each with *GG* or *AA* genotype at rs11644322, not exposed to gemcitabine, were subjected to global transcriptome analysis. Out of all identified and annotated transcripts only six showed differential expression of more than 2-fold (see Table 64). Compared with *GG*, transcription in cells with *AA* genotype was lower for *TIMP2* and *SEMA3C* and higher for *RNA5-8SP2*, *IGHA1*, *AL161626.1*, and *RNA5-8SP6*. The most pronounced ratio was observed for *RNA5*-8SP2 (ribosomal pseudogene). For this transcript, which is located on chromosome 16 like *WWOX*, correlation with EC_{50} values for gemcitabine and with *WWOX* expression was evaluated in the entire set of 89 LCLs. However, expression of *RNA5-8SP6* was neither related to EC_{50} for gemcitabine nor to *WWOX* expression (core region and last exon).

Table 64: Expression profile in LCL samples in dependence of *WWOX* rs11644322. Five non-treated LCLs each with homozygous wild-type (Coriell ID HG00096, HG00109, HG00120, HG00244, and HG00258) and homozygous variant allele (HG00100, HG00108, HG00122, HG00245, and HG00265) configuration at rs11644322 were pooled. This table lists all transcripts differing by a log2-fold change of at least 2.0 between these two groups. Data were obtained by sequencing of total RNA. Transcript data refer to RPKM values. RPKM-normalized transcripts for *AA* at rs11644322 were divided by those for *GG* genotype.

Transcript notation	Rs11644322_*GG* [RPKM]	Rs11644322_*AA* [RPKM]	Ratio *AA/GG*
TIMP2	1.50	0.18	0.12
SEMA3C	1.50	0.25	0.16
RNA5-8SP2	15.0	1653	110
IGHA1	28.14	503	17.9
AL161626.1	1757	10429	5.94
RNA5-8SP6	373	28728	77.1

4.1.3 Consequences of *SP1* overexpression for cytostatic drug sensitivity

Previously, weaker SP1 binding for the minor *A* allele at the *WWOX* rs11644322 site was identified and hypothesized to be linked to poor cytostatic response (Roppel 2013). Based on this finding, I investigated the functional consequences of *SP1* overexpression on cytostatic drug sensitivity in the pancreatic cancer cell lines AsPC1, MiaPaca-II and PancI. First, time kinetics analysis in the model cell line HEK-293 were conducted to establish proper transfection conditions. Following 48 hours upon transfection (see Methods *SP1* transfection, chapter 3.10.3), high amounts of *SP1* transcripts were detected (Figure 20). Thus, this time point was selected for starting drug exposure lasting for additional 24 h.

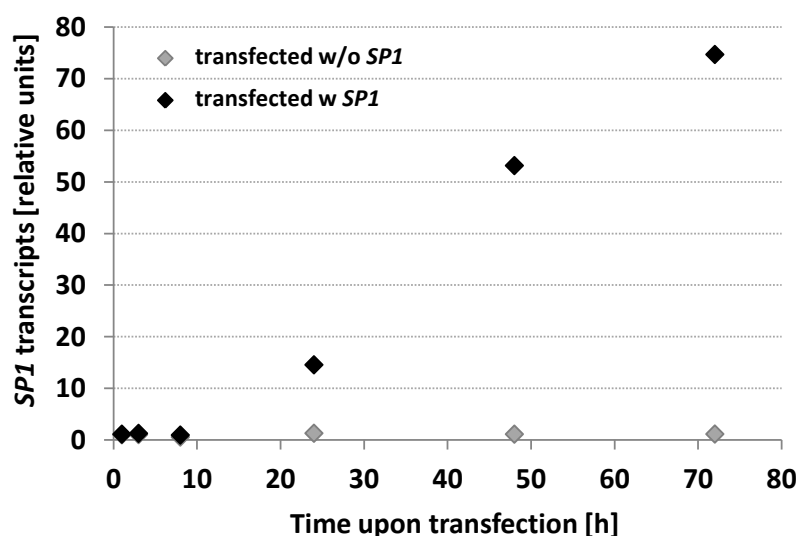**Figure 20: Time kinetics of *SP1* overexpression.** Here, easily tranfectable HEK-293 cells were used. *SP1* gene expression was assayed 1, 3, 8, 24, 48 and 72 hours upon transfection of pcDNA3 vector with and without *SP1* coding sequence. These data were normalized to a weighted mean of three reference genes (*36b4, UBC, HPRT1*) and referred to the first time point (1 h) upon vector transfection without *SP1*.

SP1 transfection resulted in different effects on *WWOX* transcription in various pancreatic cancer cell lines (see Figure 21). Expression of *WWOX* exon 4-6 appeared to be reduced by about 40 % and 20 % in AsPC1 and PancI, respectively, and induced by 70 % in MiaPaca-II. However, none of these observations based on three independent experimental series reached statistical significance. Concerning *WWOX* 8-9 transcripts, which were about 30 % in regard to *WWOX* exon 4-6 in AsPC1, 85 % in MiaPaca-II and absent in PancI without *SP1* overexpression, were not altered substantially upon *SP1* transfection.
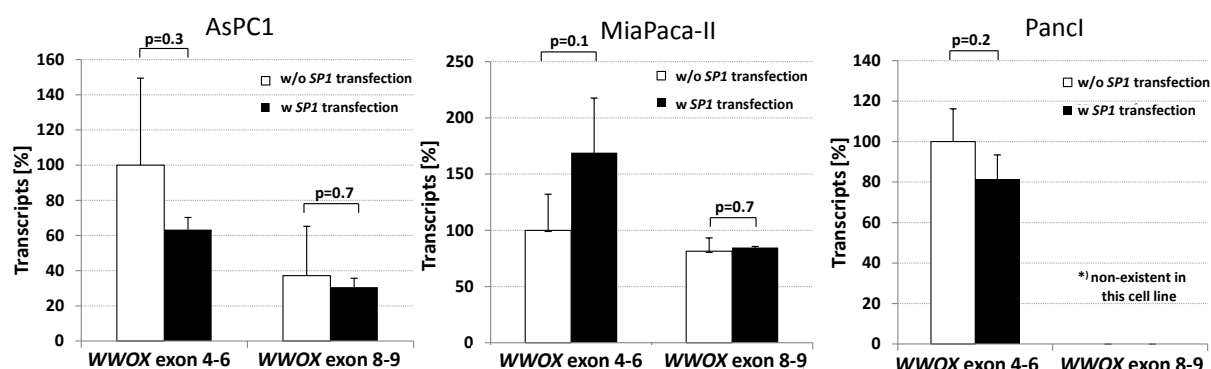
Figure 21: Impact of *SP1* overexpression on *WWOX* transcription. In each of the three investigated cell lines (AsPC1, left panel), MiaPaca-II (center), and PancI (right) expression of *WWOX* exon 4-6 and 8-9 region was quantified upon transfection of pcDNA3 vector with and w/o *SP1* and subsequent incubation at 37°C for 72 h. *WWOX* expression data were normalized to a weighted mean of three reference genes (*36b4, UBC, HPRT1*) and then referred to exon 4-6 expression w/o *SP1* transfection. Bars represent mean values of three independent experiments and the errors the respective standard deviations. Statistical differences between two groups were assessed by t-test without assuming equal variances.

In AsPC1 and MiaPaca-II cells, which exhibited detectable amounts of *WWOX* exon 8-9 transcripts, cytostatic drug effects on expression of the two interrogated *WWOX* regions elicited mostly similar (Figure 22, panel A and B). In PancI, in which transcription of the exon 8-9 region was below the detection level, conditions with and w/o *SP1* overexpression were compared for expression of the exon 4-6 region (Figure 22, panel C). In this cell line *WWOX* expression was not much affected by the tested cytostatics (besides a moderate increase induced by the lower gemcitabine concentration). In contrast, irinotecan exhibited a strong *WWOX* suppression in *SP1*-overexpressing AsPC1 and MiaPaca-II cells, regardless of the considered *WWOX* region. Respective assessment in AsPC1 without *SP1* transfection revealed similar effects for irinotecan albeit to a lesser extent. Intriguingly, gemcitabine elicited cell line-specific effects with differential affections of the *WWOX* region considered. In AsPC1, expression of the *WWOX* core region was substantially suppressed by gemcitabine whereas that of the last exon

remained virtually unaltered in relation to a drug-free control. In contrary, respective analysis in MiaPaca-II revealed a slight induction of both investigated *WWOX* regions. 5-FU, however, did not modify *WWOX* transcription neither in AsPC1 nor MiaPaca-II.
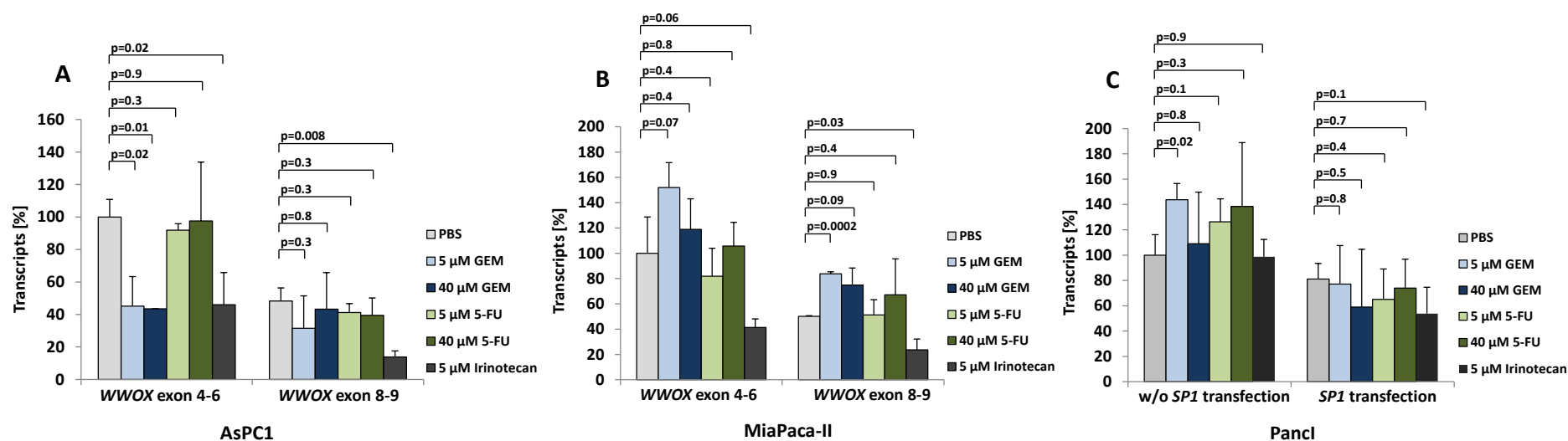
Figure 22: Modulation of *WWOX* transcription by cytostatics upon *SP1* overexpression. Experimental design was accordingly to Figure 21 with additional cytostatic treatments at the indicated drug concentrations 48 h following *SP1* transfection (i.e. drugs were present in the last 24 h period of the entire 72 h incubation at 37°C since *SP1* transfection). Drug effects were each referred to treatment with PBS and statistically assessed by t-test without assuming equal variances. Note that for AsPC1 (panel A) and MiaPaca-II (panel B), data for both transcript regions upon *SP1* overexpression are displayed (data referred to *WWOX* 4-6 expression upon PBS treatment). In case of PancI (panel C), in which *WWOX* exon 8-9 expression was not detectable, drug effects on *WWOX* exon 4-6 are illustrated w/o and with *SP1* transfection (data referred to pcDNA3 transfect w/o *SP1* and PBS treatment). With regard to reported p-values, the number of statistical tests according to the investigated parameters might be considered for interpretation.

4.1.4 *WWOX* in the context of apoptosis-related genes

After successful testing of normal distribution (p > 0.05 according to Shapiro-Wilk test for deviation from normal) bivariate correlation analysis of *WWOX* exon 4-6 transcripts with the EC_{50} values of gemcitabine were conducted in LCLs. A weak correlation was identified under basal conditions and appeared intensified after an incubation time of 72 h with 30 nM of gemcitabine (r = 0.34, p = 0.001, see Figure 23). For *WWOX* exon 8-9 correlation tendencies were the same, but less pronounced (r = 0.14, p = 0.2 at baseline level, r = 0.30, p = 0.005 at 30 nM of gemcitabine).
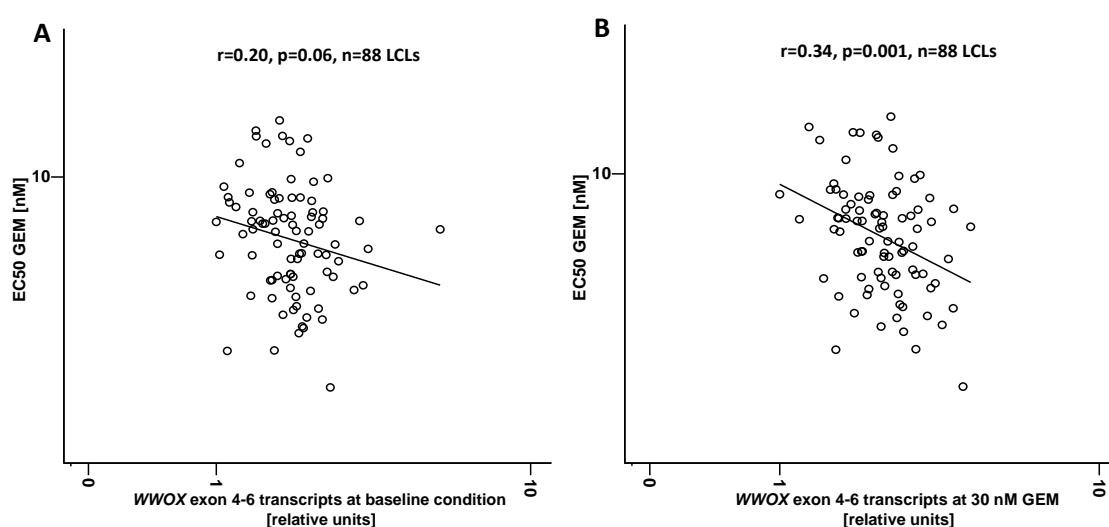
Figure 23: Correlation of *WWOX* exon 4-6 transcripts with EC_{50} values of gemcitabine. Data were based on 88 LCLs. For cell line number 247 the RNA content upon isolation was low and thus genes at low expression level like *WWOX* could not be determined. Panel A refers to baseline conditions, panel B illustrates the correlation at 30 nM of gemcitabine. Transcript numbers were normalized to the weighted mean of *36b4, B2MG, GAPDH, HPRT1* and *UBC*. P-values are according to the Pearson correlation coefficient r. EC_{50} values and expression data are denoted in a $\log_{10}$-scale. A linear regression line is delineated.

Due to the observed link between *WWOX* expression and cellular gemcitabine sensitivity an interaction with apoptosis-related genes was supposed. Therefore, expression between *WWOX* and three genes, related to apoptosis, was correlated in LCLs (see Table 65). One of those genes, *BCL2* (B-cell lymophoma 2), is known to inhibit apoptosis (JACOBSON *et al.* 1993), the second, *TP53* (Tumor protein p53), promotes apoptosis (FRIDMAN AND LOWE 2003), and the third, *GADD45A* (Growth Arrest And DNA-Damage-Inducible, alpha), fosters cell cycle arrest upon genotoxic stress and may be a crucial component in orchestrating DNA damage repair (SCHAFER *et al.* 2010, BARRETO *et al.* 2007).

Table 65: Expression correlation of *WWOX* with *BCL2*, *GADD45A*, and *TP53*. Correlation coefficients and p-values according to Pearson are listed for *WWOX* exon 4-6 and *WWOX* exon 8-9 each for baseline condition and at 30 nM gemcitabine.

Gene	*WWOX* exon 4-6		*WWOX* exon 8-9	
	Baseline	**at 30 nM GEM**	**Baseline**	**at 30 nM GEM**
BCL2	r = 0.07, p = 0.5	r = 0.15, p = 0.2	r = 0.09, p = 0.4	r = 0.16, p = 0.1
GADD45A	r = 0.08, p = 0.5	r = 0.36, p = 0.001	r = 0.16, p = 0.2	r = 0.41, p = 6×10^{-5}
TP53	r = 0.20, p = 0.06	r = 0.32, p = 0.002	r = 0.36, p = 0.001	r = 0.16, p = 0.1

Regarding the *BCL2* gene, no correlation was detected, neither with the *WWOX* core region nor with the last exon. Interestingly, *GADD45A* was substantially correlated with *WWOX* exon 4-6 and to an even stronger extent with *WWOX* exon 8-9 region upon exposure to gemcitabine, but not at baseline condition. Moreover, *GADD45A* transcription upon gemcitabine elicited highly correlated with EC_{50} of gemcitabine, but again no relationship was observed for baseline *GADD45A* expression (see Figure 24). In contrast, a different correlation pattern between the two *WWOX* transcript regions and *TP53* was noticed: Upon gemcitabine exposure, the correlation with the *WWOX* core region increased and that with the last exon decreased.
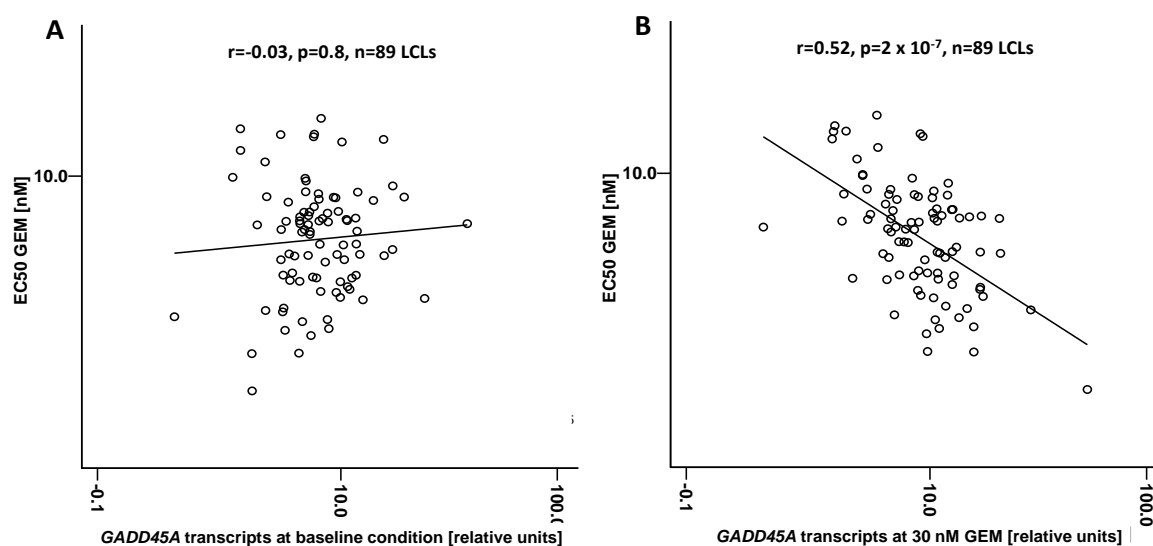
Figure 24: Correlation of *GADD45A* transcripts with EC_{50} values of gemcitabine. Data was based on 89 LCLs. Panel A refers to baseline conditions, panel B shows the correlation at 30 nm of gemcitabine. Transcript numbers were normalized to the weighted mean of *36b4, B2MG, GAPDH, HPRT1* and *UBC*. P-values are according to the Pearson correlation coefficient r. EC_{50} values and expression data are denoted in a $\log_{10}$-scale. A linear regression line is delineated.

4.1.5 *WWOX* and cytotoxicity of gemcitabine

As the SNP rs11644322 was identified as related to cellular gemcitabine sensitivity in LCLs (chapter 4.1.1) and to *WWOX* expression (see chapter 4.1.2.3) it was hypothesized that *WWOX* enhances cytotoxicity of gemcitabine. Therefore, the correlation between *WWOX* expression level and cytotoxicity of gemcitabine was examined.

WWOX transcript numbers were negatively correlated with the EC_{50} value of gemcitabine in LCLs (see Figure 25). A negative correlation implies that higher *WWOX* expression is accompanied by lower EC_{50} values for gemcitabine resulting in increased sensitivity. Expression changes of *WWOX* upon gemcitabine exposure further strengthened this correlation with EC_{50}.
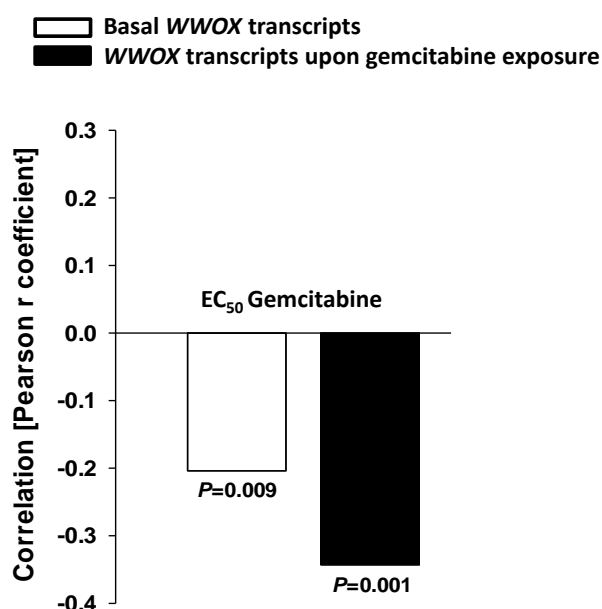
Figure 25: Correlation of *WWOX* transcripts with EC_{50} values of gemcitabine. Data are based on the same 88 LCLs as in Figure 17 (section 4.1.2.2). (For cell line number 247 the RNA content upon isolation was low and thus genes at low expression level like *WWOX* could not be determined.) Shown correlations refer to *WWOX* transcripts of the E4-6 region and were very similar for E8-9. Transcript numbers were normalized to the weighted mean of *36b4, B2MG, GAPDH, HPRT1*, and *UBC*. P-values are according to the Pearson correlation coefficient r which is displayed on the y-axis. Note that a negative correlation means higher *WWOX* expression and is accompanied by lower EC_{50} values, i.e. increased sensitivity toward cytotoxic effects. Gemcitabine was administered at 30 nM for 24 h at 37 °C prior to RNA harvesting. These drug concentrations were chosen about 5-fold higher than mean EC_{50} observed upon 72 h drug exposure (see Figure 15, section 4.1.1). This figure was generated with Sigma Plot version 12.

4.1.6 Drug sensitivity upon knock-down or overexpression of *WWOX*

4.1.6.1 *WWOX* knock-down via siRNA

SiRNA-mediated *WWOX* knock-down (see chapter 3.10.1) in the two pancreatic cancer cell lines PaTu8988t and L3.6 was performed to figure out whether *WWOX* directly affects gemcitabine sensitivity. A successful knock-down of WWOX protein expression was demonstrated for both cell lines, as shown by Western blotting (see 3.8.3 and Figure 26).

A

B
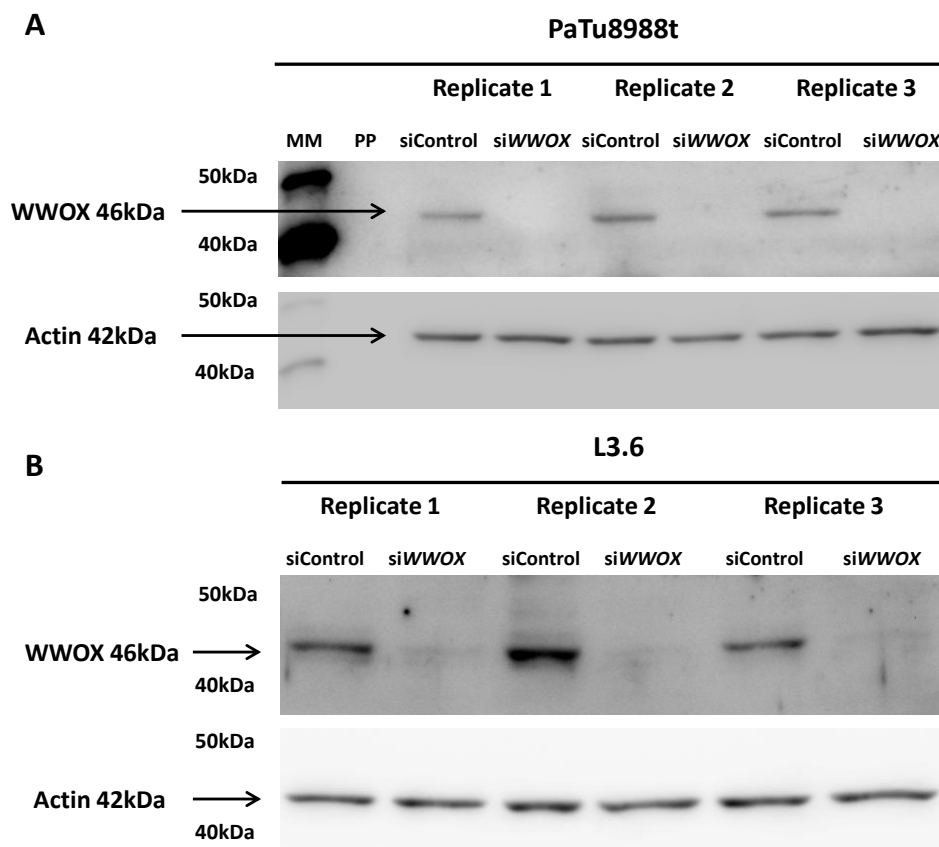
Figure 26: Western Blotting for siRNA knock-down in adenoductal pancreatic cancer cell lines PaTu8988t (A) and L3.6 (B). Actin was used as reference. "MM" = MagicMark™ XP, "PP" = pre-stained protein marker (see methods "Western Blot"). The images show samples from three independent experiments. Note that for L3.6 the marker bands were hidden from imaging to get visible bands for WWOX, which is weakly expressed in this cell line.

For both cell lines, a distinct decrease in basal proliferation was observed after *WWOX* siRNA transfection compared to control siRNA (see Figure 27).
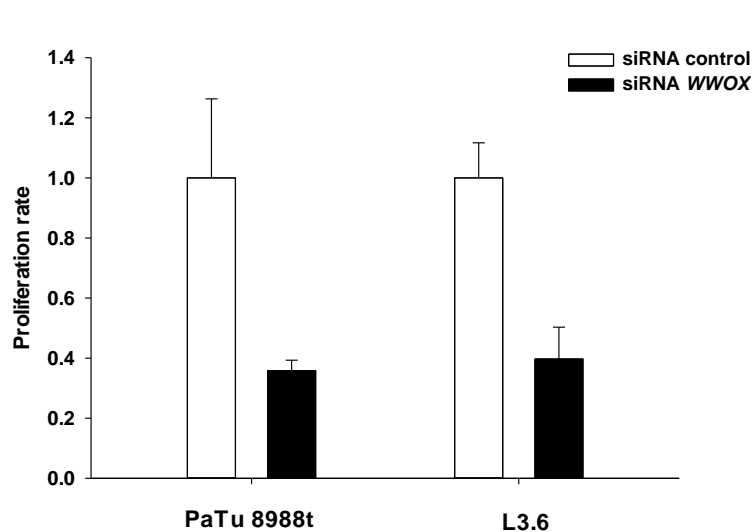
Figure 27: *WWOX* knock-down by siRNA. Effects of *WWOX* knock-down on basal proliferation rates of the two adenoductal pancreatic cancer cell lines PaTu8988t and L3.6. Cells were transfected either with a panel of four siRNAs intended to target *WWOX* or with a scrambled panel of unspecific siRNAs as control. Total incubation time upon siRNA transfection was 96 h before *PrestoBlue*® was added and recorded (recorded in methods part 3.10.4). Bars represent means of three independent experiments with the errorbars indicating one standard deviation. This figure was generated with Sigma Plot version 12.

The impact of *WWOX* knock-down on 5-FU response was moderate in the two investigated cell lines. In gemcitabine treated L3.6 cells, *WWOX* depletion moderately decreased the gemcitabine sensitivity, whereas in PaTu8988t cells an intensified resistance was recorded under knock-down conditions (see Figure 28). These findings hypothesize that the impact of *WWOX* expression on gemcitabine sensitivity differs among different pancreatic cancer cell lines.
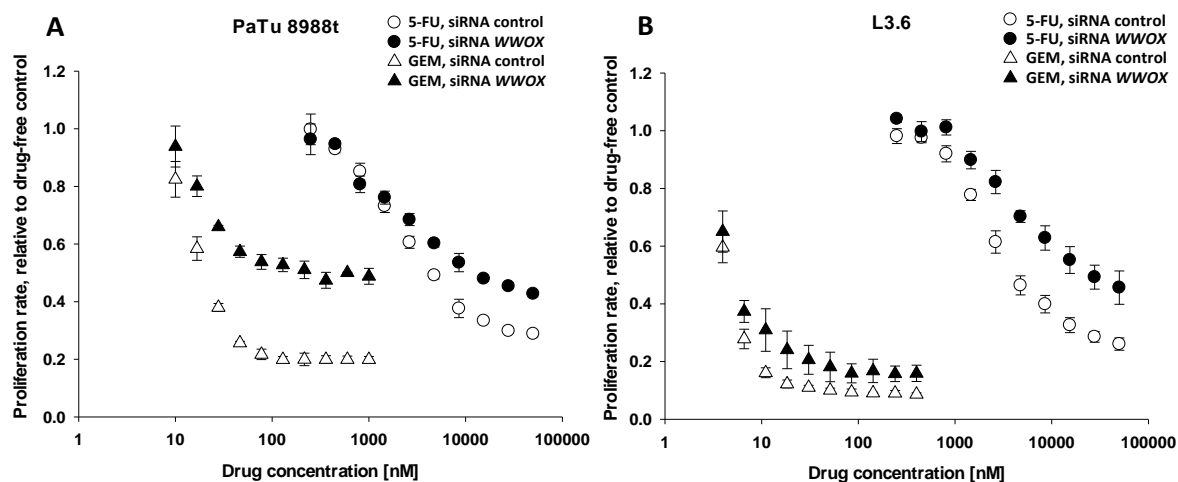
Figure 28: Consequences of *WWOX* knock-down on cytostatic drug sensitivity. Panel A displays data for the PaTu8988t and panel B for the L3.6 cell line. Drug concentrations are denoted in a $\log_{10}$-scale. Data for gemcitabine are shown as triangles (open ones for control siRNA, filled ones for siRNA against *WWOX*), for 5-FU analogously as circles. For each transfection condition and each drug, the proliferation rate for a drug-free control was set to 1.0 to which the indicated drug concentrations were each referred to. Data represent means of three independent experimental series with one standard deviation, indicated as error symbols. Within each series, each single condition was assayed in quadruplicates of which median values were taken for analysis. This figure was generated with Sigma Plot version 12.

4.1.6.2 WWOX knock-down via shRNA

The consequences of stable *WWOX* knock-down were addressed in PaTu8988t cells (see section 3.10.2). Three stably transfected clones showed more than 50 % suppression of *WWOX* expression (see Figure 29).
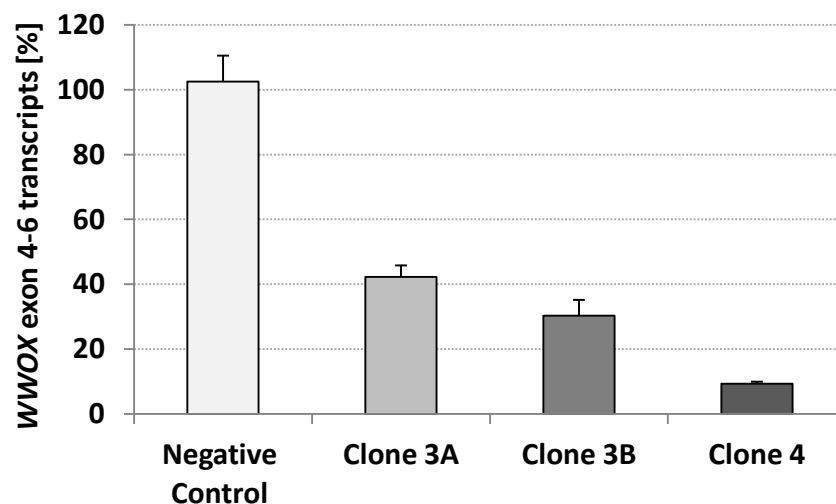
Figure 29: *WWOX* exon 4-6 expression upon suppression by shRNA. PaTu8988t cells were transfected with different shRNA plasmids targeting *WWOX* or an unspecific shRNA negative control. Clone 3A and 3B represent two subclones of a common shRNA transfection. Clone 4 was derived from a different shRNA against *WWOX*. Four different subclones of one negative control transfection were established. Expression data were normalized to the weighted mean of three reference genes (*36b4, UBC, HPRT1*) and were then referred to the unspecific shRNA negative control. Bars indicate mean values of three independent measurements and errors the respective standard deviation.

The knock-down of WWOX protein expression was affirmed by Western Blot performance (see Figure 30 and section 3.8.3). A more efficient knock-down was identified for Clone 4, which also featured the strongest knock-down on *WWOX* exon 4-6 expression level (see Figure 29).
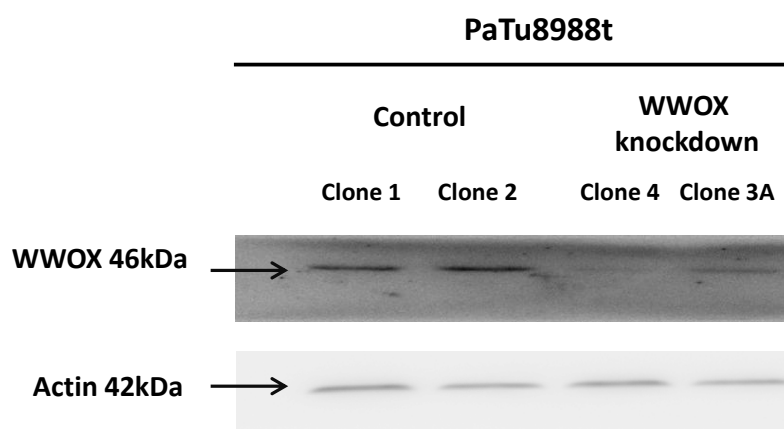
Figure 30: Western Blotting to demonstrate WWOX knock-down by shRNA. Actin was used as reference. Two clones each for shRNA negative control and shRNA *WWOX*-targeting transfection are displayed. The numbering of WWOX knock-down clones refers to Figure 29.

WWOX knock-down by shRNA (clone 4 in Figure 29 and Figure 30) surprisingly did not alter gemcitabine sensitivity (see Figure 31, panel A). However, additional siRNA-transfection of this shRNA-transfected clone resulted in profound resistance to gemcitabine (see Figure 31, panel B) in a similar extent as observed for siRNA-only knock-down of *WWOX* in PaTu8988t cells (compare with Figure 28, panel A in section 4.1.6.1).
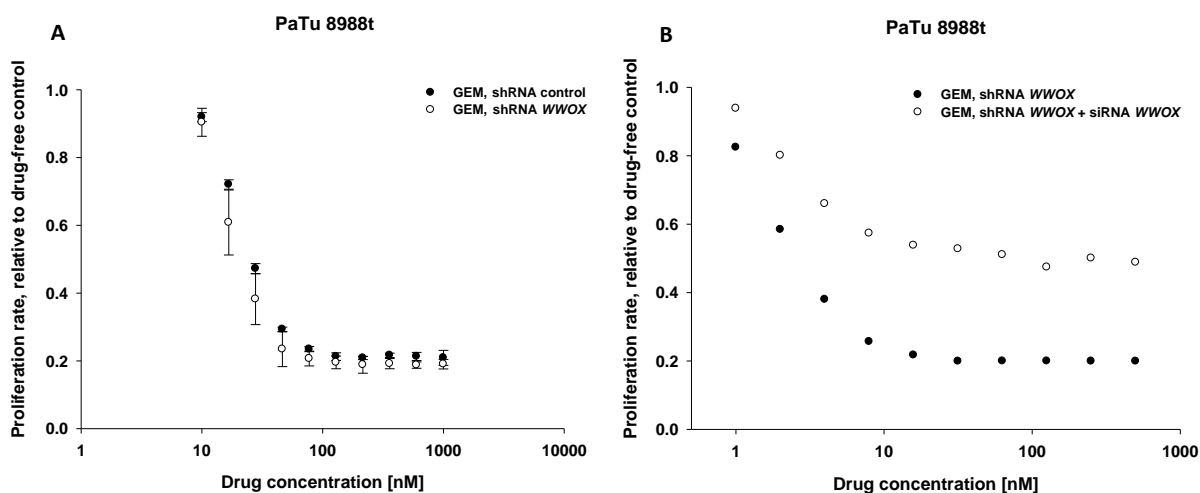
Figure 31: Gemcitabine sensitivity upon *WWOX* knock-down by shRNA and in combination with siRNA. Drug-response effects in PaTu8988t cells following shRNA-mediated *WWOX* knock-down (panel A) or with additional siRNA, targeting *WWOX* (panel B) are shown. Gemcitabine concentrations are denoted in a $\log_{10}$-scale (10 - 1000 nM for panel A, 1 - 500 nM for panel B). For each transfection condition, the proliferation rate for a drug-free control was set to 1.0, to which the indicated drug concentrations were each referred to. Data in panel A represents means of two independent experimental series with one standard deviation. Data in panel B refers to one experimental series. Within each series, each single condition was assayed in quadruplicates, of which median values were taken for analysis. This figure was generated with Sigma Plot version 12.

4.1.6.3 Transient overexpression of *WWOX*

Following the finding that siRNA knock-down of *WWOX* resulted in dramatically increased resistance toward gemcitabine in PaTu8988t (4.1.6.1), it was hypothesized that *vice versa WWOX* overexpression might increase sensitivity to this drug in this cell line. However, there is obviously a surplus of *WWOX* expression in PaTu8988t as shRNA-mediated reduction by 90 % (see Figure 29, Figure 30) did not substantially affect gemcitabine sensitivity (Figure 31, panel A) unlike virtually complete *WWOX* suppression by siRNA (Figure 28, panel A, Figure 31, panel B). Hence, assessing overexpression of *WWOX* in PaTu8988t did not appear reasonable. Thus, MiaPaca-II cells featuring a 6.6-fold less basal *WWOX* expression (according to whole transcriptome analysis, referred to RPKM) were chosen for this investigation. Overexpression of *WWOX* (see methods section 3.10.3) was repeated three times (Figure 32). In a linear

regression model, assessing gemcitabine concentration and *WWOX* transfect as independent variables, the latter did not affect cell viability (p = 0.4).
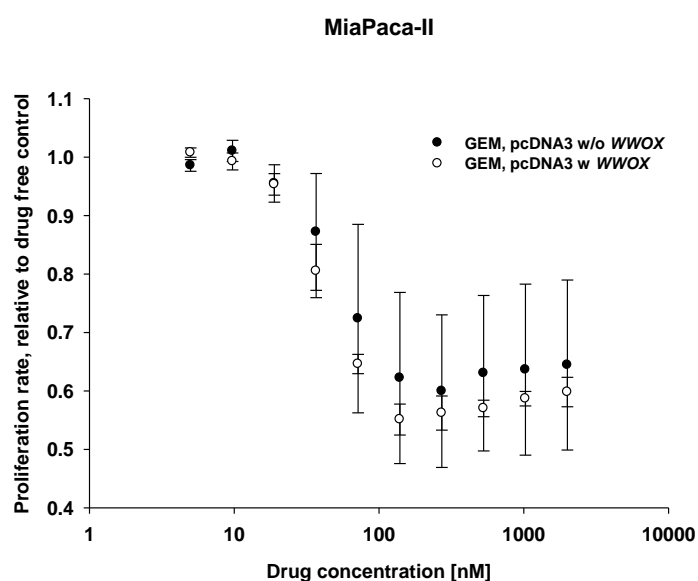
Figure 32: Gemcitabine sensitivity upon *WWOX* overexpression. Drug-response effects in MiaPaca-II cells following transient transfection w/o *WWOX* (pcDNA3 vector) and with *WWOX* (pcDNA3-*WWOX*) are displayed. Drug concentrations are denoted in a $\log_{10}$-scale. For each transfection condition, the proliferation rate for a drug-free control was set to 1.0 to which the indicated drug concentrations were each referred to. Shown data represent means of three independent experimental series with one standard deviation. Within each series, each single condition was assayed in quadruplicates, of which median values were taken for analysis. This figure was generated with Sigma Plot version 12.

4.1.6.4 *WWOX* expression in relation to whole transcriptome

Whole transcriptome analysis was conducted in PaTu8988t cells stably transfected with shRNA against *WWOX* versus transfection with unspecific shRNA. Three clones each were analyzed. None of the transcripts was altered ≥ 2-fold by shRNA (see Figure 33). Targeted *WWOX* by shRNA was the gene showing strongest downregulation in terms of mean suppression (42 %, p = 0.008). Fifteen further genes were suppressed by 30 to 41 % (0.0001 ≤ p ≤ 0.09). Statistically pronounced induction was identified for *RAB12* (p = 6.7 x 10^{-8}), *MED24* (p = 8 x 10^{-7}), *ANKRD13C* (8.3 x 10^{-5}) and *DDI2* (p = 2.7 x 10^{-4}). However, in each case the effect size in transcription increase was very moderate (between 58 and 72 %).
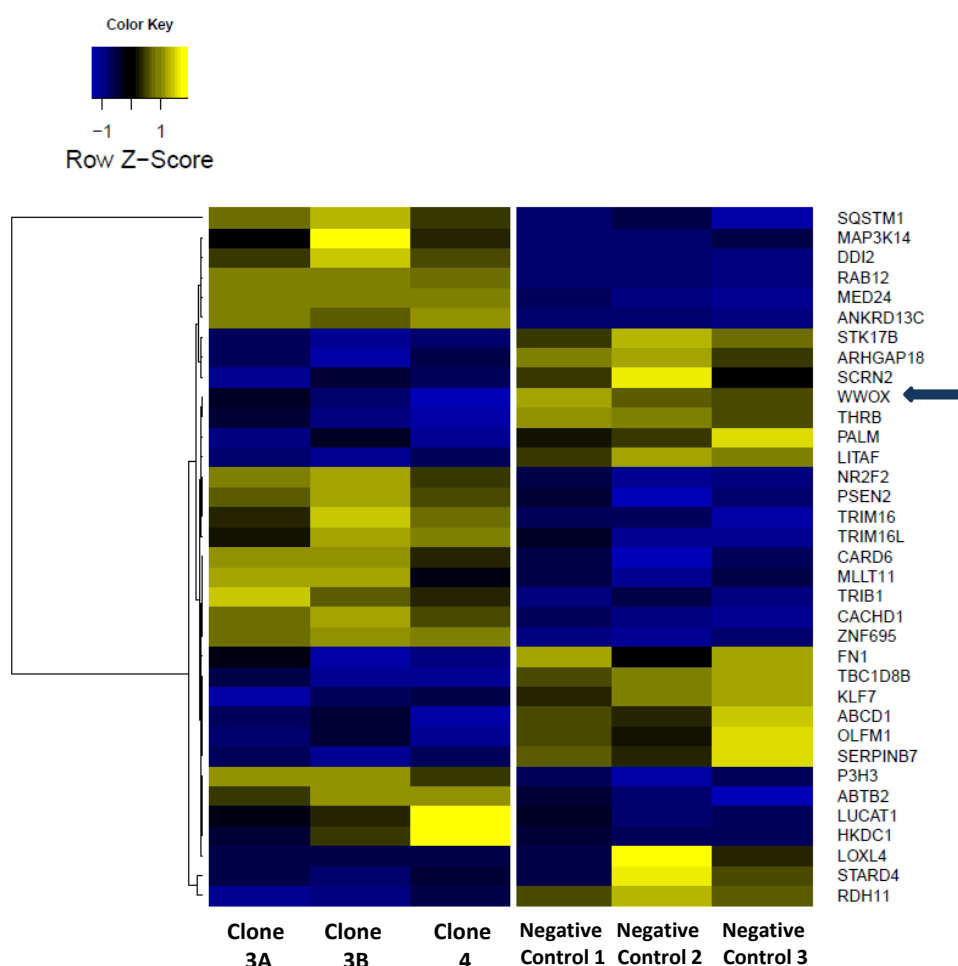
Figure 33: Differential gene expression upon *WWOX* knock-down by shRNA. The shown heatmap displays hierarchy clustering according to inter-clone correlation. Data were analyzed by RNA sequencing. Each row represents one gene. PaTu8988t cell clones with three each for specific shRNA against *WWOX* (left side) and for unspecific shRNA (controls, right) were assessed. Transcripts with a log2-fold change of at least 0.5 are displayed. Genes up-regulated upon shRNA-guided *WWOX* knock-down appear yellow, down-regulated ones in blue. Normalization was performed with regard to the total amount of sequence fragments per sample. *WWOX* is marked by a blue arrow.

4.2 Kozak region SNP in *RRM2*

The *RRM2* index SNP rs1130609 (base exchange G > T, frequency of the *T* allele 22.2 %) was identified in an in-house retrospective analysis associated with the overall survival of patients suffering from PDAC and treated with gemcitabine-containing regimens. The variant *T* allele conferred a significant better overall survival as outlined in the introduction (see Figure 4 in chapter 1.5.1, ZIMMER 2013). The following chapters describe the functional analyses that I conducted regarding *RRM2*.

4.2.1 *RRM2* expression

4.2.1.1 *RRM2* expression in relation to whole transcriptome upon gemcitabine

Total transcriptome of AsPC1 and MiaPaca-II cell lines was assayed for treatment with and without gemcitabine. In both cell lines, gemcitabine treatment for 24 h at 37 °C resulted in an increase of *RRM2* (major transcript isoform) by 1.9- and 2.8-fold for AsPC1 and MiaPaca-II, respectively. When considering the mean induction observed in these two cell lines, there was no other protein-coding transcript found with a higher basal transcription rate over the entire transcriptome to be induced stronger by gemcitabine than *RRM2*. There were only seven transcripts (all of them non-coding) which feature a stronger induction by gemcitabine at a higher basal expression level (see Table 66). Of all coding transcripts with a basal mean RPKM value of ≥ 1.0 in AsPC1 and MiaPaca-II only 54 out of 5853 showed an equal or stronger induction by gemcitabine than *RRM2*. These data highlight the role of *RRM2* in cellular response toward gemcitabine. It should be announced that these whole transcriptome data refer all to cell lines transfected with a *SP1*-overexpressing plasmid. Comparison to vector transfection without *SP1* by qRT-PCR demonstrated no statistically significant alteration ($p > 0.2$ by paired Wilcoxon signed rank test).

Table 66: *RRM2* induction by gemcitabine in relation to entire transcriptome. Expression data (basal and fold induction by gemcitabine) were averaged for AsPC1 and MiaPaca-II. Basal expression data are presented as normalized RPKM. The entire list of 57,396 transcripts was first filtered for known transcripts leaving 57,181. Second, all items with an RPKM value of zero were sorted out remaining 19,932 transcripts. These latter were sorted according to basal expression status. Then, all entries with an equal or higher expression level than *RRM2* were further sorted in relation to fold induction by gemcitabine of which the top eight are listed.

Transcript notation	RNA type	Basal expression [RPKM]	Fold induction by gemcitabine
RNA5-8SP6	rRNA[1]	240.3	13.9
RNU5F-1	snRNA[2]	130.7	6.3
MT-RNR1	Mt-rRNA[3]	45.3	4.2
SNORA80B	snoRNA[4]	106.7	3.7
RNU5A-8P	snRNA	37.6	3.3
MT-RNR2	Mt_rRNA	255.9	2.9
SNORA34	snoRNA	57.7	2.6
RRM2	Protein coding	35.6	2.3

[1]rRNA = ribosomal RNA, [2]snRNA = small nuclear RNA, [3]Mt-rRNA = mitochondrial ribosomal RNA, [4]snoRNA = small nucleolar RNA

4.2.1.2 *RRM2* transcript variant expression

The location of this SNP differs in relation to the two known transcript variants of *RRM2*. Regarding variant 1 (V1), this SNP site represents an amino acid exchange from alanine to serine at position 59, in relation to variant 2 (V2, major transcript) the SNP resides inside the Kozak sequence 6 bp prior to the methionine translation start site (see Figure 34).
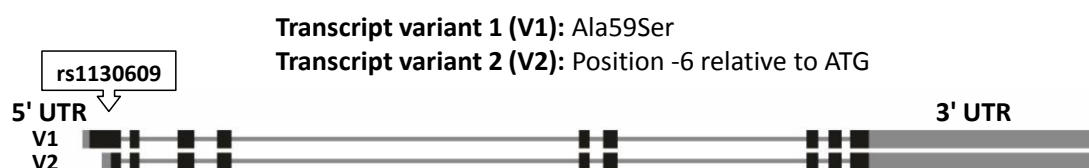
Figure 34: Relation of the index SNP (rs1130609) to the two *RRM2* transcript variants, according to NCBI GenBank. The corresponding GenBank entries are denoted as NM_001165931.1 and NP_001159403.1 for V1 mRNA and protein and as NM_001034.3 and NP_001025.1 for V2 mRNA and protein, respectively. The coding region contains 9 exons, the first one flanked by the 5' and the last by the 3'-untranslated region (UTR). The black rectangles respresent the exons. The location of the index SNP rs1130609 is marked. Relationships of sizes and distances are retained.

In order to determine the quantitative relations of V1 and V2 transcript numbers, quantitative RT-PCR (see section 3.6.4) was conducted. As the sequence of V2 is a complete substring of V1, specific primers for V2 cannot be designed. Thus, two primer pairs specifically covering V1 or both transcripts (V1+V2) were employed.

Gene expression analysis was conducted in the pancreatic cancer cell lines AsPC1, PancI and MiaPaca-II as well as in 89 LCLs (see Figure 35). In pancreatic cancer cell lines, the fraction of V1 was 3.5 % of total *RRM2* transcription, whereas in LCLs V1 represented only 1 %.
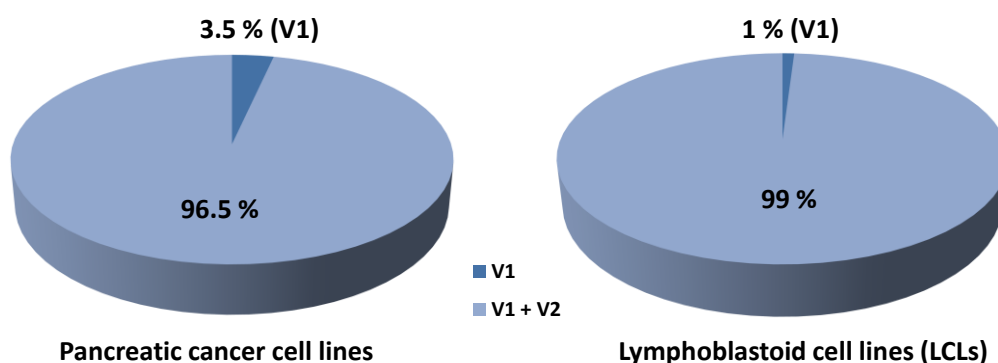
Figure 35: Quantitative proportions of *RRM2* transcript variant expression. The fraction of *RRM2* transcript variant 1 (V1) in relation to total *RRM2* (V1 + V2) is displayed for the average of three pancreatic cancer cell lines AsPC1, PancI and MiaPaca-II (left) and for 89 LCLs (right). Data were obtained by qRT-PCR.

4.2.2 *RRM2* variant expression upon gemcitabine

In LCLs, gemcitabine treatment (30 nM) resulted in a significant induction of total *RRM2* ($p = 8 \times 10^{-6}$) and a reduction of V1 ($p = 2 \times 10^{-12}$) (see Figure 36). Thus, the ratio of *RRM2v1*/*RRM2* total decreased (see Figure 37, panel A).
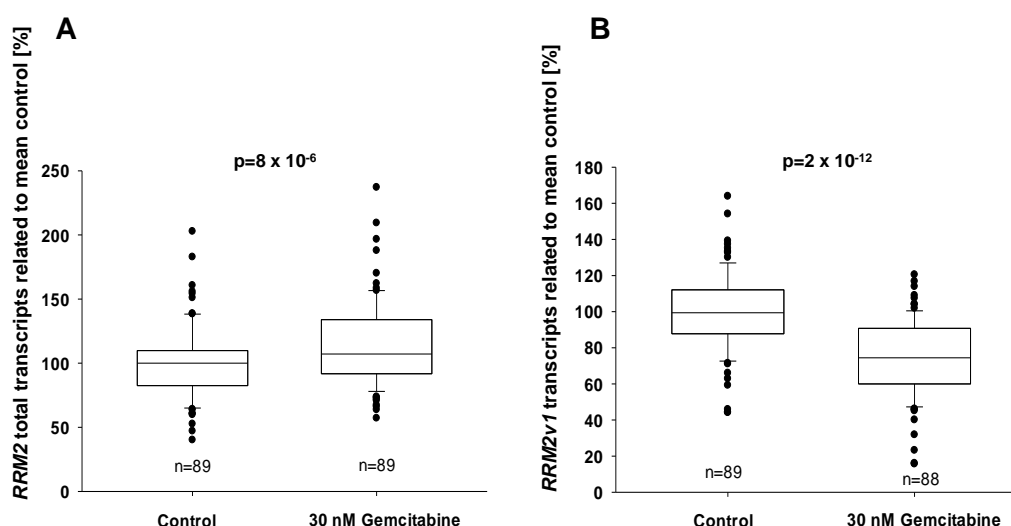
Figure 36: Gemcitabine effects on *RRM2* transcript variant expression in LCLs. Panel A features the *RRM2* total and panel B the *RRM2v1* transcript expression in 89 LCLs exposed to either PBS (control) or 30 nM of gemcitabine. Expression data obtained by qRT-PCR analysis were normalized to the weighted mean of *36b4*, *B2MG*, *GAPDH*, *HPRT1* and *UBC* serving as reference genes. The normalized data were then referred to the median of the PBS treatment, each for *RRM2* and *RRM2v1*. The p-values indicating statistical differences between PBS and gemcitabine treatment were calculated by paired Wilcoxon signed rank test.

110

Concordant to this ratio decrease in LCLs, a reduced ratio could be recorded for the pancreatic cancer cell lines AsPC1 (p = 0.001), PancI (p = 0.006) and MiaPaca-II (p = 0.07, see Figure 37, panel B) exposed to 40 µM of gemcitabine.
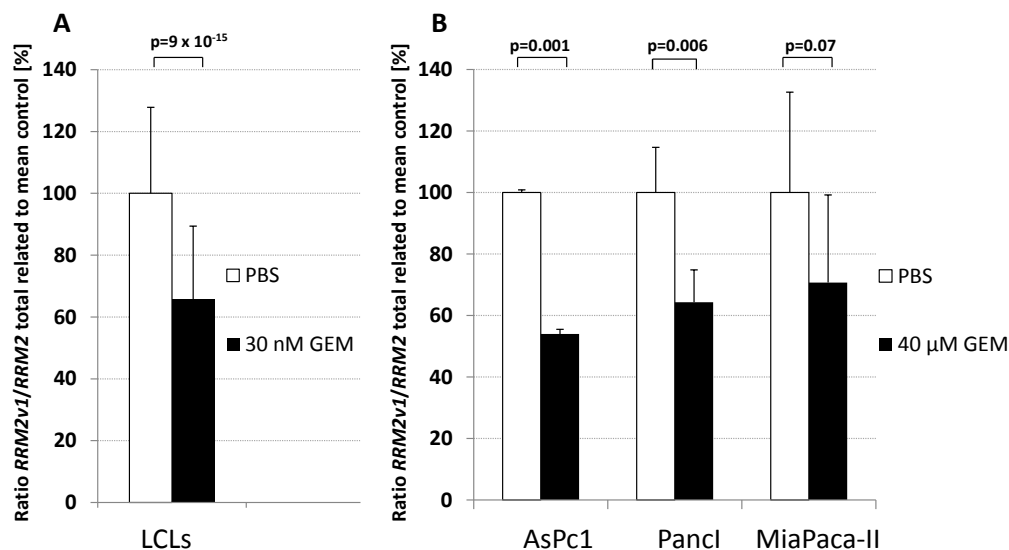
Figure 37: Consequences of gemcitabine on *RRM2* transcript variant expression ratio. Panel A displays summarized data of 89 LCLs, panel B the three denoted pancreatic cancer cell lines each representing three independent measurements. LCLs were exposed either to PBS (control) or to 30 nM of gemcitabine, pancreatic cancer cell lines to PBS or 40 µM of gemcitabine due to substantially differing sensitivity of these cell types. *RRM2v1/RRM2* ratios were calculated and then referred to the mean of PBS for each cell type. The bars represent mean values with the errors indicating standard deviation. Statistical differences were assessed by paired Wilcoxon signed rank test with the respective p-values indicated.

The differential effects of gemcitabine on *RRM2* transcript variant expression in cell lines raised the hypothesis whether analogous patterns might be present in patients as well. A marked induction of total *RRM2* within one month upon chemotherapy start (p = 0.001, n = 28) was observed and appeared sustained up to ten weeks in relation to treatment start, whereas *RRM2v1* expression did not change (see Figure 38). This data indicate that the rise in *RRM2* was due to the major transcript isoform *RRM2*.
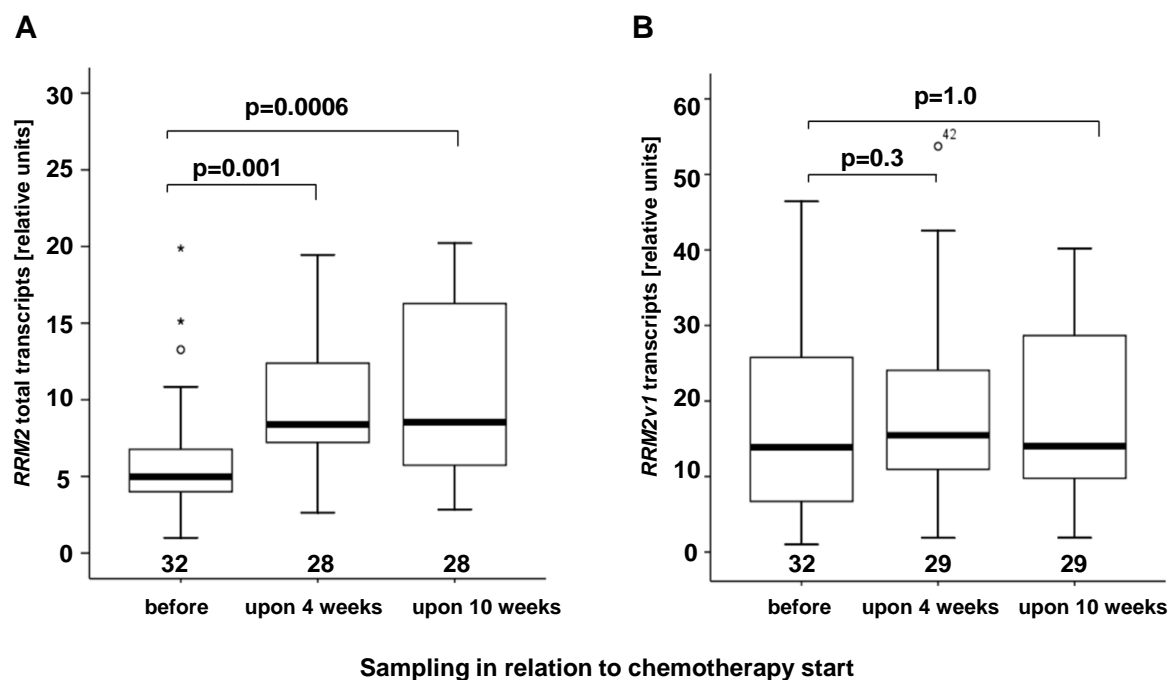
Figure 38: *RRM2* transcript variant expression in patients' blood during chemotherapy. *RRM2* total (A) and *RRM2v1* (B) transcript expression in blood before and during chemotherapy (upon 4 and 10 weeks) is shown. The data were ascertained by qRT-PCR and normalized to HPRT1. Statistical differences between each of the two sampling time points upon gemcitabine start and the reference determined prior to therapy were assessed by paired Wilcoxon signed rank test.

4.2.3 Impact of *RRM2* index SNP on *RRM2* transcript variant expression

The basal gene expression of *RRM2* in 89 LCLs was not altered by rs1130609, neither for total *RRM2* (p = 0.9) nor for *RRM2v1* (p = 0.2) (see Figure 39). Also upon gemcitabine treatment, no statistically significant SNP effect could be observed with regard to total *RRM2* expression (p = 0.2, compared to control). However, *RRM2v1* suppression by gemcitabine was weaker in case of the *T* variant allele (p_{trend} = 0.008 for number of *T* alleles compared to *G* allele). This *T* allele was associated with better clinical outcome. Due to limited sample number, assessment of *RRM2* expression in dependence on rs1130609 was not feasible for pancreatic cancer cell lines and for patients during gemcitabine treatment.
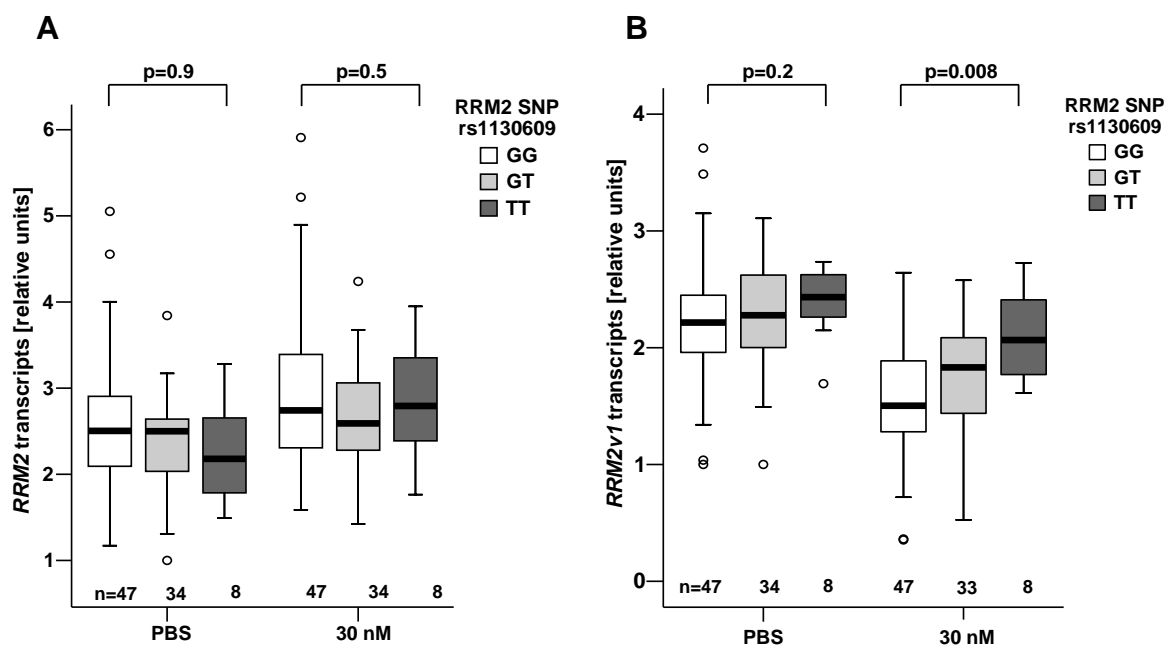
Figure 39: *RRM2* transcript variant expression in dependence on *RRM2* rs1130609. *RRM2* total (A) and *RRM2v1* (B) transcript expression data in 89 lymphoblastoid cell lines treated with PBS (left half of either panel) and upon gemcitabine exposure (30 nM, right half). Allelic effects were evaluated by Jonckheere-Terpstra trend test. Expression data are identical to those described in Figure 36, in which gemcitabine treatment effects are displayed independent of rs1130609.

4.2.4 Nuclear protein binding at *RRM2* rs1130609

With respect to the *RRM2* transcript variant 2, rs1130609 is located in the Kozak sequence, which is known as a transcription factor binding region (FITZGERALD *et al.* 2004). To investigate nuclear protein binding at rs1130609 electrophoretic mobility shift assays (EMSA, see section 3.12) were conducted using nuclear cell extracts of HEK-293 cells, LCLs and pancreatic cancer cell lines.

For nuclear extracts of LCLs, allele-specific protein binding was observed, with stronger binding for the wild type *G* allele (see Figure 40, panel A). To assess allele specificity cold competition experiments were undertaken. The radioactive labeled probe containing the *G* allele was competed with excesses (5-, 10- and 20-fold) of non-labeled probes with the *G* and the *T* allele. These competition experiments using nuclear cell extracts of LCLs indicated stronger affinity for the *G* allele (Figure 40, panel B). In a linear regression analysis based on three independent competition experiments higher affinity to the *G* *versus* the *T* allele was observed at a p-value of 0.05 adjusted for the three levels of probe excess.

113
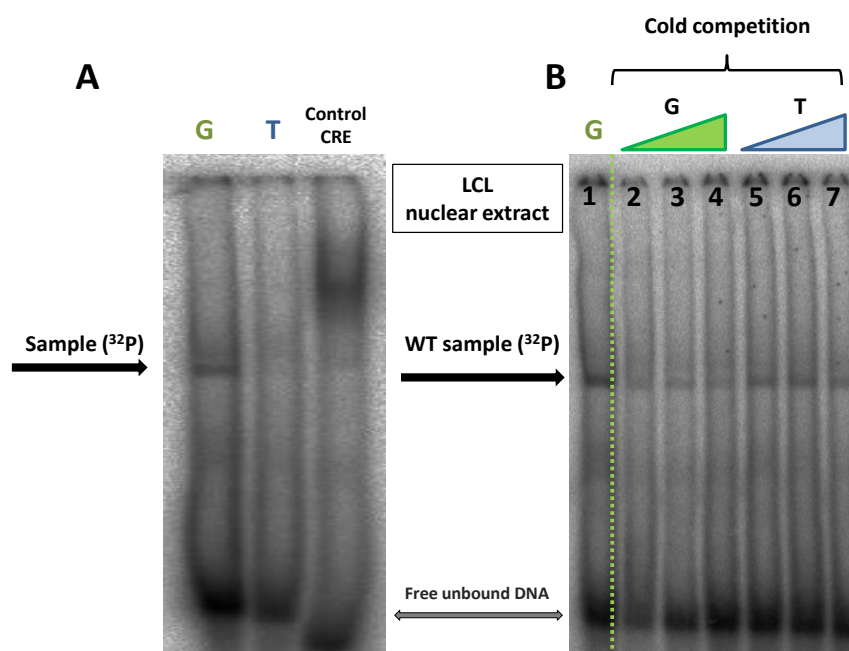
Figure 40: (A) Electrophoretic Mobility Shift Assay (EMSA) for *RRM2* rs1130609 with LCL nuclear cell extract, (B) cold competition experiments for ^{32}P labeled rs113609 wild type probe. The radioactive labeled wild type probe was competed with non-labeled wild type probe with increased concentrations (line 2 - 4 show 5-, 10- and 20-fold molar excess of the radioactive labeled probe) and competed with non-labeled variant probe (line 5 - 7, same concentrations), respectively. The unspecific probe CRE (cAMP response element) is shown as positive control in panel A. The band, indicating nuclear protein binding is marked with a black arrow.

Using nuclear extracts from HEK-293 cells, stronger binding and higher affinity to the *G* allele at rs1130609 has been confirmed (see Figure 41).
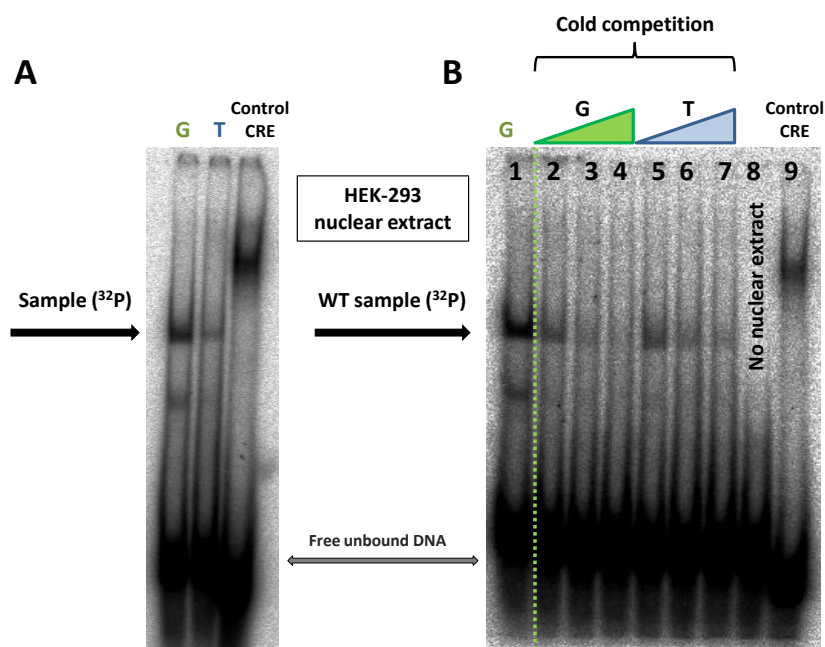
Figure 41: (A) Electrophoretic Mobility Shift Assay (EMSA) for *RRM2* rs1130609 with HEK-293 nuclear cell extract, (B) cold competition experiments for ^{32}P labeled rs113609 wild type probe. The radioactive labeled wild type probe was competed with non-labeled wild type probe with increased concentrations (line 2 - 4, 5-, 10- and 20-fold molar excess of the radioactive labeled probe) and competed with non-labeled variant probe (line 5 - 7, same concentrations), respectively. Line 8 illustrates the negative control, without nuclear extract. The unspecific probe CRE (cAMP response element) is shown as positive control in line 9. The band, indicating nuclear protein binding is marked with a black arrow.

114

Consistently, when extracts of pancreatic cancer cell lines were employed, radio-labelled probes with the *G* allele exhibited stronger protein binding than those with the *T* allele (band 1 corresponding to the interaction noticed for LCLs and HEK, see Figure 42). In contrast, an additional and larger DNA-protein complex appeared more pronounced in case of the *T* allele (band 2 in Figure 42). Though this issue was seen for all four tested pancreatic cancer cell lines, it was more distinct in PaTu8988t and PancI.
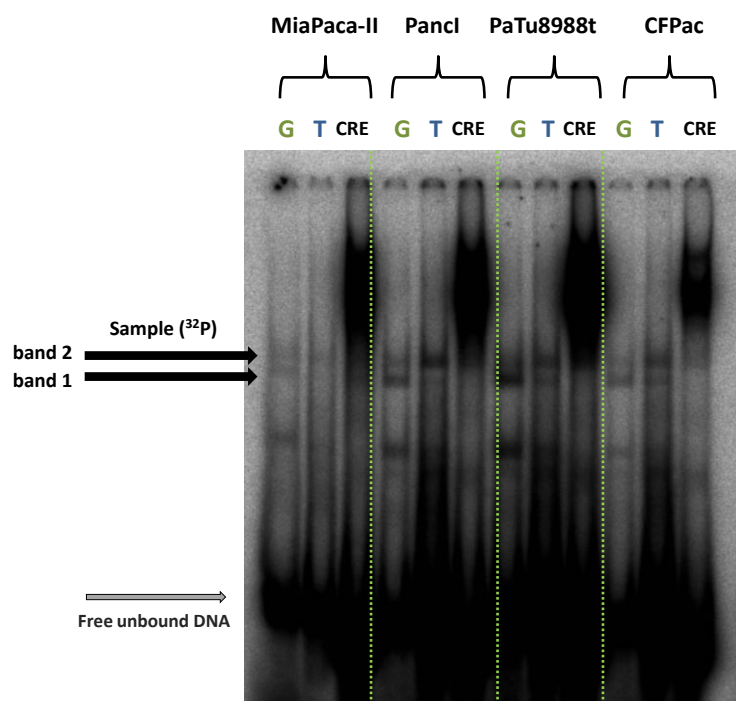
Figure 42: Electrophoretic Mobility Shift Assay (EMSA) for *RRM2* rs1130609 with nuclear extracts of the pancreatic cancer cell lines MiaPaca-II, PancI, PaTu8988t and CFPac. The unspecific probe CRE (cAMP response element) is shown as positive control for each extract. The band, indicating nuclear protein binding (supposed to be the same compared to Figure 40 and Figure 41 in LCL and HEK-293 nuclear extracts) is denoted as band 1 and an additional and larger DNA-protein complex appeared, more pronounced in case of the *T* allele denoted as band 2.

In summary, these data suggest a protein which interacts more strongly with the *G* allele, which was associated with worse clinical outcome (see section 1.5.1, Figure 4).

4.2.5 Effects on translation

To investigate the impact of *RRM2* rs1130609 on protein synthesis, GFP-tagged *RRM2* constructs (see 3.5.3) were analysed with an *in vitro* TNT® Quick Transcription/Translation system (see 3.8.4). Preliminary data via fluorescent quantification of the GFP signal suggest a 37 % lower signal in presence of the variant *T* allele, compared to the wild type *G* allele at rs1130609.

5 Discussion

In a genome-wide and a candidate gene approach the two genes *WWOX* and *RRM2* elicited as particularly promising biomarkers in gemcitabine-treated PDAC. The major findings of my thesis with regard to these two genes are discussed in the following sections.

5.1 WWOX

Based on the clinical finding that *WWOX* rs11644322 is associated with patients' OS, I could get several lines of evidence for the functional role of *WWOX* in general and of the index SNP in particular with respect to cellular gemcitabine sensitivity. The *WWOX* gene located at chromosome region 16q23.3 ‑ q24.1 encodes for a 46 kDa-sized protein described as a "fragile tumor suppressor" (SCHROCK AND HUEBNER 2015).

5.1.1 *WWOX* rs11644322 affects cytotoxicity of gemcitabine but not 5-FU

Testing of gemcitabine sensitivity in LCLs revealed increased resistance in presence of the *A* allele at rs 11644322 (see section 4.1.1, Figure 15) accordant to the clinical finding of worse OS for patients treated with gemcitabine harboring this allele (see section 1.5.2, Figure 5). In contrary, in a comparative study, using 5-FU in the same set of LCLs, cytotoxicity was not altered by rs11644322 (data provided by Mr. Ruben Pflüger, personal communication, p = 0.4).

Concerning this observation, assessment of this SNP for treatment other than gemcitabine was not possible in absence of respective patient cohorts. Thus, it is debatable if the observed SNP effect is linked to cytostatic exposure in general or specifically to gemcitabine. At present, there are no data in literature comparing OS in PDAC for different cytostatics in dependence on germline genetic variability. However, with regard to hematological toxicity, a SNP in the gemcitabine deactivating CDA was reported as associated in patients treated with gemcitabine but not with 5-FU (FARRELL *et al.* 2012).

Differential intrinsic resistance between pancreatic cancer cell lines was observed upon exposure toward gemcitabine or 5-FU (SHI *et al.* 2002). In general, pancreatic cancer cell lines appeared to be much more sensitive toward gemcitabine than 5-FU. This was also

seen in the cells I used (see Figure 28). Similar relations in sensitivity difference were found in LCLs (Figure 15). In this regard, LCLs appear as a suitable model to evaluate drug-specific cytotoxicity in dependence on genetic variability. Unlike pancreatic cancer cell lines, much higher numbers of genetically diverse LCLs are available to be tested for the impact of genetic polymorphisms. LCLs were used in previous studies as well to test for cytotoxicity of gemcitabine and cytosine arabinoside (Li *et al.* 2008). Whereas LCLs with their high sensitivity toward gemcitabine appear suitable to evaluate an impact of genetic polymorphisms, I am aware of the limitations of these cell lines with regard to pancreatic cancer. Nonetheless, common features in cellular drug response could be assumed for different cell types. Different expression levels of genes might modify sensitivity to a specific drug. A drug might be particularly efficient in a sub-group of patients with specific expression levels of genes related to handling of this drug or representing a molecular target for it. In this manner, expression levels of such candidate genes for a specific drug have been investigated in relation to clinical outcome. For instance, low expression of 5-FU-degrading *DPD* (dihydropyrimidine dehydrogenase) and high expression of the major molecular target *TS* could be favourable when this drug is applied (Shimoda *et al.* 2015). Otherwise, genes related to gemcitabine transport and metabolism might interfere with this drug's response (Iwamoto *et al.* 2015). Besides such candidate genes, for which an interaction with a specific drug is evident, there are probably numerous other genes of which a substantial contribution is present but not yet identified. A possible "new" gene in this regard might be *WWOX*.

5.1.2 *WWOX* expression affected by rs11644322

Regardless whether the core region or the last exon were considered and regardless whether LCL samples were subjected to gemcitabine or not, in all conditions homozygous *AA* allele of rs11644322 was accompanied by reduced *WWOX* expression levels (Figure 18). No relevant differences in *WWOX* transcript amounts could be detected between *AG* and *GG* genotypes in this cellular model. As the expression of the two investigated *WWOX* regions is highly correlated (Figure 17), similar association with a genetic polymorphism is obvious. This correlation appeared even intensified upon gemcitabine exposure suggesting a link between induced genotoxic stress and transcription of the entire *WWOX* gene. Regarding mean transcription rate in the entire

investigated LCL panel, that of exon 8-9 amounts to 67 % in relation to the core coding region (see Figure 17, inserted bar plot).

5.1.3 Consequences of overexpression of SP1 binding to rs11644322

Allele-specific binding at rs11644322 was demonstrated previously for SP transcription factor family members (ROPPEL 2013). Weaker SP1 protein binding for the minor *A* allele at the *WWOX* rs11644322 site was hypothesized to be related to less *WWOX* expression. Thus, I analyzed *WWOX* expression in relation to rs11644322.

In the panreatic cancer cell lines AsPC1, MiaPaca-II and PancI, I analyzed specifically the consequences of *SP1* overexpression on *WWOX* transcription. Though statistical significance was not reached by three independent experimental repetitions, cell line-specific effects could be assumed (Figure 21) with expression induction of the *WWOX* core region only in MiaPaca-II. Genotyping at rs11644322 was carried out for these three cell lines. It turned out that PancI is derived from a host with *GG* allelic configuration at rs11644322. AsPC1 seems to stem from an initially heterozyous *GA* carrier with later loss of the *A* allele during carcinogenesis. In contrast, MiaPaca-II clearly showed heterozygosity. Since these are just observations on single cell lines, conclusions derived thereof are limited. Nonetheless, one might speculate about any relationship between this genotypic configuration and the observed differential responsiveness to *SP1* overexpression in terms of *WWOX* transcription. Often, transcription factors are regulated on the activity level by phosphorylation (WHITMARSH AND DAVIS 2000) implying that expression level mostly is not limiting. However, in case of a poor interaction between a transcription factor and its DNA binding motif, it is conceivable that the full capacity of transcriptional activation is not reached under usual expression levels. Overexpression leads to an increased pool of activatable molecules, which might enhance binding according to the law of mass action in case of a less favourable binding motif. This hypothesis might argue for the idea that binding at rs11644322 is the reason for the differential effects observed upon *SP1* overexpression. However, several other binding sites for SP transcription factor family members in the *WWOX* genomic region are conceivable, which were not addressed in my thesis. Nevertheless, if the hypothesis is assumed that rs11644322 is a relevant SP binding site, which regulates *WWOX* expression, one might ask about the spatial relationships since this SNP is located far downstream in an extraordinarily huge intron.

118

In cell lines with overexpressed *SP1,* surprisingly, different effects of cytostatic drugs on *WWOX* gene expression were observed (Figure 22): Substantial suppression, moderate induction and no alteration of the *WWOX* core region transcription by gemcitabine in AsPC1, MiaPaca-II, and PancI cells, respectively, whereas virtually no alterations by 5-FU. The second interesting observation at this point was the absence of *WWOX* core region suppression by irinotecan in PancI cells. In this cell line, which was identified to be gemcitabine resistant in terms of cytostatic activity (REJIBA *et al.* 2009), transcripts of *WWOX* exon 8-9 were not detected. The lack of exon 8-9 transcripts might be involved in cytostatic resistance (e.g. towards gemcitabine or irinotecan) indicating the need of the entire *WWOX* gene transcription for efficacy of these drugs. It is conceivable that the index polymorphism rs11644322 is involved in expression of the last exon (see Figure 18). The co-association of this SNP with *WWOX* core region expression is plausible due to the high correlation of transcripts of the two investigated *WWOX* regions (displayed in Figure 17). From the data in that figure the primary effect of this SNP on *WWOX* regional expression cannot unambiguously be ascertained. In the subsequent chapters hypothesis taking into account, also spatial relationships are discussed.

5.1.4 Rs11644322 located in extraordinarily huge intron: Looping hypothesis

The last *WWOX* intron, which spans over 730 kb, is one of the longest introns in humans. The longest known intron is 1.1 Mb (intron 5 in *KCNIP4*, http://kirschner.med.harvard.edu/files/bionumbers/Human genome and human gene statistics.pdf). Large introns render the possibility of intra-molecular looping within the DNA. The involvement of genome's three-dimensional topography in transcriptional processes has become increasingly accepted within the last years (LI *et al.* 2012, SCHOENFELDER *et al.* 2010). Folded chromatin loops can bring gene regions into close proximity to cognate promoters or distant regulatory elements leading to gene activation (e.g. for the *CD68* gene spanning over a 2.5 kb distance (O'REILLY AND GREAVES 2007, MERCER *et al.* 2013) or the insulin gene looping over a range of 1.4 kb (BABU *et al.* 2008)). Further long-range enhancer-promoter communications are reported, e.g. for the sonic hedgehog (Shh) limb bud-specific enhancer, which interacts with its target promoter one megabase apart (AMANO *et al.* 2009). Another study found the SNP rs6983267 associated with higher risk of colorectal cancer to be located in a "gene desert" at the human chromosome 8q24. The rs6983267 containing region acts as an

enhancer in reporter gene assays and interacts with the promoter in the *MYC* oncogene, residing 330 kb apart (Tuupanen *et al.* 2009, Pomerantz *et al.* 2009, Schoenfelder *et al.* 2010). Remote interaction over a distance of 200 kb between the 3'-UTR region and the promoter region of *BCL2* was identified to be regulated via *SATB1* (AT-rich sequence binding protein 1)-mediated chromatin looping (Gong *et al.* 2011). Also similar non-cancer related enhancing effects were observed with intronic SNPs (e.g. rs3857080 in intron 3 in the *NR3C2* gene which was associated with increased potassium excretion (Dalila *et al.* 2015)).

As in the close vicinity of *WWOX* rs11644322, no transcripts were discovered (Figure 19), the region containing rs11644322 might act as enhancer with an upstream promoter region in a three-dimensional manner as well. SP transcription factor family members might affect such a mechanism. A similar looping mechanism has been reported for *SP1* in relation to the human heme oxygenase-1 gene in renal cells, where *SP1* siRNA and a *SP1* binding site inhibitor led to loss of looping formation between the intronic enhancer and the 6 kb distant HO-1 promoter, identified via chromosome conformation capture assay (Deshane *et al.* 2010).

This looping hypothesis is further supported by the data obtained upon exposure to the topoisomerase inhibitor irinotecan. As topoisomerases are required for proper DNA-unwinding it could be assumed that these enzymes are also involved in remote interactions between DNA elements. Thereby, it appears plausible that irinotecan suppressed expression of *WWOX* in those cell lines (AsPC1, MiaPaca-II) with relevant expression of exons 8 and 9 flanking the index SNP, but not in PancI, in which last exon transcription was below the detection level (Figure 22). This effect observed in AsPC1 and MiaPaca-II was enhanced when cells were transfected with *SP1* suggesting crucial involvement of an *SP1*-binding site like rs11644322.

Binding of the human transcription factor *SP1* to 10-bp G+C-rich elements ("GC boxes") residing at -100 and +1700 bp relative to the RNA start site was studied. A synergism of the distantly located site with the promoter-proximal site was seen resulting in strongly activated transcription *in vivo*. This synergism is regarded as direct consequence of interactions between remote and local *SP1*, whereof the remote *SP1* was translocated to the promoter via DNA looping (Mastrangelo *et al.* 1991).

The previously identified allele-specific binding of the transcription factor specificity

protein SP1 or SP3 at the rs11644322 (ROPPEL 2013) might represent such an enhancer element with mitigated function in case of the *A* allele.

5.1.5 Model linking functional and clinical findings for rs11644322

A model linking the above-mentioned functional data in conjunction with the clinical findings is presented (Figure 43). The presence of the *G* allele at the index SNP site results in stronger SP1 binding, which might lead to a stronger looping formation to the promoter region, resulting in induced *WWOX* transcription. This hypothesis would match to the finding of higher *WWOX* expression in LCLs (core region and last exon), lower EC_{50} values of gemcitabine (as *WWOX* enhances cytotoxicity of gemcitabine) resulting in better OS of patients. Gemcitabine treatment seems to be an important element in this cascade, but the mechanisms behind are still unknown.
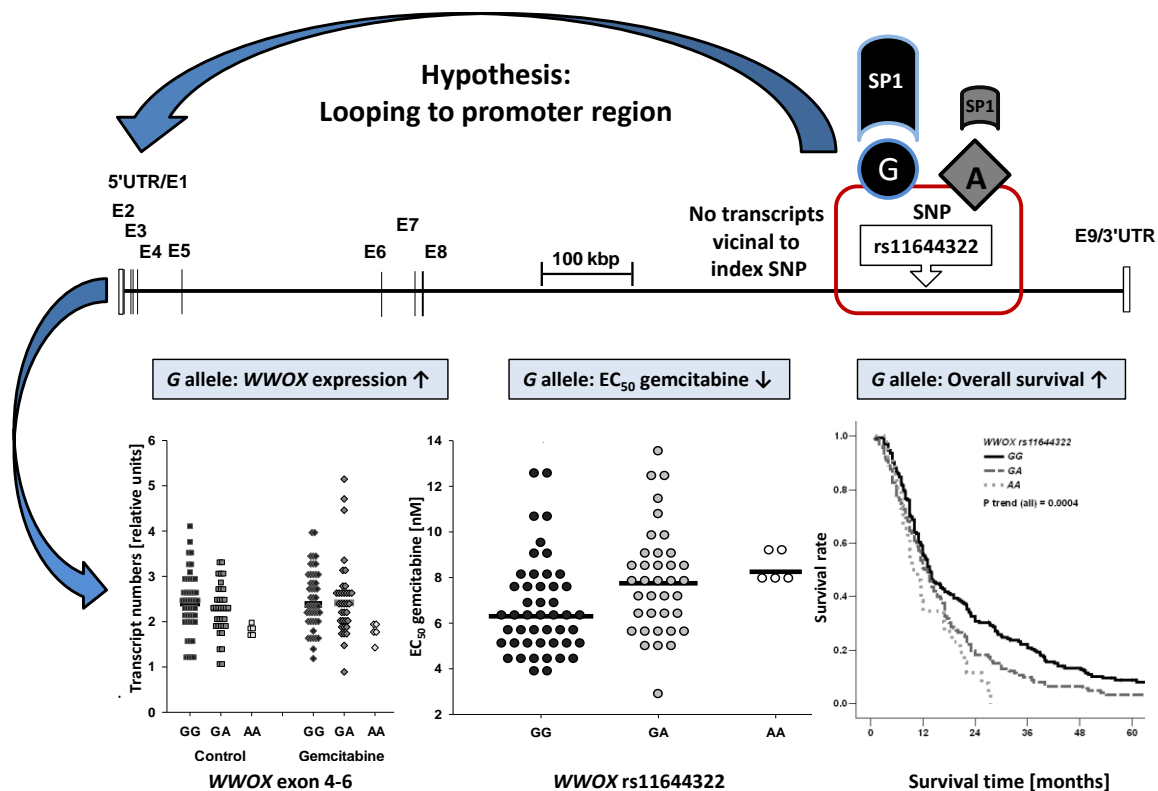
Figure 43: Hypothesis linking functional and clinical findings for rs11644322. Schematic illustration how differential *SP1* binding at the rs11644322 site might affect *WWOX* expression via looping resulting in altered cellular sensitivity towards gemcitabine affecting clinical outcome (Kaplan-Meier curve, survival data according to ROPPEL 2013). Specifically, presence of the *G* allele at rs11644322 accompanied by stronger *SP1* binding and thus by enhanced *WWOX* expression might sensitize cells to the cytotoxic effects of gemcitabine, which in turn might reason the longer survival of patients carrying this allele.

5.1.6 *WWOX* knock-down slows cell proliferation and hampers gemcitabine cytotoxicity

The finding of substantially decreased basal proliferation in PaTu8988t and L3.6 cells induced by siRNA-mediated *WWOX* knock-down (see Figure 27) is in line with decreased gemcitabine sensitivity in case of *WWOX* abrogation. However, as proliferation was reduced in a similar extent, the effects of *WWOX* knock-down differed substantially between these two cell lines. This raises the hypothesis about cell line specific interactions between gemcitabine and *WWOX*, possibly due to the respective genetic make-up. On the contrary, responsiveness of 5-FU was moderately and similarly affected in both cell lines (see Figure 28), what again suggests specific actions for gemcitabine. Consistently, the sensitivity of LCLs toward gemcitabine but not 5-FU (5-FU data in LCLs from Ruben Pflüger, personal communication) was affected by the *WWOX* SNP rs11644322 as outlined above (Figure 15).

Surprisingly, stable *WWOX* knock-down via shRNA transfection in PaTu8988t cells could not verify this effect observed for siRNA. First, the above-mentioned dramatic suppression of basal cell proliferation by siRNA-mediated *WWOX* knock-down (w/o any cytostatic drug applied) could not be detected upon shRNA transfection targeting *WWOX*. Second, gemcitabine sensitivity was not affected upon *WWOX* suppression by shRNA (Figure 31, panel A). However, when additional siRNA against *WWOX* was transfected, gemcitabine resistance was markedly increased in a similar manner (Figure 31, panel B) as seen before for the knock-down by siRNA only (Figure 28, left panel). These data indicate that shRNA-guided *WWOX* suppression by about 90 % is not sufficient, neither to slow down cell proliferation nor to alter substantially the cytotoxic effects of gemcitabine. In other words, there seems to be a surplus of *WWOX* expression in regard to the analyzed phenotypes. A relative low number of *WWOX* molecules might be sufficient to drive cell proliferation as well as gemcitabine-mediated cytotoxic reactions.

Contemporary literature addressing interactions between gemcitabine and *WWOX* is still scarce. However, some current reports indicate a relationship of *WWOX* in regard to the regulation of epithelial to mesenchymal transition (EMT). EMT is characterized by downregulation of *E-cadherin* expression leading to disruption of cell-cell junctions and distribution of cells from the primary tumor (THIERY *et al.* 2009). Thus, EMT and/or

backward (MET, reattachment of floating cells) are supposed to be crucial processes in tumor metastasis. EMT and an associated cancer stem cell phenotype are regarded as a major cause for therapy resistance in pancreatic cancer, e.g. shown for gemcitabine resistance in a panel of pancreatic cancer cell lines (MEIDHOF *et al.* 2015, ARUMUGAM *et al.* 2009, WANG *et al.* 2014). In endometrial cancer, *WWOX* was found to be related to the expression of markers for EMT/cell motility (PLUCIENNIK *et al.* 2015). In ovarian cancer stem cells, *WWOX* was identified to invert the EMT process resulting in reduced tumor invasion (YAN AND SUN 2014). This reversion to a MET phenotype may imply reinforced *E-cadherin* expression promoted by intracellular *WWOX* (BENDINELLI *et al.* 2015).

Both, decreased basal proliferation rate and enhanced resistance toward gemcitabine might represent a feature of induced EMT caused by lower *WWOX* expression in presence of the variant allele at rs11644322 (possibly due to weaker SP1 binding, see chapter 5.1.3). An increased EMT phenotype constitutes a plausible explanation for worse clinical outcome in case of an allele connected with low *WWOX* expression (see Figure 44).
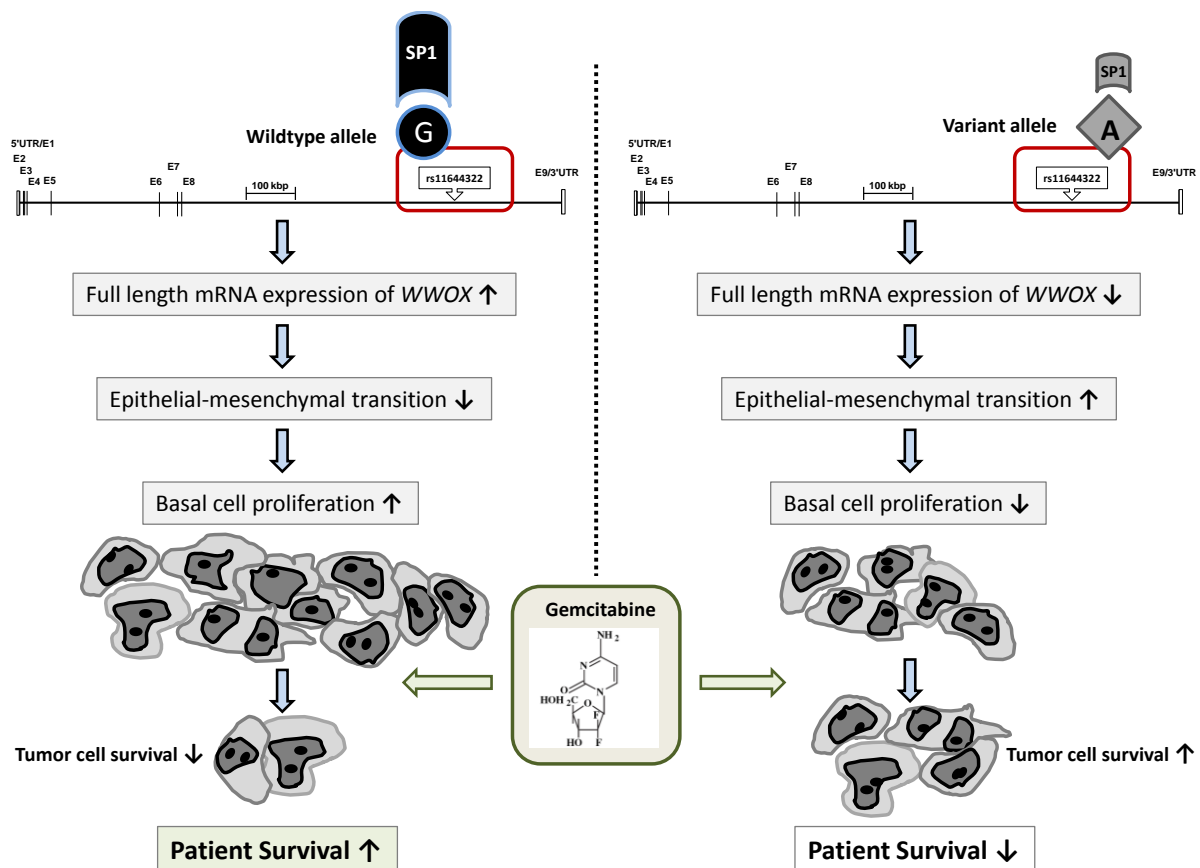
Figure 44: EMT as a putative mechanism for the effects of *WWOX* rs11644322. The chart shows hypothesized consequences for the rs11644322 wild type (left side) and variant allele (right).

5.1.7 *WWOX* in the context of genomic stability and carcinogenesis

In view of the fact that genomic instability is a feature of human cancers, it is noteworthy that *WWOX* spans the second most common fragile site in the human genome, termed *FRA16D* (BEDNAREK *et al.* 2000, RIED *et al.* 2000, BEDNAREK *et al.* 2001). Instability at the *FRA16D* site was associated with poor prognosis in human cancers. Mechanistically, this was linked to induction of aberrant *WWOX* expression with, in most cases, a lack of C-terminal sequences needed for *WWOX* acting as an oxidoreductase. As cancer cells are known to possess altered metabolism (Warburg effect), it was hypothesized that aberrant WWOX contributes to changes in metabolism in cancer (RICHARDS *et al.* 2015).

Moreover, WWOX is described to play a direct role in DNA damage response (DDR), a crucial antagonist of genomic instability. In case of *WWOX* deficiency, reduced activation of the ataxia telangiectasia-mutated (ATM) checkpoint kinase and hampered DNA repair was reported, what might explain the loss of WWOX during cancerogenesis (ABU-ODEH *et al.* 2014).

The *WWOX* SNP rs11644322 is more than 300 kb apart from the downstream end of the *FRA16D* region. Thus, an interaction is unlikely. Moreover, no genetic marker in high LD with rs11644322 was identified to touch the *FRA16D* region.

5.1.8 *WWOX* in the context of apoptosis induction and DNA damage repair

WWOX mRNA expression and cellular gemcitabine sensitivity in LCLs were identified to be correlated (see Figure 23). As WWOX is known to be involved in stress and apoptotic responses (CHANG *et al.* 2003), a connection between transcripts of *WWOX* and those of apoptosis-related genes was presumed. *In vitro* studies identified an interaction of the WWOX protein with various binding partners to regulate proliferation, cellular apoptosis and/or cell maturation (SCHROCK AND HUEBNER 2015).

Overexpression of WWOX fosters apoptosis and inhibits proliferation of cancer cells (HU *et al.* 2012, CHIANG *et al.* 2013). In addition, WWOX was found to block the Wnt/beta-catenin pathway (BOUTEILLE *et al.* 2009). Mechanistically, this effect is exerted through inhibition of transcriptional activity of a beta-catenin coactivator by WWOX (EL-HAGE *et al.* 2015). Suppression of WWOX was reported to promote Wnt/beta-catenin transcription (HUA *et al.* 2015). Recently, gemcitabine effected stronger in terms of

proliferation inhibition and apoptosis induction when Wnt/beta-catenin signalling was disrupted (JUNG *et al.* 2015). *Vice versa*, activation of this pathway was shown to enhance resistance toward gemcitabine in pancreatic cancer cell lines (NAGANO *et al.* 2013). Based on these cited reports and the data I gained it can be hypothesized that WWOX mitigates Wnt/beta-catenin signalling thereby enhancing gemcitabine efficacy. Alternatives for WWOX actions in the context of gemcitabine sensitivity are also conceivable.

WWOX was shown to interact with p53 and its homologue p73 by WW-containing domains thus enhancing stress response-induced cell death when translocated into the nucleus (ABU-ODEH *et al.* 2014, AQEILAN *et al.* 2004, CHANG *et al.* 2003). Furthermore, WWOX is able to enhance cytotoxic signalling (e.g. induced by tumor necrosis factor) by downregulating BCL2, but upregulating p53 thereby acting as a pro-apoptotic mitochondrial protein (CHANG *et al.* 2001). GADD45A constitutes an important component linking p53 downstream to DNA base excision repair (SMITH *et al.* 2000, JUNG *et al.* 2013). Intriguing, distinctions were observed for correlation of *WWOX* exon-specific transcripts and mRNA expression of *BCL2*, *GADD45A*, and *TP53* (Table 65).

WWOX protein phosphorylation at tyrosine-33 was reported necessary for p53-mediated cell death in a fibroblast cell line (CHANG *et al.* 2005). Protein interaction between p53 and WWOX was strengthened when MDM2, a nuclear localized E3 ubiquitin ligase, antagonizing p53, was blocked. Interestingly, in glioblastoma cell lines with mutant but not with wild type p53, ectopic WWOX overexpression induced apoptosis, by a mechanism independent of the intrinsic apoptotic pathway (CHIANG *et al.* 2012). This observation suggests alternative routes of WWOX-induced apoptosis when p53 is not functional. Eventually, WWOX restores chemosensitivity toward gemcitabine, which was shown to be lost in pancreatic adenocarcinoma with mutant p53 (FIORINI *et al.* 2015). With an alteration frequency of 40 - 75 % p53 is one of the most mutated genes in PDAC (LI *et al.* 2004). PDAC metastasis was reported to be driven by mutant p53 (MORTON *et al.* 2010, WEISSMUELLER *et al.* 2014). Perhaps, WWOX is involved in these processes. In LCLs, mRNA transcripts (*TP53*) coding for p53 protein did not correlate with gemcitabine sensitivity. However, there was a positive correlation between transcripts of *TP53* and the *WWOX* core region particularly upon gemcitabine exposure. In contrast, the relationship with the last *WWOX* exon transcripts was stronger under basal conditions. Thus, one might speculate whether WWOX-p53 interactions are modulated by regional *WWOX* transcription. Possibly, genotoxic stress induced by

gemcitabine triggers cellular signals inducing parallel transcriptional induction of *TP53* and the *WWOX* core region. Expression of the last exon, however, might rely on distinct mechanisms. As a limitation, it should be noted that data I obtained at this point only refer to transcription and do not address protein levels.

In the above-mentioned panel of 89 LCLs, *GADD45A* was correlated with *WWOX* expression when exposed to gemcitabine, but not at baseline conditions (Table 65). Furthermore, *GADD45A* transcript numbers at gemcitabine exposure, but again not at baseline, exhibited a strongly inverse correlation with EC_{50} for gemcitabine in LCLs (Figure 24). This relationship was not impacted by variations in LCL proliferation in a relevant manner. These data argue for stress-induced responses involving GADD45A upon a variety of genotoxic stimuli (Fornace *et al.* 1992).

GADD45A is involved in a variety of biological processes like cell cycle, senescence, apoptosis and nucleotide excision repair and its disruption results in genomic instabilty (Hollander and Fornace 2002). In hematopoietic stem cells, apoptosis was damped in absence of GADD45A (Chen *et al.* 2014). Enhanced levels of *GADD45A* mRNA and protein were reported for splenic lymphocytes from mice exposed to ionizing radiation or other agents inducing DNA damage and growth arrest (Hollander *et al.* 2001). Thus, the correlation between *GADD45A* expression and sensitivity toward gemcitabine observed in LCLs appears plausible.

Among the GADD45 family members, GADD45A is the only one responsive to p53 (Hollander *et al.* 1993). By that, GADD45A interacts with apoptosis-related genes and is involved in DNA repair (Hildesheim and Fornace 2002). Pro-apoptotic effects of GADD45A are often mediated by p38 and JNK (c-Jun N-terminal kinase), which in turn represent upstream activators of GADD45A constituting a positive feedback loop (reviewed in Salvador *et al.* 2013). GADD45A was established as a component connecting p53-dependent cell cycle checkpoint and DNA repair by interacting with the proliferating cell nuclear antigen (Smith *et al.* 1994). It counteracts mitosis by inhibiting specifically the Cdc2-cyclin B1 kinase complex (Zhan *et al.* 1999). Beyond that, the acidic GADD45A was identified to bind to chromatin structures around damaged DNA sites thus making them more accessible for DNA repair machinery components like topoisomerases (Carrier *et al.* 1999).

Whereas gemcitabine induces *GADD45A* transcription (in median by 3-fold in LCLs), this

drug was identified to specifically inhibit GADD45A-mediated DNA demethylation (SCHAFER *et al.* 2010). For *GADD45A* mutant mice, genomic instability and tumorgenesis was observed representing common features of human cancers, which were linked to changes in DNA methylation patterns (BARRETO *et al.* 2007, BIRD 2002, HOLLANDER AND FORNACE 2002). Reduced *GADD45A* expression was hypothesized to induce hypermethylation and thus inactivate tumor suppressor genes as *MLH1* (mutL homolog1) (BARRETO *et al.* 2007). At this point, the net effect of gemcitabine on GADD45A functions (increased transcription *versus* mitigated demethylation activity) remains to be elucidated.

Direct or indirect interactions between GADD45A and WWOX are likely, however, so far not addressed in literature. Exact mechanisms for the proposed interactions between WWOX and GADD45A remain to be elucidated. Transcriptional regulation of *GADD45A* by WWOX, at least, is unlikely as I could not detect any alterations in *GADD45A* expression upon siRNA-mediated *WWOX* knock-down. An interaction with the Wnt/beta-catenin pathway, as outlined above for WWOX, is conceivable as GADD45A favors distribution of beta-catenin to the cell membrane and its cytoplasmic and nuclear degradation (JI *et al.* 2007).

5.2   RRM2

RRM2 is part of physiological nucleotide synthesis and counteracts cytotoxic effects of gemcitabine on DNA synthesis. In the subsequent chapters, findings obtained during my thesis for *RRM2* in general, and the SNP rs1130609 in particular are discussed in relation to the contemporary literature.

5.2.1   *RRM2* expression increases upon gemcitabine

With regard to entire transcriptome analysis in AsPC1 and MiaPaca-II cells, *RRM2* expression increased upon gemcitabine exposure (Table 66). Intriguingly, this *RRM2* induction was highlighted as it was stronger than that of any other protein-coding transcript in this setting. Consistent with this finding, expression of the *RRM2* major isoform, which accounts for the vast majority of transcripts, was enhanced upon gemcitabine in LCLs (Figure 36, panel A) and in patients within one month after gemcitabine-based chemotherapy start (Figure 38, panel A).

Overexpression of *RRM2* is described as a hallmark of gemcitabine resistance in pancreatic cancer cell lines (WANG *et al.* 2015, NAKANO *et al.* 2007). This induction of *RRM2* by gemcitabine was reported to be mediated via *E2F1* transcriptional activation. *RRM2* upregulation is regarded as part of DNA damage response leading to enhanced cellular DNA repair. According to this, targeting gemcitabine-dependent *RRM2* expression is hypothesized as promising strategy to overcome gemcitabine resistance (LAI *et al.* 2014).

In patients suffering from PDAC, pre-therapeutic tumoral *RRM2* mRNA expression was reported as a prediction marker for sensitivity to gemcitabine-based adjuvant chemotherapy. Lower *RRM2* expression was accompanied by a better patient survival (FUJITA *et al.* 2010, ITOI *et al.* 2007). In this manner, the observed induction of *RRM2* during chemotherapy courses with gemcitabine might add the peripheral blood stream as a system to monitor occurrence of secondary resistance toward this drug. Alternatively, as gemcitabine di- and triphosphate metabolites counteract RRM2 activity, it is also possible that transcriptional induction of *RRM2* may reflect stronger gemcitabine activation and efficacy. Thus, interpretation of these observed expression changes should be done with caution since survival data of the respective patients have not been analyzed yet.

5.2.2 *RRM2* variant expression is differentially affected by gemcitabine

Two human *RRM2* transcript isoforms are known (Figure 34). The *RRM2* transcript isoform with the shorter 5'-tail represents the vast majority of *RRM2* transcripts. This implies that the data discussed in chapter 5.2.1 virtually reflect this isoform. The second variant, which features an extended 5'-region, exhibited markedly different response to gemcitabine. This resulted in a shift of the isoform ratio favoring the major one upon gemcitabine exposure in LCLs (Figure 36, Figure 37 panel A), pancreatic cancer cell lines (Figure 37, panel B) as well as in patients blood during chemotherapy (Figure 38). This finding suggests alternative promoters or interacting enhancer elements to drive versatile gene expression (AYOUBI AND VAN DE VEN 1996). To the best of my knowledge, no transcript isoform-specific investigations have been undertaken so far in literature.

5.2.3 Index SNP affects *RRM2* transcript variant-specific expression

No statistically significant impact of *RRM2* index SNP on transcription of the *RRM2* major isoform could be identified (Figure 39, panel A). However, an increased expression of the extended 5'-region variant was observed with increasing numbers of the *T* variant allele at the index SNP rs1130609. This association appeared intensified upon gemcitabine exposure (Figure 39, panel B).

The SNP rs1130609 is located in the Kozak sequence regarding the major transcript isoform and at codon 59 with respect to the isoform with 5'-extension. As only the latter was affected by this SNP a classical modulation of promoter activity is not assumed. Alternative hypotheses include an enhancer element for transcription of the extended isoform modulated by this SNP or an indirect consequence of a primary impact of this SNP on major transcript isoform expression (see below, section 5.2.4).

Isoform-specific gene transcription mediated by polymorphisms was also reported for the progesterone receptor (*PR*) gene associated with endometrial cancer risk (DE VIVO *et al.* 2002).

5.2.4 Allele-specific binding at the index SNP site

Using nuclear extracts from different cell lines, allele-specific protein binding was observed at rs1130609 with stronger binding in presence of the *G* allele (see Figure 40 and Figure 41). This allele was the one associated with poor clinical prognosis. This SNP is located in the Kozak sequence, 6 bp prior to the translation start site, which was described as a typical binding site for transcription factors as SP1, NF-Y, ETS and NRF-1 (FITZGERALD *et al.* 2004). The identity of the binding protein could not be identified. At least, SP1 was excluded. However, it is unlikely that allele-specific transcription factor binding constitutes a relevant mechanism in this issue since no impact on the expression of the respective (major) isoform could be noticed (Figure 39, panel A). That raises the assumption that translation to protein rather than gene transcription might be impacted by this SNP modifying the Kozak sequence.

5.2.5 Unifying model how the *RRM2* SNP might act

Presumed mechanisms linking the *RRM2* rs1130609 SNP effect to *RRM2* transcript expression and RRM2 protein translation are illustrated in an unifying model (see Figure 45): Di-and tri-phosphorylated gemcitabine metabolites inhibit the physiological function of RRM2 by competing with ADP, CDP, GDP, and UDP. Thus decreased levels of dADP, dCDP, dGDP, and dUDP stimulate *RRM2* transcription, most probably that of the major variant. In presence of the *G* wild type allele, translational mechanisms are supposed to work proper leading to unimpaired RRM2 protein synthesis. In this case, there is no need for enhanced transcription of the alternative 5'-extended isoform V1. *Vice verca* in presence of the *T* variant allele, the translational machinery is assumed to act less efficient, what impairs protein translation. As a consequence, expression of isoform V1 is stimulated.
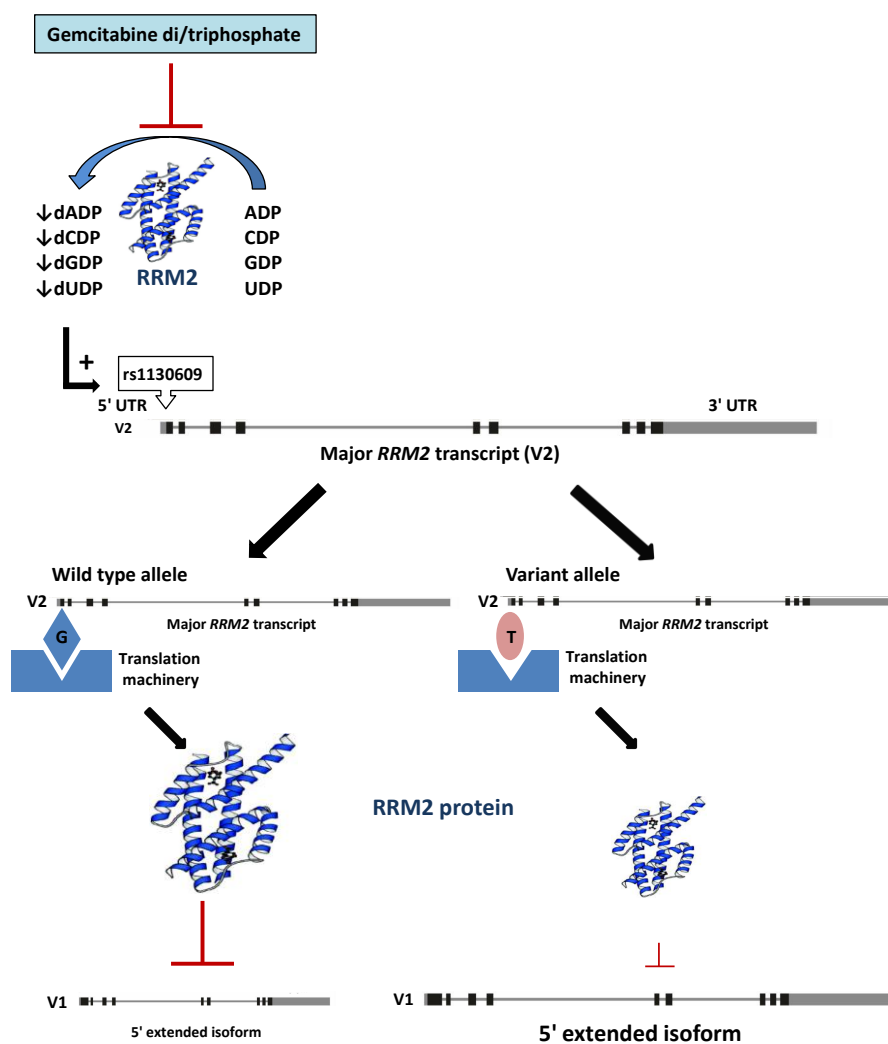
Figure 45: Hypothesized impact of *RRM2* rs1130609 on *RRM2* transcript expression and protein translation.
The major transcript isoform is denoted as V2, the 5'-extended one as V1.

5.3   Limitations

Regarding to the results of my thesis some limitations have to be considered. Sensitivity testing toward gemcitabine was performed in a set of LCLs instead in pancreatic cancer cell lines. The reason for this was the limited number of genetically divers pancreatic cancer cell lines. A clear link of *SP1* overexpression with the *WWOX* index SNP is debatable since there are several other sites containing the consensus sequence for SP1 binding. Genome-wide consequences on transcriptome were assessed upon shRNA against *WWOX*, what subsequently turned out to be insufficient. Instead, transcriptome analysis upon siRNA-mediated *WWOX* knock-down should have been performed.

Though full integrity of the generated *RRM2* vector constructs was proven, translational effects of the two *RRM2* index SNP alleles, as assessed by an *in vitro* Transcription/Translation system, were not clearly distinguishable. In view of an overall low signal intensity the difference of 37 % between the two alleles is debatable. Further elaboration is required to decipher if there is any allelic distinction in translation efficacy. Regarding the prospective patient cohort, clinical outcome data were lacking and thus the medical relevance of the observed *RRM2* induction is not clear.

5.4 Outlook

Based on the results of my thesis, further investigations are necessary to establish WWOX in general and the rs11644322 SNP in particular as biomarker in gemcitabine-treated pancreatic cancer. In clinical regard, prospective and randomized trials should address this SNP. In functional regard, deeper mechanistic understanding how WWOX interferes with cytotoxic effects provoked by gemcitabine might contribute to improve treatment efficacy. A hypothesized model for the putative role of WWOX (modulated by the SNP rs11644322) in dependence on the p53 mutation status is proposed in Figure 46: The principal assumption is that WWOX might substitute, at least in part, for p53 function, which becomes particularly relevant if the latter is inactivated by mutation what frequently occurs in cancer. In presence of the *G* allele at rs11644322 (see Figure 46, panel A) higher *WWOX* expression may foster cytotoxicity of gemcitabine by inhibiting both wnt/β-catenin signaling and EMT. In contrast, in case of the *A* allele (Figure 46, panel B) this disinhibiting effect of WWOX is assumed to be mitigated resulting in less gemcitabine cytotoxicity. These presumed interactions and analyses of components involved in the genotoxic response like the p53-inducible *GADD45A* should be elucidated in detail. Moreover, following this suggested model the effect of WWOX might be particularly relevant in case of inactivated p53, what appears promising to study in PDAC tissues with respect to clinical outcome.
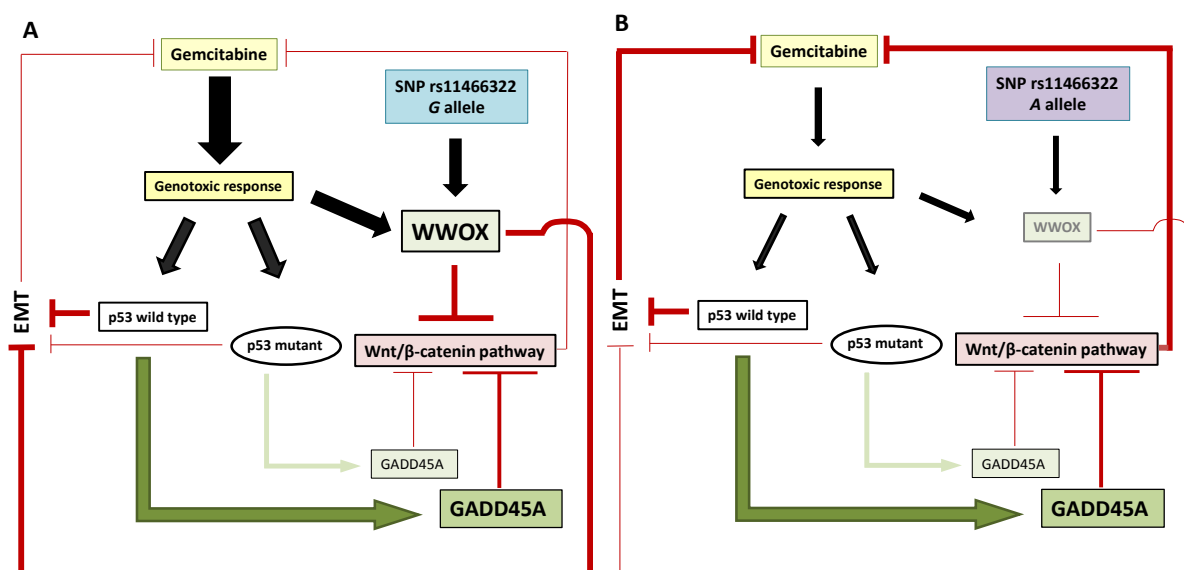
Figure 46: Hypothesized interactions of WWOX with p53, EMT and the Wnt/β-catenin pathway. Panel A demonstrates the model in case of the wild type *G* allele at the *WWOX* SNP rs11644322, panel B in case of the variant *A* allele, respectively. See text for details.

6 Conclusion

Regarding WWOX, by several lines of evidence I could delineate specific functional relations with gemcitabine supporting the clinical association. The data I gained may assist to circumvent failure of gemcitabine-based chemotherapy in PDAC. Though several mechanisms have been studied in this thesis and elicited striking results. The full interactions of WWOX in general and of the index SNP in particular with the DNA damage repair and the apoptotic machinery remains to be clarified. In view of the recently strongly increasing number of literature reports, highlighting the role of WWOX in the context of carcinogenesis, functional data addressing drug-specific interactions valuably expand the mechanistic understanding of this factor.

With respect to RRM2, a mechanism of action for a Kozak sequence polymorphism is proposed. Pending an unequivocal functional read-out for assessing an allele-specific impact on translation the data I obtained could contribute to the understanding of RRM2 in relation to gemcitabine resistance. Future strategies to overcome such resistance may consider this *RRM2* SNP. The clinical relevance of *RRM2* transcriptional induction during chemotherapy along with a possible modulation by this SNP remains to be further elaborated.

7 References

ABBRUZZESE, J. L., GRUNEWALD, R., WEEKS, E. A., GRAVEL, D., ADAMS, T.*, et al.* (1991). "A phase I clinical, plasma, and cellular pharmacology study of gemcitabine." J Clin Oncol **9**(3): 491-498.

ABU-ODEH, M., BAR-MAG, T., HUANG, H., KIM, T., SALAH, Z.*, et al.* (2014). "Characterizing WW domain interactions of tumor suppressor WWOX reveals its association with multiprotein networks." J Biol Chem **289**(13): 8865-8880.

ABU-ODEH, M., SALAH, Z., HERBEL, C., HOFMANN, T. G. AND AQEILAN, R. I. (2014). "WWOX, the common fragile site FRA16D gene product, regulates ATM activation and the DNA damage response." Proc Natl Acad Sci U S A **111**(44): E4716-4725.

AMANO, T., SAGAI, T., TANABE, H., MIZUSHINA, Y., NAKAZAWA, H.*, et al.* (2009). "Chromosomal dynamics at the Shh locus: limb bud-specific differential regulation of competence and active transcription." Dev Cell **16**(1): 47-57.

AQEILAN, R. I., PEKARSKY, Y., HERRERO, J. J., PALAMARCHUK, A., LETOFSKY, J.*, et al.* (2004). "Functional association between Wwox tumor suppressor protein and p73, a p53 homolog." Proc Natl Acad Sci U S A **101**(13): 4401-4406.

ARISAWA, T., TAHARA, T., SHIBATA, T., NAGASAKA, M., NAKAMURA, M.*, et al.* (2008). "The influence of polymorphisms of interleukin-17A and interleukin-17F genes on the susceptibility to ulcerative colitis." J Clin Immunol **28**(1): 44-49.

ARISAWA, T., TAHARA, T., SHIBATA, T., NAGASAKA, M., NAKAMURA, M.*, et al.* (2007). "Genetic polymorphisms of molecules associated with inflammation and immune response in Japanese subjects with functional dyspepsia." Int J Mol Med **20**(5): 717-723.

ARTINYAN, A., SORIANO, P. A., PRENDERGAST, C., LOW, T., ELLENHORN, J. D.*, et al.* (2008). "The anatomic location of pancreatic cancer is a prognostic factor for survival." HPB (Oxford) **10**(5): 371-376.

ARUMUGAM, T., RAMACHANDRAN, V., FOURNIER, K. F., WANG, H., MARQUIS, L.*, et al.* (2009). "Epithelial to mesenchymal transition contributes to drug resistance in pancreatic cancer." Cancer Res **69**(14): 5820-5828.

AYOUBI, T. A. AND VAN DE VEN, W. J. (1996). "Regulation of gene expression by alternative promoters." FASEB J **10**(4): 453-460.

BABU, D. A., CHAKRABARTI, S. K., GARMEY, J. C. AND MIRMIRA, R. G. (2008). "Pdx1 and BETA2/NeuroD1 participate in a transcriptional complex that mediates short-range DNA looping at the insulin gene." J Biol Chem **283**(13): 8164-8172.

BARRETO, G., SCHAFER, A., MARHOLD, J., STACH, D., SWAMINATHAN, S. K*., et al.* (2007). "Gadd45a promotes epigenetic gene activation by repair-mediated DNA demethylation." Nature **445**(7128): 671-675.

BECKER, A. E., HERNANDEZ, Y. G., FRUCHT, H. AND LUCAS, A. L. (2014). "Pancreatic ductal adenocarcinoma: risk factors, screening, and early detection." World J Gastroenterol **20**(32): 11182-11198.

BEDNAREK, A. K., KECK-WAGGONER, C. L., DANIEL, R. L., LAFLIN, K. J., BERGSAGEL, P. L*., et al.* (2001). "WWOX, the FRA16D gene, behaves as a suppressor of tumor growth." Cancer Res **61**(22): 8068-8073.

BEDNAREK, A. K., LAFLIN, K. J., DANIEL, R. L., LIAO, Q., HAWKINS, K. A*., et al.* (2000). "WWOX, a novel WW domain-containing protein mapping to human chromosome 16q23.3-24.1, a region frequently affected in breast cancer." Cancer Res **60**(8): 2140-2145.

BENDINELLI, P., MARONI, P., MATTEUCCI, E. AND DESIDERIO, M. A. (2015). "HGF and TGFbeta1 differently influenced Wwox regulatory function on Twist program for mesenchymal-epithelial transition in bone metastatic versus parental breast carcinoma cells." Mol Cancer **14**: 112.

BERGMAN, A. M., PINEDO, H. M. AND PETERS, G. J. (2002). "Determinants of resistance to 2',2'-difluorodeoxycytidine (gemcitabine)." Drug Resist Updat **5**(1): 19-33.

BIRD, A. (2002). "DNA methylation patterns and epigenetic memory." Genes Dev **16**(1): 6-21.

BOUTEILLE, N., DRIOUCH, K., HAGE, P. E., SIN, S., FORMSTECHER, E*., et al.* (2009). "Inhibition of the Wnt/beta-catenin pathway by the WWOX tumor suppressor protein." Oncogene **28**(28): 2569-2580.

BRENNAN, M. F., MOCCIA, R. D. AND KLIMSTRA, D. (1996). "Management of adenocarcinoma of the body and tail of the pancreas." Ann Surg **223**(5): 506-511; discussion 511-502.

BURRIS, H. A., 3RD, MOORE, M. J., ANDERSEN, J., GREEN, M. R., ROTHENBERG, M. L*., et al.* (1997). "Improvements in survival and clinical benefit with gemcitabine as first-line therapy for patients with advanced pancreas cancer: a randomized trial." J Clin Oncol **15**(6): 2403-2413.

CALDAS, C., HAHN, S. A., DA COSTA, L. T., REDSTON, M. S., SCHUTTE, M*., et al.* (1994). "Frequent somatic mutations and homozygous deletions of the p16 (MTS1) gene in pancreatic adenocarcinoma." Nat Genet **8**(1): 27-32.

CALHOUN, E. S., JONES, J. B., ASHFAQ, R., ADSAY, V., BAKER, S. J*., et al.* (2003). "BRAF and FBXW7 (CDC4, FBW7, AGO, SEL10) mutations in distinct subsets of pancreatic cancer: potential therapeutic targets." Am J Pathol **163**(4): 1255-1260.

CARRIER, F., GEORGEL, P. T., POURQUIER, P., BLAKE, M., KONTNY, H. U*., et al.* (1999). "Gadd45, a p53-responsive stress protein, modifies DNA accessibility on damaged chromatin." Mol Cell Biol **19**(3): 1673-1685.

CHAN, T. A., HERMEKING, H., LENGAUER, C., KINZLER, K. W. AND VOGELSTEIN, B. (1999). "14-3-3Sigma is required to prevent mitotic catastrophe after DNA damage." Nature **401**(6753): 616-620.

CHANG, N. S., DOHERTY, J., ENSIGN, A., LEWIS, J., HEATH, J.*, et al.* (2003). "Molecular mechanisms underlying WOX1 activation during apoptotic and stress responses." Biochem Pharmacol **66**(8): 1347-1354.

CHANG, N. S., DOHERTY, J., ENSIGN, A., SCHULTZ, L., HSU, L. J.*, et al.* (2005). "WOX1 is essential for tumor necrosis factor-, UV light-, staurosporine-, and p53-mediated cell death, and its tyrosine 33-phosphorylated form binds and stabilizes serine 46-phosphorylated p53." J Biol Chem **280**(52): 43100-43108.

CHANG, N. S., PRATT, N., HEATH, J., SCHULTZ, L., SLEVE, D.*, et al.* (2001). "Hyaluronidase induction of a WW domain-containing oxidoreductase that enhances tumor necrosis factor cytotoxicity." J Biol Chem **276**(5): 3361-3370.

CHEN, Y., MA, X., ZHANG, M., WANG, X., WANG, C.*, et al.* (2014). "Gadd45a regulates hematopoietic stem cell stress responses in mice." Blood **123**(6): 851-862.

CHIANG, M. F., CHOU, P. Y., WANG, W. J., SZE, C. I. AND CHANG, N. S. (2013). "Tumor Suppressor WWOX and p53 Alterations and Drug Resistance in Glioblastomas." Front Oncol **3**: 43.

CHIANG, M. F., YEH, S. T., LIAO, H. F., CHANG, N. S. AND CHEN, Y. J. (2012). "Overexpression of WW domain-containing oxidoreductase WOX1 preferentially induces apoptosis in human glioblastoma cells harboring mutant p53." Biomed Pharmacother **66**(6): 433-438.

CHUE, B. M. (2009). "Five-year survival of metastatic pancreatic carcinoma: a study of courage and hope." Gastrointest Cancer Res **3**(5): 208-211.

CONROY, T., DESSEIGNE, F., YCHOU, M., BOUCHE, O., GUIMBAUD, R.*, et al.* (2011). "FOLFIRINOX versus gemcitabine for metastatic pancreatic cancer." N Engl J Med **364**(19): 1817-1825.

CONROY, T., GAVOILLE, C., SAMALIN, E., YCHOU, M. AND DUCREUX, M. (2013). "The role of the FOLFIRINOX regimen for advanced pancreatic cancer." Curr Oncol Rep **15**(2): 182-189.

CONROY, T. AND MITRY, E. (2011). "[Chemotherapy of metastatic pancreatic adenocarcinoma: challenges and encouraging results]." Bull Cancer **98**(12): 1439-1446.

CUNNINGHAM, D., CHAU, I., STOCKEN, D. D., VALLE, J. W., SMITH, D.*, et al.* (2009). "Phase III randomized comparison of gemcitabine versus gemcitabine plus capecitabine in patients with advanced pancreatic cancer." J Clin Oncol **27**(33): 5513-5518.

DALILA, N., BROCKMOLLER, J., TZVETKOV, M. V., SCHIRMER, M., HAUBROCK, M., *et al.* (2015). "Impact of mineralocorticoid receptor polymorphisms on urinary electrolyte excretion with and without diuretic drugs." Pharmacogenomics **16**(2): 115-127.

DE VIVO, I., HUGGINS, G. S., HANKINSON, S. E., LESCAULT, P. J., BOEZEN, M., *et al.* (2002). "A functional polymorphism in the promoter of the progesterone receptor gene associated with endometrial cancer risk." Proc Natl Acad Sci U S A **99**(19): 12263-12268.

DELPERO, J. R., TURRINI, O. AND RAOUL, J. L. (2015). "[Management of localized, locally advanced and metastatic pancreatic adenocarcinoma]." Rev Prat **65**(3): 382-389.

DESHANE, J., KIM, J., BOLISETTY, S., HOCK, T. D., HILL-KAPTURCZAK, N., *et al.* (2010). "Sp1 regulates chromatin looping between an intronic enhancer and distal promoter of the human heme oxygenase-1 gene in renal cells." J Biol Chem **285**(22): 16476-16486.

DI MAGLIANO, M. P. AND LOGSDON, C. D. (2013). "Roles for KRAS in pancreatic tumor development and progression." Gastroenterology **144**(6): 1220-1229.

DUXBURY, M. S., ITO, H., ZINNER, M. J., ASHLEY, S. W. AND WHANG, E. E. (2004). "RNA interference targeting the M2 subunit of ribonucleotide reductase enhances pancreatic adenocarcinoma chemosensitivity to gemcitabine." Oncogene **23**(8): 1539-1548.

EL-HAGE, P., PETITALOT, A., MONSORO-BURQ, A. H., MACZKOWIAK, F., DRIOUCH, K., *et al.* (2015). "The Tumor-Suppressor WWOX and HDAC3 Inhibit the Transcriptional Activity of the beta-Catenin Coactivator BCL9-2 in Breast Cancer Cells." Mol Cancer Res **13**(5): 902-912.

ELLI LILY AND COMPANY DRUG INFORMATION SHEET GEMZAR (2014) Drug information Gemzar. available from: www.gemzar.com

ESER, S., SCHNIEKE, A., SCHNEIDER, G. AND SAUR, D. (2014). "Oncogenic KRAS signalling in pancreatic cancer." Br J Cancer **111**(5): 817-822.

FARRELL, J. J., BAE, K., WONG, J., GUHA, C., DICKER, A. P., *et al.* (2012). "Cytidine deaminase single-nucleotide polymorphism is predictive of toxicity from gemcitabine in patients with pancreatic cancer: RTOG 9704." Pharmacogenomics J **12**(5): 395-403.

FARRELL, J. J., ELSALEH, H., GARCIA, M., LAI, R., AMMAR, A., *et al.* (2009). "Human equilibrative nucleoside transporter 1 levels predict response to gemcitabine in patients with pancreatic cancer." Gastroenterology **136**(1): 187-195.

FIORINI, C., CORDANI, M., PADRONI, C., BLANDINO, G., DI AGOSTINO, S., *et al.* (2015). "Mutant p53 stimulates chemoresistance of pancreatic adenocarcinoma cells to gemcitabine." Biochim Biophys Acta **1853**(1): 89-100.

FISHER, S. B., PATEL, S. H., BAGCI, P., KOOBY, D. A., EL-RAYES, B. F., *et al.* (2013). "An analysis of human equilibrative nucleoside transporter-1, ribonucleoside reductase subunit M1, ribonucleoside reductase subunit M2, and excision repair cross-complementing gene-1 expression in patients with resected pancreas adenocarcinoma: implications for adjuvant treatment." Cancer **119**(2): 445-453.

FITZGERALD, P. C., SHLYAKHTENKO, A., MIR, A. A. AND VINSON, C. (2004). "Clustering of DNA sequences in human promoters." Genome Res **14**(8): 1562-1574.

FORNACE, A. J., JR., JACKMAN, J., HOLLANDER, M. C., HOFFMAN-LIEBERMANN, B. AND LIEBERMANN, D. A. (1992). "Genotoxic-stress-response genes and growth-arrest genes. gadd, MyD, and other genes induced by treatments eliciting growth arrest." Ann N Y Acad Sci **663**: 139-153.

FRIDMAN, J. S. AND LOWE, S. W. (2003). "Control of apoptosis by p53." Oncogene **22**(56): 9030-9040.

FUJITA, H., OHUCHIDA, K., MIZUMOTO, K., ITABA, S., ITO, T., *et al.* (2010). "Gene expression levels as predictive markers of outcome in pancreatic cancer after gemcitabine-based adjuvant chemotherapy." Neoplasia **12**(10): 807-817.

FUKUNAGA, A. K., MARSH, S., MURRY, D. J., HURLEY, T. D. AND MCLEOD, H. L. (2004). "Identification and analysis of single-nucleotide polymorphisms in the gemcitabine pharmacologic pathway." Pharmacogenomics J **4**(5): 307-314.

GILLEN, S., SCHUSTER, T., MEYER ZUM BUSCHENFELDE, C., FRIESS, H. AND KLEEFF, J. (2010). "Preoperative/neoadjuvant therapy in pancreatic cancer: a systematic review and meta-analysis of response and resection percentages." PLoS Med **7**(4): e1000267.

GIOVANNETTI, E., DEL TACCA, M., MEY, V., FUNEL, N., NANNIZZI, S., *et al.* (2006). "Transcription analysis of human equilibrative nucleoside transporter-1 predicts survival in pancreas cancer patients treated with gemcitabine." Cancer Res **66**(7): 3928-3935.

GONG, F., SUN, L., WANG, Z., SHI, J., LI, W., *et al.* (2011). "The BCL2 gene is regulated by a special AT-rich sequence binding protein 1-mediated long range chromosomal interaction between the promoter and the distal element located within the 3'-UTR." Nucleic Acids Res **39**(11): 4640-4652.

GREENHALF, W., GHANEH, P., NEOPTOLEMOS, J. P., PALMER, D. H., COX, T. F., *et al.* (2014). "Pancreatic cancer hENT1 expression and survival from gemcitabine in patients from the ESPAC-3 trial." J Natl Cancer Inst **106**(1): djt347.

GREENLEE, R. T., MURRAY, T., BOLDEN, S. AND WINGO, P. A. (2000). "Cancer statistics, 2000." CA Cancer J Clin **50**(1): 7-33.

GRUNEWALD, R., ABBRUZZESE, J. L., TARASSOFF, P. AND PLUNKETT, W. (1991). "Saturation of 2',2'-difluorodeoxycytidine 5'-triphosphate accumulation by mononuclear cells during a phase I trial of gemcitabine." Cancer Chemother Pharmacol **27**(4): 258-262.

HAHN, S. A., SCHUTTE, M., HOQUE, A. T., MOSKALUK, C. A., DA COSTA, L. T*., et al.* (1996). "DPC4, a candidate tumor suppressor gene at human chromosome 18q21.1." Science **271**(5247): 350-353.

HAINAUT, P. AND HOLLSTEIN, M. (2000). "p53 and human cancer: the first ten thousand mutations." Adv Cancer Res **77**: 81-137.

HEINEMANN, V., LABIANCA, R., HINKE, A. AND LOUVET, C. (2007). "Increased survival using platinum analog combined with gemcitabine as compared to single-agent gemcitabine in advanced pancreatic cancer: pooled analysis of two randomized trials, the GERCOR/GISCAD intergroup study and a German multicenter study." Ann Oncol **18**(10): 1652-1659.

HEINEMANN, V., XU, Y. Z., CHUBB, S., SEN, A., HERTEL, L. W*., et al.* (1992). "Cellular elimination of 2',2'-difluorodeoxycytidine 5'-triphosphate: a mechanism of self-potentiation." Cancer Res **52**(3): 533-539.

HILDESHEIM, J. AND FORNACE, A. J., JR. (2002). "Gadd45a: an elusive yet attractive candidate gene in pancreatic cancer." Clin Cancer Res **8**(8): 2475-2479.

HOLLANDER, M. C., ALAMO, I., JACKMAN, J., WANG, M. G., MCBRIDE, O. W*., et al.* (1993). "Analysis of the mammalian gadd45 gene and its response to DNA damage." J Biol Chem **268**(32): 24385-24393.

HOLLANDER, M. C. AND FORNACE, A. J., JR. (2002). "Genomic instability, centrosome amplification, cell cycle checkpoints and Gadd45a." Oncogene **21**(40): 6228-6233.

HOLLANDER, M. C., KOVALSKY, O., SALVADOR, J. M., KIM, K. E., PATTERSON, A. D*., et al.* (2001). "Dimethylbenzanthracene carcinogenesis in Gadd45a-null mice is associated with decreased DNA repair and increased mutation frequency." Cancer Res **61**(6): 2487-2491.

HORII, A., NAKATSURU, S., MIYOSHI, Y., ICHII, S., NAGASE, H*., et al.* (1992). "Frequent somatic mutations of the APC gene in human pancreatic cancer." Cancer Res **52**(23): 6696-6698.

HOWLADER, N., NOONE, A., KRAPCHO, M., GARSHELL, J., NEYMAN, N*., et al.* (2013). "SEER Cancer Statistics Review 1975-2010." National Cancer Institute, availiable from: http://seer.cancer.gov/csr/1975_2010 , updated June 14, 2013.

HU, B. S., TAN, J. W., ZHU, G. H., WANG, D. F., ZHOU, X*., et al.* (2012). "WWOX induces apoptosis and inhibits proliferation of human hepatoma cell line SMMC-7721." World J Gastroenterol **18**(23): 3020-3026.

HUA, H. W., JIANG, F., HUANG, Q., LIAO, Z. AND DING, G. (2015). "MicroRNA-153 promotes Wnt/beta-catenin activation in hepatocellular carcinoma through suppression of WWOX." Oncotarget **6**(6): 3840-3847.

HUANG, P., CHUBB, S., HERTEL, L. W., GRINDEY, G. B. AND PLUNKETT, W. (1991). "Action of 2',2'-difluorodeoxycytidine on DNA synthesis." Cancer Res **51**(22): 6110-6117.

INNOCENTI, F., OWZAR, K., COX, N. L., EVANS, P., KUBO, M.*, et al.* (2012). "A genome-wide association study of overall survival in pancreatic cancer patients treated with gemcitabine in CALGB 80303." Clin Cancer Res **18**(2): 577-584.

ITOI, T., SOFUNI, A., FUKUSHIMA, N., ITOKAWA, F., TSUCHIYA, T.*, et al.* (2007). "Ribonucleotide reductase subunit M2 mRNA expression in pretreatment biopsies obtained from unresectable pancreatic carcinomas." J Gastroenterol **42**(5): 389-394.

IWAMOTO, K., NAKASHIRO, K., TANAKA, H., TOKUZEN, N. AND HAMAKAWA, H. (2015). "Ribonucleotide reductase M2 is a promising molecular target for the treatment of oral squamous cell carcinoma." Int J Oncol **46**(5): 1971-1977.

JACOBSON, M. D., BURNE, J. F., KING, M. P., MIYASHITA, T., REED, J. C.*, et al.* (1993). "Bcl-2 blocks apoptosis in cells lacking mitochondrial DNA." Nature **361**(6410): 365-369.

JI, J., LIU, R., TONG, T., SONG, Y., JIN, S.*, et al.* (2007). "Gadd45a regulates beta-catenin distribution and maintains cell-cell adhesion/contact." Oncogene **26**(44): 6396-6405.

JONES, S., ZHANG, X., PARSONS, D. W., LIN, J. C., LEARY, R. J.*, et al.* (2008). "Core signaling pathways in human pancreatic cancers revealed by global genomic analyses." Science **321**(5897): 1801-1806.

JUNG, D. B., YUN, M., KIM, E. O., KIM, J., KIM, B.*, et al.* (2015). "The heparan sulfate mimetic PG545 interferes with Wnt/beta-catenin signaling and significantly suppresses pancreatic tumorigenesis alone and in combination with gemcitabine." Oncotarget **6**(7): 4992-5004.

JUNG, H. J., KIM, H. L., KIM, Y. J., WEON, J. I. AND SEO, Y. R. (2013). "A novel chemopreventive mechanism of selenomethionine: enhancement of APE1 enzyme activity via a Gadd45a, PCNA and APE1 protein complex that regulates p53-mediated base excision repair." Oncol Rep **30**(4): 1581-1586.

KIM, R., TAN, A., LAI, K. K., JIANG, J., WANG, Y.*, et al.* (2011). "Prognostic roles of human equilibrative transporter 1 (hENT-1) and ribonucleoside reductase subunit M1 (RRM1) in resected pancreatic cancer." Cancer **117**(14): 3126-3134.

KOCABAS, N. A., AKSOY, P., PELLEYMOUNTER, L. L., MOON, I., RYU, J. S.*, et al.* (2008). "Gemcitabine pharmacogenomics: deoxycytidine kinase and cytidylate kinase gene resequencing and functional genomics." Drug Metab Dispos **36**(9): 1951-1959.

LAI, I. L., CHOU, C. C., LAI, P. T., FANG, C. S., SHIRLEY, L. A.*, et al.* (2014). "Targeting the Warburg effect with a novel glucose transporter inhibitor to overcome gemcitabine resistance in pancreatic cancer cells." Carcinogenesis **35**(10): 2203-2213.

LI, D., XIE, K., WOLFF, R. AND ABBRUZZESE, J. L. (2004). "Pancreatic cancer." Lancet **363**(9414): 1049-1057.

LI, G., RUAN, X., AUERBACH, R. K., SANDHU, K. S., ZHENG, M.*, et al.* (2012). "Extensive promoter-centered chromatin interactions provide a topological basis for transcription regulation." Cell **148**(1-2): 84-98.

LI, L., FRIDLEY, B., KALARI, K., JENKINS, G., BATZLER, A.*, et al.* (2008). "Gemcitabine and cytosine arabinoside cytotoxicity: association with lymphoblastoid cell expression." Cancer Res **68**(17): 7050-7058.

MARECHAL, R., BACHET, J. B., MACKEY, J. R., DALBAN, C., DEMETTER, P.*, et al.* (2012). "Levels of gemcitabine transport and metabolism proteins predict survival times of patients treated with gemcitabine for pancreatic adenocarcinoma." Gastroenterology **143**(3): 664-674 e661-666.

MARECHAL, R., MACKEY, J. R., LAI, R., DEMETTER, P., PEETERS, M.*, et al.* (2009). "Human equilibrative nucleoside transporter 1 and human concentrative nucleoside transporter 3 predict survival after adjuvant gemcitabine therapy in resected pancreatic adenocarcinoma." Clin Cancer Res **15**(8): 2913-2919.

MASTRANGELO, I. A., COUREY, A. J., WALL, J. S., JACKSON, S. P. AND HOUGH, P. V. (1991). "DNA looping and Sp1 multimer links: a mechanism for transcriptional synergism and enhancement." Proc Natl Acad Sci U S A **88**(13): 5670-5674.

MEIDHOF, S., BRABLETZ, S., LEHMANN, W., PRECA, B. T., MOCK, K.*, et al.* (2015). "ZEB1-associated drug resistance in cancer cells is reversed by the class I HDAC inhibitor mocetinostat." EMBO Mol Med **7**(6): 831-847.

MERCER, T. R., EDWARDS, S. L., CLARK, M. B., NEPH, S. J., WANG, H.*, et al.* (2013). "DNase I-hypersensitive exons colocalize with promoters and distal regulatory elements." Nat Genet **45**(8): 852-859.

MINI, E., NOBILI, S., CACIAGLI, B., LANDINI, I. AND MAZZEI, T. (2006). "Cellular pharmacology of gemcitabine." Ann Oncol **17 Suppl 5**: v7-12.

MIYAKI, M. AND KUROKI, T. (2003). "Role of Smad4 (DPC4) inactivation in human cancer." Biochem Biophys Res Commun **306**(4): 799-804.

MORTON, J. P., TIMPSON, P., KARIM, S. A., RIDGWAY, R. A., ATHINEOS, D.*, et al.* (2010). "Mutant p53 drives metastasis and overcomes growth arrest/senescence in pancreatic cancer." Proc Natl Acad Sci U S A **107**(1): 246-251.

NAGANO, H., TOMIMARU, Y., EGUCHI, H., HAMA, N., WADA, H.*, et al.* (2013). "MicroRNA-29a induces resistance to gemcitabine through the Wnt/beta-catenin signaling pathway in pancreatic cancer cells." Int J Oncol **43**(4): 1066-1072.

NAKAHIRA, S., NAKAMORI, S., TSUJIE, M., TAKAHASHI, Y., OKAMI, J*., et al.* (2007)*.* "Involvement of ribonucleotide reductase M1 subunit overexpression in gemcitabine resistance of human pancreatic cancer." International Journal of Cancer **120**(6): 1355-1363.

NAKANO, Y., TANNO, S., KOIZUMI, K., NISHIKAWA, T., NAKAMURA, K*., et al.* (2007). "Gemcitabine chemoresistance and molecular markers associated with gemcitabine transport and metabolism in human pancreatic cancer cells." Br J Cancer **96**(3): 457-463.

NANDA, R. H., EL-RAYES, B., MAITHEL, S. K. AND LANDRY, J. (2015). "Neoadjuvant modified FOLFIRINOX and chemoradiation therapy for locally advanced pancreatic cancer improves resectability." J Surg Oncol.

NEOPTOLEMOS, J. P., STOCKEN, D. D., BASSI, C., GHANEH, P., CUNNINGHAM, D*., et al.* (2010). "Adjuvant chemotherapy with fluorouracil plus folinic acid vs gemcitabine following pancreatic cancer resection: a randomized controlled trial." JAMA **304**(10): 1073-1081.

O'REILLY, D. AND GREAVES, D. R. (2007). "Cell-type-specific expression of the human CD68 gene is associated with changes in Pol II phosphorylation and short-range intrachromosomal gene looping." Genomics **90**(3): 407-415.

OKAZAKI, T., JAVLE, M., TANAKA, M., ABBRUZZESE, J. L. AND LI, D. (2010). "Single nucleotide polymorphisms of gemcitabine metabolic genes and pancreatic cancer survival and drug toxicity." Clin Cancer Res **16**(1): 320-329.

PAPROSKI, R. J., YAO, S. Y., FAVIS, N., EVANS, D., YOUNG, J. D*., et al.* (2013). "Human concentrative nucleoside transporter 3 transfection with ultrasound and microbubbles in nucleoside transport deficient HEK293 cells greatly increases gemcitabine uptake." PLoS One **8**(2): e56423.

PLUCIENNIK, E., NOWAKOWSKA, M., POSPIECH, K., STEPIEN, A., WOLKOWICZ, M*., et al.* (2015). "The role of WWOX tumor suppressor gene in the regulation of EMT process via regulation of CDH1-ZEB1-VIM expression in endometrial cancer." Int J Oncol **46**(6): 2639-2648.

PLUNKETT, W., HUANG, P. AND GANDHI, V. (1995). "Preclinical characteristics of gemcitabine." Anticancer Drugs **6 Suppl 6**: 7-13.

POMERANTZ, M. M., AHMADIYEH, N., JIA, L., HERMAN, P., VERZI, M. P*., et al.* (2009). "The 8q24 cancer risk variant rs6983267 shows long-range interaction with MYC in colorectal cancer." Nat Genet **41**(8): 882-884.

RACHAKONDA, P. S., BAUER, A. S., XIE, H., CAMPA, D., RIZZATO, C*., et al.* (2013). "Somatic mutations in exocrine pancreatic tumors: association with patient survival." PLoS One **8**(4): e60870.

REJIBA, S., BIGAND, C., PARMENTIER, C. AND HAJRI, A. (2009). "Gemcitabine-based chemogene therapy for pancreatic cancer using Ad-dCK::UMK GDEPT and TS/RR siRNA strategies." Neoplasia **11**(7): 637-650.

RICHARDS, R. I., CHOO, A., LEE, C. S., DAYAN, S. AND O'KEEFE, L. (2015). "WWOX, the chromosomal fragile site FRA16D spanning gene: its role in metabolism and contribution to cancer." Exp Biol Med (Maywood) **240**(3): 338-344.

RIED, K., FINNIS, M., HOBSON, L., MANGELSDORF, M., DAYAN, S.*, et al.* (2000). "Common chromosomal fragile site FRA16D sequence: identification of the FOR gene spanning FRA16D and homozygous deletions and translocation breakpoints in cancer cells." Hum Mol Genet **9**(11): 1651-1663.

ROBERT-KOCH INSTITUT (2012). "Krebs in Deutschland 2005 - 2006, Häufigkeiten und Trends: Bauchspeicheldrüse." **7. Auflage 2010**(40 - 43. 3).

ROPPEL, S. (2013). "Functional Assessment of Biomarkers in Gemcitabine-Treated Pancreatic Cancer with Specific Focus on Nucleoside Transporter ENT1". Doctoral Thesis**:** 1-159.

RUIZ VAN HAPEREN, V. W., VEERMAN, G., VERMORKEN, J. B. AND PETERS, G. J. (1993). "2',2'-Difluoro-deoxycytidine (gemcitabine) incorporation into RNA and DNA of tumour cell lines." Biochem Pharmacol **46**(4): 762-766.

SAIF, M. W. AND KIM, R. (2007). "Role of platinum agents in the management of advanced pancreatic cancer." Expert Opin Pharmacother **8**(16): 2719-2727.

SALVADOR, J. M., BROWN-CLAY, J. D. AND FORNACE, A. J., JR. (2013). "Gadd45 in stress signaling, cell cycle control, and apoptosis." Adv Exp Med Biol **793**: 1-19.

SANGER, F. AND COULSON, A. R. (1975). "A rapid method for determining sequences in DNA by primed synthesis with DNA polymerase." J Mol Biol **94**(3): 441-448.

SCHAFER, A., SCHOMACHER, L., BARRETO, G., DODERLEIN, G. AND NIEHRS, C. (2010). "Gemcitabine functions epigenetically by inhibiting repair mediated DNA demethylation." PLoS One **5**(11): e14060.

SCHOENFELDER, S., CLAY, I. AND FRASER, P. (2010). "The transcriptional interactome: gene expression in 3D." Curr Opin Genet Dev **20**(2): 127-133.

SCHROCK, M. S. AND HUEBNER, K. (2015). "WWOX: a fragile tumor suppressor." Exp Biol Med (Maywood) **240**(3): 296-304.

SHI, X., LIU, S., KLEEFF, J., FRIESS, H. AND BUCHLER, M. W. (2002). "Acquired resistance of pancreatic cancer cells towards 5-Fluorouracil and gemcitabine is associated with altered expression of apoptosis-regulating genes." Oncology (Williston Park) **62**(4): 354-362.

SHIMODA, M., KUBOTA, K., SHIMIZU, T. AND KATOH, M. (2015). "Randomized clinical trial of adjuvant chemotherapy with S-1 versus gemcitabine after pancreatic cancer resection." Br J Surg **102**(7): 746-754.

SHRIKHANDE, S. V., KLEEFF, J., REISER, C., WEITZ, J., HINZ, U*., et al.* (2007). "Pancreatic resection for M1 pancreatic ductal adenocarcinoma." Ann Surg Oncol **14**(1): 118-127.

SIEGEL, R., NAISHADHAM, D. AND JEMAL, A. (2013). "Cancer statistics, 2013." CA Cancer J Clin **63**(1): 11-30.

SMIT, V. T., BOOT, A. J., SMITS, A. M., FLEUREN, G. J., CORNELISSE, C. J*., et al.* (1988). "KRAS codon 12 mutations occur very frequently in pancreatic adenocarcinomas." Nucleic Acids Res **16**(16): 7773-7782.

SMITH, M. L., CHEN, I. T., ZHAN, Q., BAE, I., CHEN, C. Y*., et al.* (1994). "Interaction of the p53-regulated protein Gadd45 with proliferating cell nuclear antigen." Science **266**(5189): 1376-1380.

SMITH, M. L., FORD, J. M., HOLLANDER, M. C., BORTNICK, R. A., AMUNDSON, S. A*., et al.* (2000). "p53-mediated DNA repair responses to UV radiation: studies of mouse cells lacking p53, p21, and/or gadd45 genes." Mol Cell Biol **20**(10): 3705-3714.

SPERTI, C., PASQUALI, C., PICCOLI, A. AND PEDRAZZOLI, S. (1997). "Recurrence after resection for ductal adenocarcinoma of the pancreas." World J Surg **21**(2): 195-200.

SPRATLIN, J., SANGHA, R., GLUBRECHT, D., DABBAGH, L., YOUNG, J. D*., et al.* (2004). "The absence of human equilibrative nucleoside transporter 1 is associated with reduced survival in patients with gemcitabine-treated pancreas adenocarcinoma." Clin Cancer Res **10**(20): 6956-6961.

STALEY, C. A., LEE, J. E., CLEARY, K. R., ABBRUZZESE, J. L., FENOGLIO, C. J*., et al.* (1996). "Preoperative chemoradiation, pancreaticoduodenectomy, and intraoperative radiation therapy for adenocarcinoma of the pancreatic head." Am J Surg **171**(1): 118-124; discussion 124-115.

STOFFEL, E. M. (2015). "Screening in GI Cancers: The Role of Genetics." J Clin Oncol **33**(16): 1721-1728.

TANAKA, M., JAVLE, M., DONG, X., ENG, C., ABBRUZZESE, J. L*., et al.* (2010). "Gemcitabine metabolic and transporter gene polymorphisms are associated with drug toxicity and efficacy in patients with locally advanced pancreatic cancer." Cancer **116**(22): 5325-5335.

THIERY, J. P., ACLOQUE, H., HUANG, R. Y. AND NIETO, M. A. (2009). "Epithelial-mesenchymal transitions in development and disease." Cell **139**(5): 871-890.

TOKINO, T. AND NAKAMURA, Y. (2000). "The role of p53-target genes in human cancer." Crit Rev Oncol Hematol **33**(1): 1-6.

TUUPANEN, S., TURUNEN, M., LEHTONEN, R., HALLIKAS, O., VANHARANTA, S*., et al.* (2009). "The common colorectal cancer predisposition SNP rs6983267 at chromosome 8q24 confers potential to enhanced Wnt signaling." Nat Genet **41**(8): 885-U837.

UENO, H., KIYOSAWA, K. AND KANIWA, N. (2007). "Pharmacogenomics of gemcitabine: can genetic studies lead to tailor-made therapy?" Br J Cancer **97**(2): 145-151.

VACCARO, V., SPERDUTI, I., VARI, S., BRIA, E., MELISI, D*., et al.* (2015). "Metastatic pancreatic cancer: Is there a light at the end of the tunnel?" World J Gastroenterol **21**(16): 4788-4801.

VALSECCHI, M. E., HOLDBROOK, T., LEIBY, B. E., PEQUIGNOT, E., LITTMAN, S. J*., et al.* (2012). "Is there a role for the quantification of RRM1 and ERCC1 expression in pancreatic ductal adenocarcinoma?" BMC Cancer **12**: 104.

VAN LAETHEM, J. L., VERSLYPE, C., IOVANNA, J. L., MICHL, P., CONROY, T*., et al.* (2012). "New strategies and designs in pancreatic cancer research: consensus guidelines report from a European expert panel." Ann Oncol **23**(3): 570-576.

VINCENT, A., HERMAN, J., SCHULICK, R., HRUBAN, R. H. AND GOGGINS, M. (2011). "Pancreatic cancer." Lancet **378**(9791): 607-620.

VON HOFF, D. D., ERVIN, T., ARENA, F. P., CHIOREAN, E. G., INFANTE, J*., et al.* (2013). "Increased survival in pancreatic cancer with nab-paclitaxel plus gemcitabine." N Engl J Med **369**(18): 1691-1703.

WANG, C., ZHANG, W., FU, M., YANG, A., HUANG, H*., et al.* (2015). "Establishment of human pancreatic cancer gemcitabineresistant cell line with ribonucleotide reductase overexpression." Oncol Rep **33**(1): 383-390.

WANG, J. P., WU, C. Y., YEH, Y. C., SHYR, Y. M., WU, Y. Y*., et al.* (2015). "Erlotinib is effective in pancreatic cancer with epidermal growth factor receptor mutations: a randomized, open-label, prospective trial." Oncotarget.

WANG, R., CHENG, L., XIA, J., WANG, Z., WU, Q*., et al.* (2014). "Gemcitabine resistance is associated with epithelial-mesenchymal transition and induction of HIF-1alpha in pancreatic cancer cells." Curr Cancer Drug Targets **14**(4): 407-417.

WEISSMUELLER, S., MANCHADO, E., SABOROWSKI, M., MORRIS, J. P. T., WAGENBLAST, E*., et al.* (2014). "Mutant p53 drives pancreatic cancer metastasis through cell-autonomous PDGF receptor beta signaling." Cell **157**(2): 382-394.

WHITMARSH, A. J. AND DAVIS, R. J. (2000). "Regulation of transcription factor function by phosphorylation." Cell Mol Life Sci **57**(8-9): 1172-1183.

WOLFGANG, C. L., HERMAN, J. M., LAHERU, D. A., KLEIN, A. P., ERDEK, M. A*., et al.* (2013). "Recent progress in pancreatic cancer." CA Cancer J Clin **63**(5): 318-348.

WONG, A., SOO, R. A., YONG, W. P. AND INNOCENTI, F. (2009). "Clinical pharmacology and pharmacogenetics of gemcitabine." Drug Metab Rev **41**(2): 77-88.

YAN, H. AND SUN, Y. (2014). "Evaluation of the mechanism of epithelial-mesenchymal transition in human ovarian cancer stem cells transfected with a WW domain-containing oxidoreductase gene." Oncol Lett **8**(1): 426-430.

ZHAN, Q., ANTINORE, M. J., WANG, X. W., CARRIER, F., SMITH, M. L.*, et al.* (1999). "Association with Cdc2 and inhibition of Cdc2/Cyclin B1 kinase activity by the p53-regulated protein Gadd45." Oncogene **18**(18): 2892-2900.

ZIMMER, C. (2013). "Identifizierung von Biomarkern für die Prognose der Gemcitabin-Therapie beim Pankreaskarzinom: RNA-, DNA- und Immunhistochemische-Analysen". Doctoral Thesis**:** 1-89.

8 Curriculum Vitae

PERSONAL INFORMATION:

Name: Claudia Lüske

Date of birth: February 28th, 1986

Place of birth: Oldenburg i.O.

EDUCATION:

1992 - 1996:	Primary School, Molbergen
1996 - 1998:	Orientation stage, Molbergen
1998 - 2005:	Academic High School
	(Clemens-August-Gymnasium Cloppenburg)
June 2005:	University-entrance diploma
	(Allgemeinbildendes Abitur,
	Clemens-August-Gymnasium Cloppenburg)
2005 - 2008:	**Studies in Environmental Science**
	(Carl Von Ossietzky Universität Oldenburg)

<u>**First University qualification**</u>**:** Bachelor of Science "Umweltwissenschaften"

<u>Topic of my bachelor thesis:</u>

(performed at ICBM (Institut für Chemie und Biologie des Meeres)-Terramare Wilhelmshaven, Department of Marine Chemistry):

"Gelöste freie Aminosäuren in Porenwässern von Wattsedimenten."

2009 – 2012:	**Studies in Toxicology**
	(Technische Universität Kaiserslautern)

<u>**Second University qualification**</u>**:** Master of Science "Toxikologie"

<u>Topic of my master thesis:</u>

(performed at Bayer Health Care AG, Wuppertal, Department of Immunotoxicology):

"Analyse der Genexpressionsveränderungen in der Rattenlunge nach Inhalation verschieden großer Nano-Partikel."

since 08/2012: **PhD position** in the Molecular Medicine program at the Institute of Clinical Pharmacology at the University Medical Center of the George August University Göttingen.

08/2012 - 12/2014: Scholarship of the DFG Research Training Group (GRK1034).

Additional Qualifications:

• Certificate in ICH/GCP-Good Clinical Practice
(IFS GmbH, Institut für anwendungsorientierte Forschung und klinische Studien).

• Certificate: Module „Lebensmitteltoxikologie"
(Gesellschaft für Toxikologie in der DGPT (Deutsche Gesellschaft für experimentelle und klinische Pharmakologie und Toxikologie e.V.) und dem Helmholtz Zentrum München).

9 Appendix

Sequence of the pGeneClip™ Hygromycin vector used for sh-RNA (*WWOX*)-Transfection in section 3.10.2

3'GGGCGAATTGGGCCCGATATCTCTAGAGTCGACGAATTCGGATCCCTAAGGACCAGCTTCTTTGGGAGAGAACAGACGCAGGGGCGGGAGGGAAAAA
GGGAGAGGCAGACGTCACTTCCCCTTGGCGGCTCTGGCAGCAGATTGGTCGGTTGAGTGGCAGAAAGGCAGACGGGGACTGGGCAAGGCACTGTCGGT
GACATCACGGACAGGGCGACTTCTATGTAGATGAGGCAGCGCAGAGGCTGCTGCTTCGCCACTTGCTGCTTCACCACGAAGGAGTTCCCGTGCCCTGGGA
GCGGGTTCAGGACCGCTGATCGGAAGTGAGAATCCCAGCTGTGTGTCAGGGCTGGAAAGGGCTCGGGAGTGCGCGGGGCAAGTGACCGTGTGTGTAAA
GAGTGAGGCGTATGAGGCTGTGTCGGGGCAGAGGCCCAAGATCTCGCAGTCTGGAGTTTCAAAAGTAGACTGGGCGGCCGCATCGATGTTAACCTCGAG
GAGCTCCCAACGCGTTGGATGCATAGCTTGAGTATTCTATAGTGTCACCTAAATAGCTTGGCGTAATCATGGTCATAGCTGTTTCCTGTGTGAAATTGTTAT
CCGCTCACAATTCCACACAACATACGAGCCGGAAGCATAAAGTGTAAAGCCTGGGGTGCCTAATGAGTGAGCTAACTCACATTAATTGCGTTGCGCTCACT
GCCCGCTTTCCAGTCGGGAAACCTGTCGTGCCAGCTGCATTAATGAATCGGCCAACGCGCGGGGAGAGGCGGTTTGCGTATTGGGCGCTCTTCCGCTGAT
CTGCGCAGCACCATGGCCTGAAATAACCTCTGAAAGAGGAACTTGGTTAGGTACCTTCTGAGGCGGAAAGAACCAGCTGTGGAATGTGTGTCAGTTAGGG
TGTGGAAAGTCCCCAGGCTCCCCAGCAGGCAGAAGTATGCAAAGCATGCATCTCAATTAGTCAGCAACCAGGTGTGGAAAGTCCCCAGGCTCCCCAGCAG
GCAGAAGTATGCAAAGCATGCATCTCAATTAGTCAGCAACCATAGTCCCGCCCCTAACTCCGCCCATCCCGCCCCTAACTCCGCCCAGTTCCGCCCATTCTCC
GCCCCATGGCTGACTAATTTTTTTTATTTATGCAGAGGCCGAGGCCGCCTCGGCCTCTGAGCTATTCCAGAAGTAGTGAGGAGGCTTTTTTGGAGGCCTAG
GCTTTTGCAAAAAGCTTGATTCTTCTGACGCTAGCGATCGCCCGGGCCACCATGAAAAAGCCTGAACTCACCGCGACGTCTGTCGAGAAGTTTCTGATCGA
AAAGTTCGACAGCGTGTCCGACCTGATGCAGCTCTCGGAGGGCGAAGAATCTCGTGCTTTCAGCTTCGATGTAGGAGGGCGTGGATATGTCCTGCGGGTA
AATAGCTGCGCCGATGGTTTCTACAAAGATCGTTATGTTTATCGGCACTTTGCATCGGCCGCGCTCCCGATTCCGGAAGTGCTTGACATTGGGGAATTCAGC
GAGAGCCTGACCTATTGCATCTCCCGCCGTGCACAGGGTGTCACGTTGCAAGACCTGCCTGAAACCGAACTGCCCGCTGTTCTGCAGCCGGTCGCGGAGG
CCATGGATGCGATCGCTGCGGCCGATCTTAGCCAGACGAGCGGGTTCGGCCCATTCGGACCGCAAGGAATCGGTCAATACACTACATGGCGTGATTTCAT
ATGCGCGATTGCTGATCCCCATGTGTATCACTGGCAAACTGTGATGGACGACACCGTCAGTGCGTCCGTCGCGCAGGCTCTCGATGAGCTGATGCTTTGGG
CCGAGGACTGCCCCGAAGTCCGGCACCTCGTGCACGCGGATTTCGGCTCCAACAATGTCCTGACGGACAATGGCCGCATAACAGCGGTCATTGACTGGAG
CGAGGCGATGTTCGGGGATTCCCAATACGAGGTCGCCAACATCTTCTTCTGGAGGCCGTGGTTGGCTTGTATGGAGCAGCAGACGCGCTACTTCGAGCGG
AGGCATCCGGAGCTTGCAGGATCGCCGCGGCTCCGGGCGTATATGCTCCGCATTGGTCTTGACCAACTCTATCAGAGCTTGGTTGACGGCAATTTCGATGA
TGCAGCTTGGGCGCAGGGTCGATGCGACGCAATCGTCCGATCCGGAGCCGGGACTGTCGGGCGTACACAAATCGCCCGCAGAAGCGCGGCCGTCTGGAC
CGATGGCTGTGTAGAAGTACTCGCCGATAGTGGAAACCGACGCCCCAGCACTCGTCCGAGGGCAAAGGAATAGCTCGAGTTTAAACTCTAGAACCGGTCA
TGGCCGCAATAAAATATCTTTATTTTCATTACATCTGTGTGTTGGTTTTTTGTGTGTTCGAACTAGAAGCTTGCTTCCTCGCTCACTGACTCGCTGCGCTCGGT
CGTTCGGCTGCGGCGAGCGGTATCAGCTCACTCAAAGGCGGTAATACGGTTATCCACAGAATCAGGGGATAACGCAGGAAAGAACATGTGAGCAAAAGG
CCAGCAAAAGGCCAGGAACCGTAAAAAGGCCGCGTTGCTGGCGTTTTTCCATAGGCTCCGCCCCCCTGACGAGCATCACAAAAATCGACGCTCAAGTCAG
AGGTGGCGAAACCCGACAGGACTATAAAGATACCAGGCGTTTCCCCCTGGAAGCTCCCTCGTGCGCTCTCCTGTTCCGACCCTGCCGCTTACCGGATACCT
GTCCGCCTTTCTCCCTTCGGGAAGCGTGGCGCTTTCTCATAGCTCACGCTGTAGGTATCTCAGTTCGGTGTAGGTCGTTCGCTCCAAGCTGGGCTGTGTGCA
CGAACCCCCCGTTCAGCCCGACCGCTGCGCCTTATCCGGTAACTATCGTCTTGAGTCCAACCCGGTAAGACACGACTTATCGCCACTGGCAGCAGCCACTG
GTAACAGGATTAGCAGAGCGAGGTATGTAGGCGGTGCTACAGAGTTCTTGAAGTGGTGGCCTAACTACGGCTACACTAGAAGAACAGTATTTGGTATCTG
CGCTCTGCTGAAGCCAGTTACCTTCGGAAAAAGAGTTGGTAGCTCTTGATCCGGCAAACAAACCACCGCTGGTAGCGGTGGTTTTTTTGTTTGCAAGCAGC
AGATTACGCGCAGAAAAAAAGGATCTCAAGAAGATCCTTTGATCTTTTCTACGGGGTCTGACGCTCAGTGGAACGAAAACTCACGTTAAGGGATTTTGGTC
ATGAGATTATCAAAAAGGATCTTCACCTAGATCCTTTTAAATTAAAAATGAAGTTTTAAATCAATCTAAAGTATATATGAGTAAACTTGGTCTGACAGTTACC
AATGCTTAATCAGTGAGGCACCTATCTCAGCGATCTGTCTATTTCGTTCATCCATAGTTGCCTGACTCCCCGTCGTGTAGATAACTACGATACGGGAGGGCT
TACCATCTGGCCCCAGTGCTGCAATGATACCGCGAGACCCACGCTCACCGGCTCCAGATTTATCAGCAATAAACCAGCCAGCCGGAAGGGCCGAGCGCAG
AAGTGGTCCTGCAACTTTATCCGCCTCCATCCAGTCTATTAATTGTTGCCGGGAAGCTAGAGTAAGTAGTTCGCCAGTTAATAGTTTGCGCAACGTTGTTGC
CATTGCTACAGGCATCGTGGTGTCACGCTCGTCGTTTGGTATGGCTTCATTCAGCTCCGGTTCCCAACGATCAAGGCGAGTTACATGATCCCCCATGTTGTG
CAAAAAAGCGGTTAGCTCCTTCGGTCCTCCGATCGTTGTCAGAAGTAAGTTGGCCGCAGTGTTATCACTCATGGTTATGGCAGCACTGCATAATTCTCTTAC
TGTCATGCCATCCGTAAGATGCTTTTCTGTGACTGGTGAGTACTCAACCAAGTCATTCTGAGAATAGTGTATGCGGCGACCGAGTTGCTCTTGCCCGGCGTC
AATACGGGATAATACCGCGCCACATAGCAGAACTTTAAAAGTGCTCATCATTGGAAAACGTTCTTCGGGGCGAAAACTCTCAAGGATCTTACCGCTGTTGA
GATCCAGTTCGATGTAACCCACTCGTGCACCCAACTGATCTTCAGCATCTTTTACTTTCACCAGCGTTTCTGGGTGAGCAAAAACAGGAAGGCAAAATGCCG
CAAAAAAGGGAATAAGGGCGACACGGAAATGTTGAATACTCATACTCTTCCTTTTTCAATATTATTGAAGCATTTATCAGGGTTATTGTCTCATGAGCGGAT
ACATATTTGAATGTATTTAGAAAAATAAACAAATAGGGGTTCCGCGCACATTTCCCCGAAAAGTGCCACCTGATGCGGTGTGAAATACCGCACAGATGCGT
AAGGAGAAAATACCGCATCAGGAAATTGTAAGCGTTAATATTTTGTTAAAATTCGCGTTAAATTTTTGTTAAATCAGCTCATTTTTTAACCAATAGGCCGAA
ATCGGCAAAATCCCTTATAAATCAAAAGAATAGACCGAGATAGGGTTGAGTGTTGTTCCAGTTTGGAACAAGAGTCCACTATTAAAGAACGTGGACTCCAA
CGTCAAAGGGCGAAAAACCGTCTATCAGGGCGATGGCCCACTACGTGAACCATCACCCTAATCAAGTTTTTTGGGGTCGAGGTGCCGTAAAGCACTAAATC
GGAACCCTAAAGGGAGCCCCCGATTTAGAGCTTGACGGGGAAAGCCGGCGAACGTGGCGAGAAAGGAAGGGAAGAAAGCGAAAGGAGCGGGCGCTAG
GGCGCTGGCAAGTGTAGCGGTCACGCTGCGCGTAACCACCACACCCGCCGCGCTTAATGCGCCGCTACAGGGCGCGTCCATTCGCCATTCAGGCTGCGCA
ACTGTTGGGAAGGGCGATCGGTGCGGGCCTCTTCGCTATTACGCCAGCTGGCGAAAGGGGGATGTGCTGCAAGGCGATTAAGTTGGGTAACGCCAGGGT
TTTCCCAGTCACGACGTTGTAAAACGACGGCCAGTGAATTGTAATACGACTCACTATA 5'